A peer-reviewed version of this preprint was published in PeerJ on 30 August 2016.

Parker WG. 2016. Osteology of the Late Triassic aetosaur *Scutarx deltatylus* (Archosauria: Pseudosuchia) PeerJ 4:e2411 https://doi.org/10.7717/peerj.2411

Osteology of the Late Triassic aetosaur *Scutarx deltatylus* (Archosauria: Pseudosuchia).

William G Parker

Aetosaurs are some of the most common fossils collected from the Upper Triassic Chinle Formation of Arizona, especially at the Petrified Forest National Park. Four partial skeletons collected from the park from 2002 through 2009 represent the holotype and referred specimens of *Scutarx deltatylus*. These specimens include much of the carapace, as well as the vertebral column, and shoulder and pelvic girldles. A partial skull represents the first aetosaur skull recovered from Arizona since the 1930s. *Scutarx deltatylus* can be distinguished from closely related forms *Calyptosuchus wellesi* and *Adamanasuchus eisenhardtae* not only morphologically, but also stratigraphically. Thus, *Scutarx deltatylus* is potentially an index taxon for the upper part of the Adamanian biozone.

PeerJ Preprints | https://doi.org/10.7287/peerj.preprints.1924v1 | CC-BY 4.0 Open Access | rec: 3 Apr 2016, publ: 3 Apr 2016

Osteology of the Late Triassic aetosaur *Scutarx deltatylus* (Archosauria: Pseudosuchia).

William G. Parker[1,2]

[1] Division of Resource Management, Petrified Forest National Park, Petrified Forest, Arizona, U.S.A.

[2] Department of Geosciences, The University of Texas, Austin, Texas, U.S.A.

Corresponding Author:

William Parker

1 Park Road, #2217, Petrified Forest, Arizona, 86028, U.S.A.

Email address: William_Parker@nps.gov

PeerJ Preprints | https://doi.org/10.7287/peerj.preprints.1924v1 | CC-BY 4.0 Open Access | rec: 3 Apr 2016, publ: 3 Apr 2016

Abstract

Aetosaurs are some of the most common fossils collected from the Upper Triassic Chinle Formation of Arizona, especially at the Petrified Forest National Park. Aetosaurs collected from lower levels of the park include *Desmatosuchus spurensis*, *Paratypothorax*, *Adamanasuchus eisenhardtae*, *Calyptosuchus wellesi*, and *Scutarx deltatylus*. Four partial skeletons collected from the park from 2002 through 2009 represent the holotype and referred specimens of *Scutarx deltatylus*. These specimens include much of the carapace, as well as the vertebral column, and shoulder and pelvic girldles. A partial skull represents the first aetosaur skull recovered from Arizona since the 1930s. *Scutarx deltatylus* can be distinguished from closely related forms *Calyptosuchus wellesi* and *Adamanasuchus eisenhardtae* not only morphologically, but also stratigraphically. Thus, *Scutarx deltatylus* is potentially an index taxon for the upper part of the Adamanian biozone.

Introduction

The Triassic Period is a key transitional point in Earth history, when remnants of Paleozoic biotas were replaced by a Mesozoic biota including components of recent ecosystems (e.g., Fraser 2006). Prominent in this new radiation were the archosaurs, which include the common ancestor of birds and crocodylians and all of their descendants (Gauthier 1986). The early appearance and diversification of this important clade is of interest because beginning in the Triassic, the archosaurs almost completely dominated all continental ecosystems throughout the entire Mesozoic (e.g., Nesbitt 2011). Because the Triassic globe had a coalesced supercontinent, Pangaea, the Laurasian and Gondwanan continental faunas are often considered to be cosmopolitan in their distribution, presumably because of a lack of major oceanic barriers

PeerJ Preprints | https://doi.org/10.7287/peerj.preprints.1924v1 | CC-BY 4.0 Open Access | rec: 3 Apr 2016, publ: 3 Apr 2016

(Colbert 1971). Thus many Triassic taxa were considered widespread and widely applicable for global biostratigraphy (e.g., Lucas 1998a).

More recent work suggests that this is a gross oversimplification of the taxonomic diversity present at the time (e.g., Irmis et al. 2007a; Nesbitt, Irmis & Parker 2007; Nesbitt et al. 2009a; Nesbitt et al. 2009b) and new research on many Triassic groups is showing evidence for endemism of species-level taxa (e.g., Martz & Small 2006; Parker 2008a; Parker 2008b; Stocker 2010), with distinct patterns of radiation of more inclusive clades into new areas (e.g., Nesbitt et al. 2010). Key to this change in thinking are the utilization of testable techniques such as apomorphy-based identification of fossils (e.g., Irmis et al. 2007b; Nesbitt & Stocker 2008) and improved phylogenetic approaches to archosaur relationships and paleobiogeography (e.g., Irmis 2008; Nesbitt 2011; Nesbitt et al. 2010). The apomorphy-based approach reveals hidden diversity in faunal assemblages resulting in the recognition of new distinct taxa (e.g., Nesbitt & Stocker 2008).

Aetosaurians are quadrupedal, heavily armored, suchian archosaurs with a global distribution, restricted to non-marine strata of the Late Triassic (Desojo et al. 2013). Aetosaurians are characterized by their specialized skull with partially edentulous jaws, an upturned premaxillary tip, and laterally facing supratemporal fenestrae. Another key feature of aetosaurians is a heavy carapace consisting of four columns of rectangular dermal armor, two paramedian columns that straddle the midline, and two lateral columns (Walker 1961). Ventral and appendicular osteoderms are also present in most taxa. Aetosaurian osteoderms possess detailed ornamentation on the dorsal surface, the patterning of which is diagnostic for taxa (Long & Ballew 1985). Thus, the type specimens of several aetosaurian taxa consist solely of osteoderms (e.g., *Typothorax coccinarum* Cope 1875; *Paratypothorax andressorum* Long and

PeerJ Preprints | https://doi.org/10.7287/peerj.preprints.1924v1 | CC-BY 4.0 Open Access | rec: 3 Apr 2016, publ: 3 Apr 2016

Ballew 1985; *Lucasuchus hunti* Long and Murry 1995; *Rioarribasuchus chamaensis* Zeigler, Heckert & Lucas 2003; *Apachesuchus heckerti* Spielmann & Lucas 2012) or consist chiefly of osteoderms (e.g., *Calyptosuchus wellesi* Long & Ballew 1985; *Typothorax antiquus* Lucas, Heckert & Hunt 2003; *Tecovasuchus chatterjeei* Martz & Small 2006; *Adamanasuchus eisenhardtae* Lucas, Hunt, and Spielmann 2007; *Sierritasuchus macalpini* Parker, Stocker & Irmis 2008). Aetosaurian osteoderms and osteoderm fragments are among the most commonly recovered fossils from Upper Triassic strata (Heckert & Lucas 2000). Because of this abundance, in concert with the apparent ease of taxonomic identification, global distribution in non-marine strata, and limited stratigraphic range (e.g., Upper Triassic) aetosaurians have been proposed as key index fossils for use in regional and global non-marine biostratigraphy (e.g., Heckert et al. 2007a; Heckert et al. 2007b; Long & Ballew 1985; Lucas 1998; Lucas & Heckert 1996; Lucas et al. 1997; Lucas & Hunt 1993; Lucas et al. 2007; Parker & Martz 2011). Four Land Vertebrate Faunachrons (LVF) were erected that use aetosaurians to divide the Late Triassic Epoch (Lucas & Hunt 1993), from oldest to youngest these are the Otischalkian (middle Carnian); Adamanian (late Carnian); Revueltian (Norian), and the Apachean (Rhaetian). These were redefined as biozones by Parker and Martz (2011).

Aetosaurians are one of the most commonly recovered vertebrate fossils in the Upper Triassic Chinle Formation at Petrified Forest National Park (PEFO), Arizona. Paleontological investigations in the park between 2001 and 2009 resulted in the discovery of four partial skeletons that are considered a new taxon (Parker 2016). The first specimen (PEFO 31217), discovered in 2001 and collected in 2002 from Petrified Forest Vertebrate Locality (PFV) 169 (Battleship Quarry; Figure 1), was initially assigned to *Calyptosuchus* (=*Stagonolepis*) *wellesi* based on characters of the armor and vertebrae (Parker & Irmis 2005). The second partial

PeerJ Preprints | https://doi.org/10.7287/peerj.preprints.1924v1 | CC-BY 4.0 Open Access | rec: 3 Apr 2016, publ: 3 Apr 2016

skeleton was collected in 2004 from PFV 304 (Milkshake Quarry), at the south end of the park (Figure 1). That specimen (PEFO 34045) was also mentioned by Parker and Irmis (2005), who noted differences in the armor from *Calyptosuchus wellesi* and suggested that might represent a distinct species. The other two specimens were collected in 2007 and 2009. The first (PEFO 34616), from the Billings Gap area (PFV 355; Figure 1) is notable because it included the first aetosaurian skull to be recovered in the park. The second specimen (PEFO 34919) was recovered from the Saurian Valley area of the Devils Playground (PFV 224; Figure 1). All four of these specimens were originally assigned to *Calyptosuchus wellesi* by Parker and Martz (2011) and used to construct the stratigraphic range for that taxon. *Calyptosuchus* is considered to be an index taxon of the Adamanian biozone (Lucas & Hunt 1993; Parker & Martz 2011).

Subsequent preparation and more detailed examination of these four specimens led to the discovery that they all shared a key autapomorphy, the presence of a prominent, raised triangular protuberance in the posteromedial corner of the paramedian osteoderms. The protuberance is not present on any of the osteoderms of the holotype of *Calyptosuchus wellesi* (UMMP 13950). It is also absent on the numerous paramedian osteoderms of *Calyptosuchus wellesi* recovered from the *Placerias* Quarry of Arizona in collections at the UCMP and the MNA. That autapomorphy and several features of the cranium and pelvis differentiate these specimens from all other known aetosaurians and form the basis for assigning these materials to a new taxon, *Scutarx deltatylus* (Parker 2016).

.

Institutional abbreviations –**DMNH**, Perot Museum of Natural History, Dallas, Texas, USA; **MCZD**, Marischal College Zoology Department, University of Aberdeen, Aberdeen, Scotland, UK; **NCSM**, North Carolina State Museum, Raleigh, North Carolina, USA; **NHMUK**, The

PeerJ Preprints | https://doi.org/10.7287/peerj.preprints.1924v1 | CC-BY 4.0 Open Access | rec: 3 Apr 2016, publ: 3 Apr 2016

Natural History Museum, London, United Kingdom; **NMMNH**, New Mexico Museum of Natural History and Science, Albuquerque, New Mexico, USA; **MNA**, Museum of Northern Arizona, Flagstaff, Arizona, USA; **PEFO**, Petrified Forest National Park, Petrified Forest, Arizona, USA; **PFV**, Petrified Forest National Park Vertebrate Locality, Petrified Forest, Arizona, USA; **PVL**, Paleontología de Vertebrados, Instituto 'Miguel Lillo', San Miguel de Tucumán, Argentina; **PVSJ,** División de Paleontologia de Vertebrados del Museo de Ciencias Naturales y Universidad Nacional de San Juan, San Juan, Argentina; **TMM**, Vertebrate Paleontology Laboratory, University of Texas, Austin, Texas, USA; **TTU P**, Museum of Texas Tech, Lubbock, Texas, USA; **UCMP**, University of California, Berkeley, California, USA; **UMMP**, University of Michigan, Ann Arbor, Michigan, USA; **USNM**, National Museum of Natural History, Smithsonian Institution, Washington, D.C., USA; **VPL**, Vertebrate Paleontology Lab, University of Texas at Austin, Austin, Texas, USA; **YPM**, Yale Peabody Museum of Natural History, New Haven, Connecticut, USA; **ZPAL,** Institute of Paleobiology of the Polish Academy of Sciences in Warsaw, Warsaw; Poland.

GEOLOGICAL SETTING

The four localities from which the material of *Scutarx deltatylus* was collected all occur in the lower part of the Sonsela Member of the Chinle Formation (Martz & Parker 2010) (Figure 2). In the PEFO region the Sonsela Member can be divided into five distinct beds, the Camp Butte, Lot's Wife, Jasper Forest, Jim Camp Wash, and Martha's Butte beds (Martz & Parker 2010). The Lot's Wife, Jasper Forest, and Martha's Butte beds are sandstone dominated, cliff forming units with source areas to the south and west (Howell & Blakey 2013), whereas the Lot's Wife and Martha's Butte beds are slope forming units with a higher proportion of mudrocks than sandstones (Martz & Parker 2010). All of these localities represent proximal

PeerJ Preprints | https://doi.org/10.7287/peerj.preprints.1924v1 | CC-BY 4.0 Open Access | rec: 3 Apr 2016, publ: 3 Apr 2016

floodplain facies associated with a braided river system (Howell & Blakey 2013; Martz & Parker 2010; Woody 2006).

PFV 169 and PFV 224 occur in the upper part of the Lot's Wife beds, PFV 355 is situated in the base of the Jasper Forest bed, and PFV 304 marks the highest stratigraphic occurrence, located in the lower part of the Jim Camp Wash beds (Figure 2). All of these sites are below the 'persistent red silcrete,' a thick, chert, marker bed that approximates the stratigraphic boundary between the Adamanian and Revueltian biozones (Martz & Parker 2010; Parker & Martz 2011). Exact locality information is available at Petrified Forest National Park to qualified researchers. Non-disclosure of locality information is protected by the Paleontological Resources Preservation Act of 2009.

A high concentration of volcanic material in mudrocks of the Chinle Formation includes detrital zircons and allows for determination of high precision radioisotopic dates for studied beds (Figure 2; Ramezani et al. 2011). Zircons from the top of the Lot's Wife beds provided an age of 219.317 ± 0.080 Ma (sample SBJ; Ramezani et al. 2011). The base of the unit is constrained by an age of 223.036 ± 0.059 Ma for the top of the underlying Blue Mesa Member (sample TPs; Ramezani et al. 2011). Ages of 218.017 ± 0.088 Ma (sample GPL) and 213.870 ± 0.078 (sample KWI) are known from the Jasper Forest bed and the overlying Jim Camp Wash beds constraining the upper age for the fossil specimens (Ramezani et al. 2011).

MATERIALS AND METHODS

All specimens were excavated utilizing small hand tools, although a backhoe tractor was used initially to remove overburden at PFV 304. B-15 Polyvinyl Acetate "Vinac" (Air Products & Chemicals, Inc.) and B-76 Butvar (Eastman Chemical Company) dissolved in acetone were used as a consolidant in the field. PEFO 31217 was discovered partly in unconsolidated, heavily

PeerJ Preprints | https://doi.org/10.7287/peerj.preprints.1924v1 | CC-BY 4.0 Open Access | rec: 3 Apr 2016, publ: 3 Apr 2016

weathered sediment with numerous plant roots growing over and through the bones. Small handtools, including brushes, caused damage to the bone surface so plastic drinking straws were used to blow away sediment from the bone surface, which was then quickly hardened with a consolidant. In the lab the same specimen quickly deteriorated upon exposure, and liberal amounts of extremely thin Paleobond cyanoacrylate (Uncommon Conglomerates) was applied to stop disintegration. Because of the delicate nature of this specimen and the application of the cyanoacrylate, many of the bones cannot be prepared further or removed from the original field jackets. Furthermore, during collection the condition of the bones and surrounding matrix proved to be so poor that a portion of the jacket with the scapulocoracoid in it was lost during turning. This lost material consisted mostly of trunk vertebrae, ribs, and osteoderms.

The other three skeletons were consolidated in the lab using B-72 Butvar (Eastman Chemical Company), with Paleobond (Uncommon Conglomerates) cyanoacrylate used in many cases for permanent bonds. Paleobond (Uncommon Conglomerates) accelerator was originally used on some of the bones in PEFO 34045, but was halted because it was causing discoloration of the bone surface during the curing process. PEFO 34919 is coated with thin layers of hematite as is common for fossil specimens recovered from sandy facies in the Devils Playground region of PEFO. Mechanical preparation with pneumatic tools damaged the bone surface upon removing the coating and revealed that the hematite had permeated numerous microfractures in the bones, expanding them slightly, or in some bones significantly. As a result, the non-osteoderm bones from PFV 224 are highly deformed and often ‘mashed’ into the associated osteoderms. Further preparation to remove the hematite coating was not attempted.

Naming Conventions for Aetosaurian Osteoderms

PeerJ Preprints | https://doi.org/10.7287/peerj.preprints.1924v1 | CC-BY 4.0 Open Access | rec: 3 Apr 2016, publ: 3 Apr 2016

Traditionally, identification and naming of aetosaurian osteoderms, which cover the dorsal, ventral, and appendicular areas, utilizes terms first originated by Long & Ballew (1985). In this convention the dorsal armor (carapace) consists of two midline 'paramedian' columns flanked laterally by two 'lateral' columns (Desojo et al. 2013; Long & Ballew 1985). By convention, osteoderms of the dorsal region are named from the type of vertebrae they cover (e.g., cervical, dorsal, and caudal; (Long & Ballew 1985)). However, the anteriormost paramedian osteoderms lack equivalent lateral osteoderms causing a potention numbering offset between the presacral paramedian and lateral rows (Heckert et al. 2010). Aetosaurians also possess ventral armor at the throat, as well as ventral armor (plastron) that underlies the 'dorsal' (=trunk) and caudal vertebrae. The presence of ventral armor of the 'dorsal' series creates the awkward combination of 'ventral-dorsal' osteoderms. Therefore there is a need to standardize the positional nomenclature for aetosaurian osteoderms.

The term carapace properly refers only to the dorsally situated network of osteoderms, thus the term 'dorsal carapace' is incorrect and redundant. In this study the term carapace refers only to the dorsally situated osteoderms and the term ventral osteoderms (or in some cases, plastron) is used for all ventrally situated osteoderms.

The carapace can be divided into four anteroposteriorly trending columns of osteoderms (Heckert et al. 2010). Those that straddle the mid-line are referred to as the paramedians and the flanking osteoderms are called the lateral armor (Long & Ballew 1985). Each column is divided into rows and as noted above these have traditionally been given names based on the vertebral series they cover (in most taxa there is a 1:1 ratio between osteoderms and vertebrae).

The two anteriormost paramedian osteoderms fit into the back of the skull and are generally mediolaterally oval and lack corresponding lateral osteoderms. These osteoderms are termed the nuchal series (Figure 3; Desojo et al. 2013; Sawin 1947; Schoch & Desojo 2016). Posterior to these are roughly five, six, or nine rows of paramedian and lateral osteoderms that

PeerJ Preprints | https://doi.org/10.7287/peerj.preprints.1924v1 | CC-BY 4.0 Open Access | rec: 3 Apr 2016, publ: 3 Apr 2016

cover the entire cervical vertebral series, termed cervical osteoderms (Figure 3; Long & Ballew 1985). The patch of osteoderms beneath the cervical vertebrae in the throat area would be called the gular osteoderms, based on the name given to these osteoderms in phytosaurians (Long & Murry 1995).

The next vertebral series initiates with the 10th presacral vertebra. On this vertebra the parapophysis has moved up to the top of the centrum, just below the level of the neurocentral suture. In the previous nine vertebrae (the cervical series), the parapophysis is situated at the base of the centrum, and in the eleventh vertebra the parapophysis is situated on the tranverse process. Thus the 10th presacral is transitional in form and has been considered to be the first of the 'dorsal' series (Case 1922; Parker 2008a; Walker 1961), and that convention is followed here.

Historically in aetosaurians these vertebrae have been referred to as the dorsal series and osteoderms covering these vertebrae are the 'dorsal osteoderms' (e.g., Desojo et al. 2013; Heckert & Lucas 2000; Long & Ballew 1985; Long & Murry 1995); however, this term has become problematic because whereas all of the osteoderms below the vertebral column are termed the ventral osteoderms, only those of above the vertebral column in the trunk region are called the dorsals. Thus technically the osteoderms beneath the caudal vertebrae would be the caudal ventral osteoderms and those beneath the 'dorsal' vertebrae would be the dorsal ventral osteoderms. This is non-sensical so a new term is suggested be used for what have been known as the dorsal vertebrae and osteoderms in aetosaurians. The terms thoracic and lumbar vertebrae reflect the chest and loin areas respectively and are assigned depending on the presence or absence of free ribs. This is not readily applicable to aetosaurians where there are ribs through the entire series. Instead the term trunk vertebrae is used, which is commonly used for amphibians and lepidosaurs, which also tend to have a ribs throughout the entire series (e.g., Wake 1992). The osteoderms above the trunk vertebrae are the dorsal trunk paramedian and dorsal trunk lateral osteoderms. The osteoderms located beneath the trunk vertebrae are the ventral trunk osteoderms and consists of numerous columns of osteoderms (Figure 3; Walker 1961). Heckert et al. (2010) utilized the term ventral thoracic osteoderms, which effectively

PeerJ Preprints | https://doi.org/10.7287/peerj.preprints.1924v1 | CC-BY 4.0 Open Access | rec: 3 Apr 2016, publ: 3 Apr 2016

239 solves the 'ventral dorsal' problem; however, the term ventral trunk osteoderms is preferred here
240 to maintain consistency with the term dorsal trunk osteoderms.
241 The osteoderms above the caudal vertebrae are termed the dorsal caudal osteoderms and
242 consist of paramedian and lateral columns (Figure 3; Long & Ballew 1985). The osteoderms
243 beneath the caudal vertebrae are the ventral caudal osteoderms (Heckert et al. 2010) and also
244 consist of paramedian and lateral columns behind the cloacal area (fourth row) to the tip of the
245 tail (Jepson 1948; Walker 1961), the first two lateral rows bear spines in *Typothorax coccinarum*
246 (Heckert et al. 2010). An assemblage of irregular shaped osteoderms are located anterior to the
247 cloacal area is preserved in *Stagonolepis robertsoni*, *Aetosaurus ferratus*, and *Typothorax*
248 *coccinarum* (Heckert et al. 2010; Schoch 2007; Walker 1961), which can be called the cloacal
249 osteoderms. Small masses of irregular shaped osteoderms cover the limb elements of
250 aetosaurians (e.g., Heckert & Lucas 1999; Heckert et al. 2010; Schoch 2007). These have
251 collectively been termed as simply appendicular osteoderms. However, when found in
252 articulation they can be differentiated by the limb that is covered, including the humeral,
253 radioulnar, femoral, and tibiofibular osteoderms (Hill 2010).
254
255

256 **SYSTEMATIC PALEONTOLOGY**

257 Archosauria Cope 1869 *sensu* Gauthier & Padian 1985.

258 Pseudosuchia Zittel 1887-90 *sensu* Gauthier & Padian 1985.

259 Aetosauria Marsh 1884 *sensu* Parker, 2007.

260 Stagonolepididae Lydekker 1887 *sensu* Heckert & Lucas 2000.

261 ***Scutarx deltatylus*** Parker 2016

262 (Figs. 4 – 25)

263

PeerJ Preprints | https://doi.org/10.7287/peerj.preprints.1924v1 | CC-BY 4.0 Open Access | rec: 3 Apr 2016, publ: 3 Apr 2016

1985 *Calyptosuchus wellesi*: Long and Ballew, p. 54, fig. 13a.
1995 *Stagonolepis wellesi*: Long and Murry, p. 82, figs, 71b, 72b, e.
2005 *Stagonolepis wellesi*: Parker and Irmis, p. 49, fig. 4a.
2005a *Stagonolepis wellesi*: Parker, p. 44.
2005b *Stagonolepis wellesi*: Parker, p. 35.
2006 *Stagonolepis wellesi*: Parker, p. 53.
2011 *Calyptosuchus wellesi*: Parker and Martz, p. 242.
2013 *Calyptosuchus wellesi*: Martz et al., p. 342, figs. 7a-d.
2014 *Calyptosuchus wellesi*: Roberto-Da-Silva et al., p. 247.
2016 *Scutarx deltatylus*: Parker, p. 27, figs. 2-5.

Holotype – PEFO 34616, posterior portion of skull with braincase, cervical and dorsal trunk paramedian and dorsal trunk lateral osteoderms, ventral osteoderms, rib fragments, and paired gastral ribs.

Paratypes -- PEFO 31217, much of a postcranial skeleton including vertebrae, ribs, pectoral and pelvic girdles, osteoderms; PEFO 34919, much of a postcranial skeleton including vertebrae, ribs, osteoderms, girdle fragments, ilium; PEFO 34045, much of a postcranial skeleton including vertebrae, ribs, and osteoderms.

Referred Specimens -- UCMP 36656, UCMP 35738, dorsal trunk paramedian and dorsal trunk lateral osteoderms (lower part of the Chinle Formation, Nazlini, Arizona); TTU P-09240, left and right dorsal trunk paramedian osteoderms (Cooper Canyon Formation, Dockum Group, Post, Texas).

Locality, Horizon, and Age -- PFV 255 (The Sandcastle), Petrified Forest National Park, Arizona; lower part of the Sonsela Member, Chinle Formation; Adamanian biozone, Norian, ~217 Ma (Ramezani et al. 2011).

Diagnosis – From Parker (2016): Medium-sized aetosaurian diagnosed by the following autapomorphies; the cervical and dorsal trunk paramedian osteoderms bear a strongly raised, triangular tuberosity in the posteromedial corner of the dorsal surface of the osteoderm; the

PeerJ Preprints | https://doi.org/10.7287/peerj.preprints.1924v1 | CC-BY 4.0 Open Access | rec: 3 Apr 2016, publ: 3 Apr 2016

occipital condyle lacks a distinct neck because the condylar stalk is mediolaterally broad; the base of the cultriform process of the parabasisphenoid bears deep lateral fossae; the frontals and parietals are very thick dorsoventrally; and there is a distinct fossa or recess on the lateral surface of the ilium between the supraacetabular crest and the posterior portion of the iliac blade. *Scutarx deltatylus* can also be differentiated from other aetosaurs a unique combination of characters including moderately wide dorsal trunk paramedian osteoderms with a strongly raised anterior bar that possesses anteromedial and anterolateral processes (shared with all aetosaurians except Desmatosuchini); osteoderm surface ornamentation of radiating ridges and pits that emanate from a posterior margin contacting a dorsal eminence (shared with *Calyptosuchus wellesi*, *Stagonolepis robertsoni*, *Adamanasuchus eisenhardtae*, *Neoaetosauroides engaeus*, and *Aetosauroides scagliai*); lateral trunk osteoderms with an obtuse angle between the dorsal and lateral flanges (shared with non-desmatosuchines); a dorsoventrally short pubic apron with two proximally located 'obturator' fenestrae (shared with *Stagonolepis robertsoni*); and an extremely anteroposteriorly short parabasisphenoid, with basal tubera and basipterygoid processes almost in contact and a reduced cultriform process (shared with *Desmatosuchus*).

DESCRIPTION

Skull

Much of the posterodorsal portion of the skull is present in PEFO 34616 (Figures 4-10). Elements preserved include much of the left nasal, both frontals (the right is incomplete), both postfrontals, the left parietal (badly damaged), the left and right squamosals, the right postorbital, a portion of the left postorbital, and a nearly complete occipital region and braincase. The skull was already heavily eroded when discovered and although the skull roof/braincase portion was

PeerJ Preprints | https://doi.org/10.7287/peerj.preprints.1924v1 | CC-BY 4.0 Open Access | rec: 3 Apr 2016, publ: 3 Apr 2016

collected *in situ*, the remaining elements had to be carefully pieced back together from many fragments collected as float. Accordingly many of the skull roof elements are incomplete.

Much of the skull appears to have separated originally along some of the sutures, notably those between the prefrontal-frontal, squamosal-quadrate, and postorbital-quadratojugal contacts. The left frontoparietal suture is also visible because of bone separation, and the sockets in the squamosals for reception of the proximal heads of the quadrates are well-preserved. Thus, the skull appears to have mostly fallen apart before burial and many of the anterior and ventral elements were presumably scattered and lost during disarticulation, with the exception of the left nasal, which is represented as an isolated piece. Similar preservation exists for the skull roof of the holotype of *Stagonolepis olenkae* (ZPAL AbIII/466/17) in which the frontal, parietals, occipital, and braincase are preserved as a single unit. This may suggest that the posterodorsal portion of the skull fuses earlier in ontogeny in these taxa. The skull of *Scutarx deltatylus* features a well-preserved braincase, which is described in detail below. Sutures are difficult to observe because of the state of preservation of the specimen, and the skull of *Longosuchus meadei* (TMM 31185-98) was used to infer the locations of various sutures, based on observable landmarks present in PEFO 34616.

Nasal

The proximal half of the left nasal is preserved, consisting of the main body and the posterior portion of the anterior projection through the mid-point of the external naris (Figure 4). The main body is dorsoventrally thick and the entire element is slightly twisted dorsomedially so that the dorsal surface is noticeably concave. Any surface ornamentation is obscured by a thin coating of hematite. The midline symphysis is straight and slightly rugose (Figure 4). The lateral surface is damaged along the lacrimal suture; however, more anteriorly, the sutural surface for

PeerJ Preprints | https://doi.org/10.7287/peerj.preprints.1924v1 | CC-BY 4.0 Open Access | rec: 3 Apr 2016, publ: 3 Apr 2016

the ascending process of the maxilla is preserved and is strongly posteroventrally concave (Figure 4). Anteriorly the nasal narrows mediolaterally where it forms the dorsal margin of the external naris. The ventral process of the nasal that borders the posterior edge of the naris is missing its tip but it is clear from what is preserved that it was not elongate as in *Aetosauroides scagliai* but rather short as in *Stagonolepis olenkae* (ZPAL AbIII/346).

Frontal

Both frontals are present, with the left nearly complete and the right missing the posterior portion (Figure 5). The extreme dorsoventral thickness of the element is evident, as the dorsoventral thickness is 0.35 times the midline length of the element. The frontals appear to be hollow; however, this is most likely from damage during deposition and subsequent weathering before the skull roof was collected and pieced back together. In dorsal view the posterior margin of the frontal is slanted posterolaterally as in *Stagonolepis robertsoni* (Walker 1961) so that the lateral margin of the frontal is longer than the medial margin, forming a distinct posterolateral process (Figure 5). The anterior portion of that process meets the postfrontal laterally and the parietal posteriorly as in *Stagonolepis olenkae* (Sulej 2010). Just anterior to the posterolateral process the frontal forms the dorsal margin of the orbit. The position of the suture with the postfrontal is not clear, but it should have been present as in all other aetosaurians.

The dorsal surfaces of the frontals are rugose, ornamented with deep pits, some associated with more elongate grooves. Laterally above the round orbits and anteriorly there is are wider, anteroposteriorly oriented grooves as in *Stagonolepis olenkae* (Sulej 2010). These grooves demarcate a raised central portion of the frontals as described for *Stagonolepis robertsoni* by Walker (1961). The anterolateral margins of the frontals are dorsoventrally thick,

PeerJ Preprints | https://doi.org/10.7287/peerj.preprints.1924v1 | CC-BY 4.0 Open Access | rec: 3 Apr 2016, publ: 3 Apr 2016

rugose, anteromedially sloping areas that are bounded posteriorly by a thin curved ridge. These are the sutures for the prefrontals (Figures 5-6). There is no clear evidence for articulation of a palpebral bone at this position as in *Stenomyti huangae* (Small & Martz 2013), but the posteriormost portion of the articular surface (Figure 6) is probably a suture for a palpebral as in *Longosuchus meadei* (TMM 31184-98). The anterior margins of the frontals are thick and rugose for articulation with the nasals (Figures 5, 7). The frontal/nasal suture is nearly transverse. The frontal also lacks the distinct, raised midline ridge present in *Stenomyti huangae* (Small & Martz 2013).

The ventral surfaces of the frontals are broadly ventrally concave and smooth (Figure 7). Medial to the orbital fossa is a distinct, slightly curved ridge that is the articulation point with the laterosphenoid.

Postfrontal

The postfrontals are roughly triangular bones that form the posterodorsal margin of the orbit. Both are certainly preserved in PEFO 34616, as in all aetosaurians, but the positions of their sutures are not clear.

Parietal

The dorsal portions of both parietals are mostly missing, although the posterolateral corner of the left one remains as well as a small fragment of the posterior portion of the right where it contacts the dorsal process of the squamosal (Figure 5). The frontal/parietal suture is visible along the posterior margin of the frontals, so it is clear that these elements were not fused. The posterolateral portion forms the dorsal border of the supratemporal fenestra, but few other details are visible.

PeerJ Preprints | https://doi.org/10.7287/peerj.preprints.1924v1 | CC-BY 4.0 Open Access | rec: 3 Apr 2016, publ: 3 Apr 2016

The posterior flanges of both parietals are preserved (Figure 8). Their posteroventrally sloping surfaces form the upper portion of the back of the skull. Ventrally, they contact the paroccipital processes of the opisthotics. There is no evidence for a posttemporal fenestrae, which may have been obliterated by slight ventral crushing of the skull roof. The parietal flanges contact the supraoccipital medially and the posterior process of the squamosal laterally. The upper margins are damaged so that the presence of a shelf for articulation of the nuchal paramedian osteoderms cannot be confirmed.

Squamosal

The majority of both squamosals is present. As is typical for aetosaurians the squamosals are elongate bones that are fully exposed in lateral view, forming the posterior corner of the skull, as well as the posteroventral margin of the oval supratemporal fenestra (Figure 6). The anterior and posterior portions are separated by a dorsoventrally thin neck. The anterior portion divides into two distinct rami, a large, but mediolaterally thin, ventral lobe that presumably contacted the upper margin of the quadratojugal, and a much smaller triangular dorsal ramus that forms much of the anteroventral margin of the supratemporal fenestra. These two rami are separated by a posterior process of the postorbital. On the right side of PEFO 34616, the dorsal ramus is broken, clearly showing the articulation with the postorbital and exposing the prootic in this view (Figure 6). The ventral margin of the main body is concave and bears a flat surface that is the articulation surface with the quadrate (s.qu; Figure 7). Anterior to that articular surface the ventral margin of the anterior portion of the squamosal is confluent with the ventral margin of the postorbital. This arrangement suggests that the squamosal contributed little if anything to the margin of the lateral temporal fenestra. This is similar to the condition in *Stagonolepis robertsoni*

PeerJ Preprints | https://doi.org/10.7287/peerj.preprints.1924v1 | CC-BY 4.0 Open Access | rec: 3 Apr 2016, publ: 3 Apr 2016

(Walker 1961) and differs from that in *Stenomyti huangae* (Small & Martz 2013) in which the ventral margin of the squamosal is situated much lower that the ventral margin of the postorbital, and the squamosal contributes significantly to the margin of the infratemporal fenestra.

The posterior portion of the squamosal expands dorsally into dorsal and ventral posterior processes. The dorsal process forms the posterior border of the supratemporal fenestra and is mediolaterally thickened with a smooth anterior concave area that represents the supratemporal fossa. The apex of the upper process contacts the parietal. The ventral posterior process forms a small hooked knob that projects off of the back of

the skull. Medial to this is a deep pocket in the medial surface of the squamosal that receives the dorsal head of the quadrate.. Dorsomedial to this pocket is the contact between the squamosal and the distal end of the paroccipital process of the opisthotic (Figure 7).

Postorbital

A portion of the left and almost the complete right postorbital are preserved in PEFO 34616 (Figures 6-7). They are mediolaterally thin, triradiate bones that contact the postfrontal and parietal dorsally, the jugal anteriorly, and the squamosal posteriorly. The upper bar forms the posterior margin of the orbit and the anterior margin of the supratemporal fenestra. The posterior process is triangular and inserts into a slot in the anterior portion of the squamosal. The ventral margin is flat, and forms the dorsal border of the infratemporal fenestra and more anteriorly that edge bears an articular surface with the jugal. The tip of the anterior process is broken, but it would have overlain the posterior process of the jugal and formed the posteroventral margin of the orbit.

PeerJ Preprints | https://doi.org/10.7287/peerj.preprints.1924v1 | CC-BY 4.0 Open Access | rec: 3 Apr 2016, publ: 3 Apr 2016

Supraoccipital

The supraoccipital is present but poorly preserved (Figure 8). A median element, it forms much of the dorsal portion of the occiput and roofs the foramen magnum. Laterally it contacts the parietal flanges and ventrally the otooccipitals.

Exocipital/opisthotic

The exocciptals and opisthotics are indistinguishably fused into a single structure, the otooccipital. The exoccipital portions form the lateral margins of the foramen magnum (Figure 8). A protuberance is present on the left exoccipital at the dorsolateral corner of the foramen magnum (Figures 5, 8). The presence of similar structures in *Neoaetosauroides engaeus* (e.g., PVL 5698) was noted by Desojo and Báez (2007), and interpreted by them to be facets for reception of the proatlantes. Those authors considered the facets located on the supraoccipital; however, in *Longosuchus meadei* (TMM 31185-84) they are located on the exoccipital and the same appears to be true for PEFO 34616.

Anteriorly, a strong lateral ridge forms the posteroventral margin of the 'stapedial groove' as is typical for aetosaurs (Gower & Walker 2002). In aetosaurians there are typically two openings for the hypoglossal nerve (XII) that straddle the lateral ridge (Gower & Walker 2002); however, they are not apparent in PEFO 34616, and where the posterior opening of the left side should be situated there is a fragment of bone missing.

Both paroccipital processes are present and well-preserved (Figures 5-8). They are mediolaterally short (14 mm) and stout, dorsoventrally taller than anteroposteriorly long (8 mm tall, 4 mm long), and contact the parietal flanges dorsally and the squamosal laterally. The distal end expands slightly dorsoventrally (Figure 8). The posterior surface is flat and distally the process forms the posterior border of the pocket for reception of the quadrate head, therefore there was a sizeable contact between the opisthotic and the quadrate.

PeerJ Preprints | https://doi.org/10.7287/peerj.preprints.1924v1 | CC-BY 4.0 Open Access | rec: 3 Apr 2016, publ: 3 Apr 2016

The proximoventral portion of the paroccipital process opens into the 'stapedial groove'. That groove continues into the main body of the opisthotic, bounded by the lateral ridge of the exoccipital posteroventrally and the crista prootica anterodorsally Figure 9). Here there is a large opening for the fenestra ovalis and the metotic foramen; however, the two cannot be distinguished because the ventral ramus of the opisthotic that divides the two openings in aetosaurians (Gower & Walker 2002) is not preserved (Figure 9). It is not clear if the ventral ramus was never originally preserved or if it was removed during preparation of the braincase. Thus the perilymphatic foramen is not preserved as well. The embryonic metotic fissure is undivided in aetosaurs and therefore the glossopharyngeal, vagal, and accessory (IX, X, XI) nerves and the jugular vein would have exited the braincase via a single opening, the metotic foramen (Gower & Walker 2002; Rieppel 1985; Walker 1990). Just lateral to the metotic foramen on the ventral surface of the crista prootica there should be a small opening for the facial nerve (VII); however, it is not visible through the hematite build-up on the lateral wall of the cranium.

A second distinct groove extends from the ventral border of the fenestra ovalis anteroventrally along the lateral face of the parabasisphenoid to the posterodorsal margin of the basipterygoid process, and is bordered anterodorsally by the anteroventral continuation of the crista prootica (Figure 9). The termination of that groove houses the entrance of the cerebral branch of the internal carotid artery (Gower & Walker 2002; Sulej 2010).

Prootic

The entire braincase is slightly crushed and rotated dorsolaterally so that the left side of the otic capsule is easier to view (Figure 9). Both prootics are preserved. Posteriorly, the prootic overlaps the opisthotic medially, and ventrolaterally forms a thin ridge (crista prootica), which is

PeerJ Preprints | https://doi.org/10.7287/peerj.preprints.1924v1 | CC-BY 4.0 Open Access | rec: 3 Apr 2016, publ: 3 Apr 2016

bounded ventrally by the upper part of the 'stapedial groove' and the groove in the parabasisphenoid leading to an opening for the internal carotid. Anteroventrally, the prootic meets the anterior portion of the parabasisphenoid, just posterior to the hypophyseal fossa. Anteriorly and anterodorsally, the prootic meets the laterosphenoid and dorsally it is bounded by the parietal. The uppermost margin is deformed by a thick anteroposteriorly oriented mass of bone, which could represent crushing of the parietal margin. Just posterior to the anterior suture with the laterosphenoid is the opening for the trigeminal nerve (V) which is deformed and closed by crushing (Figure 9). In PEFO 34616 the opening for the trigeminal nerve is completely enclosed by the prootic.

Laterosphenoid

The laterosphenoids are ossified but poorly preserved. On the left side anterodorsal to the opening for the trigeminal nerve (V), there is the cotylar crest, which is crescentic and opens posteriorly (Figure 9). No other details of the laterosphenoid can be determined.

Basioccipital/Parabasisphenoid

The basioccipital and parabasisphenoid are complete and together comprise the best preserved and most distinctive portion of the braincase in *Scutarx deltatylus* (Figure 10). The occipital condyle is transversely ovate in posterior view rather than round like in other aetosaurs such as *Longosuchus meadei* (TMM 31185-98). The dorsal surface is broad with a wide shallow groove for the spinal cord.

The condylar stalk is also broad (25 mm wide), and wider than the condyle. Thus there is no distinct 'neck,' nor does a sharp ridge delineate the condyle from the stalk as in *Longosuchus meadei* (TMM 31185-98; Parrish 1994) or *Desmatosuchus smalli* (TTU P-9024; Small 2002). The ventral surface of the condylar stalk bears two low rounded 'keels' separated by a shallow,

PeerJ Preprints | https://doi.org/10.7287/peerj.preprints.1924v1 | CC-BY 4.0 Open Access | rec: 3 Apr 2016, publ: 3 Apr 2016

but distinct, oblong pit. The broad stalk, lack of a distinct neck, and ventral keels all appear to be autapomorphic for *Scutarx deltatylus*. Anterolaterally the condylar stalk expands laterally to form the ventral margin of the metotic fissure. The contacts with the exoccipitals are dorsal and posterior to that margin.

The right basal tuber of the basioccipital is present, but the left is missing. The basioccipital tuber is separated from the crescentic basal tuber of the parabasisphenoid by an unossified cleft, typical for aetosaurians and other suchians (Figure 10; Gower & Walker 2002). The basal tubera of the basioccipital are divided medially by an anteroposteriorly oriented bony ridge that bifurcates anteriorly to form the crescentic basal tubera of the parabasisphenoid and enclose the posterior portion of the basisphenoid recess (sensu Witmer 1997). Posteriorly that bony ridge is confluent with the posteriorly concave posterior margin of the basioccipital basal tubera (Figure 10). The short, anterolaterally directed basipterygoid processes are located anteriorly and in contact posteriorly with the anterior margin of the basal tubera of the parabasisphenoid. The upper portion of the distal end of the left basipterygoid process is broken, but the right is complete and bears a slightly expanded and slightly concave distal facet that faces anterolaterally to contact the posterior process of the pterygoid.

The basipterygoid processes and the basal tubera are positioned in the same horizontal plane (Figure 9), which is typical for aetosaurians and differs significantly from the condition in *Revueltosaurus callenderi* (PEFO 34561) and *Postosuchus kirkpatricki* (TTU P-9000; Weinbaum 2011) in which the basicranium is oriented more more vertically, with the basipterygoid processes situated much lower dorsoventrally than the basal tubera.

Scutarx deltatylus differs from aetosaurians such as *Stagonolepis robertsoni* (MCZD 2) and *Aetosauroides scagliai* (PVSJ 326) in that there is a broad contact between the basal tubera

PeerJ Preprints | https://doi.org/10.7287/peerj.preprints.1924v1 | CC-BY 4.0 Open Access | rec: 3 Apr 2016, publ: 3 Apr 2016

519 and the basipterygoid processes and that the basipterygoid processes are not elongate (Figure
520 10). This is nearly identical to the condition in *Desmatosuchus smalli* (TTU P-9023) and
521 *Desmatosuchus spurensis* (UMMP 7476; Case 1922). There are two basicrania (UCMP 27414,
522 UCMP 27419) from the *Placerias* Quarry with widely separated (anteroposteriorly) basal tubera
523 and (elongate) basipterygoid processes that apparently do not pertain to either *Desmatosuchus* or
524 *Scutarx deltatylus*, and may belong to *Calyptosuchus wellesi*. This would demonstrate a potential
525 important braincase difference between *Calyptosuchus wellesi* and *Scutarx deltatylus*, despite the
526 nearly identical structure of the osteoderms shared between these two taxa.
527 In the anteroposteriorly short area between the basal tubera and the basipterygoid
528 processes, a deep, subrounded fossa (Figure 10) represents the basisphenoid recess (=median
529 pharyngeal recess of Gower and Walker, 2002; =parabasisphenoid recess of Nesbitt, 2011),
530 which is formed by the median pharyngeal system (Witmer 1997). The presence of a 'deep
531 hemispherical fontanelle' (= basisphenoid recess) between the basal tubera and the basipterigoid
532 processes has been proposed as a synapomorphy of *Desmatosuchus* and *Longosuchus* (Parrish
533 1994), but as discussed by Gower and Walker (2002), that condition is present in many
534 archosauriforms. The number of aetosaurian taxa with this feature was expanded by Heckert and
535 Lucas (1999), who also reported that a 'hemispherical fontanelle' is absent in *Typothorax* and
536 *Aetosaurus*. Unfortunately they did not list catalog numbers for examined specimens, and
537 scoring of character occurrences cannot be replicated. The basisphenoid recess is actually present
538 in *Aetosaurus* (Schoch 2007) and *Typothorax* (TTU P-9214; Martz 2002). Thus, the presence of
539 that recess is an aetosaurian synapomorphy.
540 Small (2002) found the shape and size of the basisphenoid recess to be variable in his
541 hypodigm of *Desmatosuchus haplocerus*, and recommended that the character be dropped from

PeerJ Preprints | https://doi.org/10.7287/peerj.preprints.1924v1 | CC-BY 4.0 Open Access | rec: 3 Apr 2016, publ: 3 Apr 2016

phylogenetic analysis pending further review. However, rather than utilizing the presence or absence of the structure, it has been proposed that the shape and depth may be of phylogenetic significance (Gower & Walker 2002). As noted above, it appears that there are two types of aetosaurian basicrania, those with anteroposteriorly short parabasisphenoids and those with long parabasisphenoids. These differences were used as rationale for splitting *Desmatosuchus haplocerus* into two species (Parker 2005b). Among taxa with short parabasisphenoids, *Scutarx deltatylus* (PEFO 34616) and *Desmatosuchus spurensis* (UMMP 7476) have deep, more or less round basisphenoid recesses, and *Desmatosuchus smalli* has a shallow subtriangular recess. In *Longosuchus meadei* (TMM 31185-98) the recess is round and shallow. Among taxa with elongate basisphenoids, *Aetosauroides scagliai* (PVSJ 326) has a shallow, round recess and *Tecovasuchus chatterjeei* (TTU P-545) has a deep, round recess. However, in *Coahomasuchus kahleorum* (NMMNH P-18496; TMM 31100-437), which has an elongate basisphenoid, the recess has the form of a moderately deep, anteroposteriorly elongate oval (Desojo & Heckert 2004; pers. obs. of TMM 31100-437). Thus, the shape of this structure is highly variable and most likely not phylogenetically informative, although the elongate form of the recess in *C. kahleorum* may prove autapomorphic.

Anterior to the basisphenoid recess and between the bases of the basipterygoid processes there is another shallow, anteroventrally opening recess (Figure 10). This recess is at the base of the parasphenoid process, in the same position as the subsellar recess in theropod dinosaurs (Rauhut 2004; Witmer 1997) and may be homologous to the latter. However, the function and origin of the recess are not understood (Witmer 1997).

Dorsal to the basipterygoid processes, two crescentic and dorsally expanding clinoid processes flank the circular, concave hypophyseal fossa, which housed the pituitary gland

PeerJ Preprints | https://doi.org/10.7287/peerj.preprints.1924v1 | CC-BY 4.0 Open Access | rec: 3 Apr 2016, publ: 3 Apr 2016

(Figure 9). No openings are visible because of poor preservation, but the dorsum sellae should be pierced by two canals for the abducens (VI) nerves (Gower & Walker 2002; Hopson 1979). At the base of the hypophyseal fossa in *Stagonolepis robertsoni* (MCZD 2) and *Longosuchus meadei* (TMM 31185-98) there is a triangular flange of bone termed the parabasisphenoid prow (Gower & Walker 2002). This structure is mostly eroded in PEFO 34616, although its base is preserved as a small dorsal protuberance.

Anterior to this, the cultriform process of the parasphenoid is completely preserved (Figures 9-10). This structure is delicate and usually missing or obscured in the few known aetosaur skulls, making comparisons difficult. However, the process is notably short in PEFO 34616, barely extending past the anterior margins of the orbits (Figure 9). In PEFO 34616 the basisphenoid has a length of 34.2 mm, whereas the cultriform process measures 20.2 mm in length (cultriform process/basisphenoid ratio = 0.59). This is noticeably different from the parabasisphenoid in *Aetosauroides scagliai* (PVSJ 326) which has a basisphenoid length of 51 mm and a cultriform process length of at least 63 mm, although the anterior end of the process is concealed (ratio = 1.23) beneath the left pterygoid. The cultriform process is also preserved in *Desmatosuchus spurensis* (UMMP 7476), which has a relatively short parabasisphenoid and a cultriform process/basisphenoid ratio of 0.96.

The cultriform process is elongate and tapers anteriorly. It is Y-shaped in cross-section with a ventral ridge, and dorsal trough for the ethmoid cartilage. Its posterolateral margins bear distinct oval recesses bound posterodorsally by strong ridges that are confluent with the posterodorsal edge of the process (Figures 9-10). Thus the process is broader posteriorly, with these recesses contributing greatly to the thinning of the element anteriorly. The parasphenoid

PeerJ Preprints | https://doi.org/10.7287/peerj.preprints.1924v1 | CC-BY 4.0 Open Access | rec: 3 Apr 2016, publ: 3 Apr 2016

recesses appear to be unique to PEFO 34616, although the general lack of known aetosaurian cultriform processes makes it difficult to determine this with certainty.

Postcranial skeleton

Vertebrae

Cervical Series

Axis/Atlas

The axis and atlas are not preserved in any presently known specimens of *Scutarx deltatylus*.

Post-axial Cervicals

Two articulated cervical vertebrae are preserved in PEFO 31217 (Figure 11). Although both are crushed mediolaterally, they are nearly complete and preserve many details. The centra are taller than long (Figure 11a) suggesting they represent part of the anterior (post-axial) series (i.e., positions 3-6). Most notably, the difference in dimensions is not as pronounced as in *Typothorax coccinarum* and *Neoaetosauroides engaeus*, in which the centra are greatly reduced in length (Desojo & Báez 2005; Long & Murry 1995). The centrum faces are subcircular in anterior and posterior views and slightly concave, with slightly flared rims (Figures 11b-c). The ventral surface of each centrum consists of two concave, ventromedially inclined, rectangular surfaces divided by a sharp and deep mid-line keel (Figure 11d).

The short parapophyses are oval in cross-section and situated at the anteroventral corners of the centrum. The parapophyses are directed posteriorly, and each forms the beginning of a prominent ridge that continues posteriorly to the posterior margin of the centrum. The lateral faces of the centra are concave mediolaterally and dorsoventrally forming discrete, but shallow, lateral fossae that contact the neural arch dorsally (Figure 11a). However, PEFO 31217 lacks the

PeerJ Preprints | https://doi.org/10.7287/peerj.preprints.1924v1 | CC-BY 4.0 Open Access | rec: 3 Apr 2016, publ: 3 Apr 2016

deep lateral fossae, which are considered an autapomorphy of *Aetosauroides scagliai* (Desojo & Ezcurra 2011). The neurocentral sutures are not apparent on this specimen, suggesting closure of the sutures and that this individual is osteologically 'mature' although this cannot be completely confirmed without histological sectioning of the sutural contact (Brochu 1996; Irmis 2007).

The diapophyses are centrally located at the base of the neural arch (Figure 11b). The best preserved vertebra shows that they are slightly elongate, oval in cross-section, and curved ventrolaterally. Because none of the diapophyses appears to be complete their exact length cannot be determined. The neural canal is round in posterior view (Figure 11c) rather than rectangular as in *Desmatosuchus spurensis* (UMMP 7504). The entire neural arch is taller than the corresponding centrum face. The zygapophyses are well-formed, elongate, and oriented at approximately 45 degrees from the horizontal.

Aetosaurian vertebrae bear several vertebral laminae and associated fossae. The terminology for these structures follows Wilson (1999) and Wilson et al. (2011). There is a weakly developed posterior centrodiapophyseal lamina (pcdl) that originates at the posteroventral corner of the diapophysis and continues posteroventrally to the posterior edge of the neurocentral suture. The only other apparent vertebral laminae are paired intrapostzygapophyseal laminae (tpol) that originate on the posteroventral surface of the postzygapophyses and form two sharp ridges (laminae) that meet at the dorsomedial margin of the neural canal (Figure 11b). Those laminae delineate the medial margins of a pair of distinct subzygapophyseal fossae, called the postzygapophyseal centrodiapophyseal fossae (pocdf), as well as a sizeable intrazygapophyseal fossa, called the spinopostzygapophseal fossa (spof). This represents the first recognition of distinct intrapostzygapophyseal laminae in an aetosaurian. *Desmatosuchus spurensis* (MNA V9300) has struts of bone from the dorsomedial margins of the

PeerJ Preprints | https://doi.org/10.7287/peerj.preprints.1924v1 | CC-BY 4.0 Open Access | rec: 3 Apr 2016, publ: 3 Apr 2016

postzygapophyses that join medially and then extend ventrally as a single thickened unit to form a Y-shaped hyposphene (Parker 2008a: fig. 10a), similar to the pattern formed by the intrapostzygapophyseal laminae in *Scutarx deltatylus*. Thus, it is possible that the structure of the hyposphene in aetosaurians is homologous (i.e., the hyposphene is actually formed by paired vertebral laminae) with the presence of paired (but not joined) intrapostzygapophyseal laminae, but this interpretation requires further investigation.

The neural spines are not complete; however, the base of the one on the second preserved vertebra shows that the spine was anteroposteriorly elongate, with prominent spinopostzygapophyseal laminae (spol) that are confluent with the dorsal surfaces of the postzygapophyses (Figure 11b). Spinopostzygapophyseal laminae are also present on the cervical vertebrae of *Desmatosuchus spurensis* (Parker 2008a).

Trunk Series

Mid-trunk vertebrae

Four mid-trunk vertebrae are preserved in PEFO 34045. In aetosaurs the cervical to trunk transition occurs when the parapophysis fully migrates from the base of the neural arch, laterally onto the ventral surface of the transverse process (Case 1922; Parker 2008a). PEFO 34045/FF-51 is well preserved, missing only the postzygapophyses (Figures 12a-c). The articular faces of the centra are round and slightly concave with broad flaring rims. The centrum is longer (45.78 mm) than tall (41.81 mm), its lateral faces are deeply concave, and its ventral surface is narrow and smooth. The neural canal is large and in anterior view, the margins of the neural arch lateral to the canal are mediolaterally thin with sharp anterior edges.

The prezygapophyses are inclined at about 45 degrees from the horizontal and are confluent laterally with a short horizontally oriented prezygadiapophyseal lamina (prdl) that

PeerJ Preprints | https://doi.org/10.7287/peerj.preprints.1924v1 | CC-BY 4.0 Open Access | rec: 3 Apr 2016, publ: 3 Apr 2016

terminates laterally at the parapophysis (Figure 12b). Between the prezygapophyses and ventral to the base of the neural spine there is a well-developed broad, sub-triangular spinoprezygapophyseal fossa (sprf). In combination with the flat prezygapophyses this creates a broad shelf for reception of the posterior portion of the neural arch of the preceding vertebra (Figure 12b). There is a horizontal, ventral bar that roofs the opening of the neural canal between the ventromedial edges of the prezygapophyses (Figure 12d); thus, there is no developed hypantrum as in *Desmatosuchus spurensis* or *Aetobarbakinoides brasiliensis* (Desojo, Ezcurra & Kischlat 2012; Parker 2008a). The ventral bar also occurs in *Stagonolepis robertsoni* (Walker 1961: fig 7j). Ventrolateral to the prezygapophysis there is a deep fossa termed the centroprezygapophyseal fossa (cprf), which is bordered posteriorly by the main strut of the transverse process (Figure 12b). Although the positions of these fossae are homologous with those of saurischian dinosaurs because they share distinct topological landmarks, it is not clear if these features are similarly related to the respiratory system (Butler, Barrett & Gower 2012; Wilson et al. 2011).

In posterior view, the postzygapophyses (best preserved in PEFO 34045/14-R) are also oriented about 45 degrees above the horizontal. They are triangular in posterior view with a well-developed lateral postzygodiapophyseal lamina (podl). That lamina extends laterally to the diapophysis and forms a broad dorsal shelf of the transverse process in dorsal view (Figure 12a). The shelf is wider proximally and significantly narrows distally along the transverse process. Along the dorsal surface of the shelf, between the postzygapophyses and the neural spine is a pair of shallow postzygapophyseal spinodiapophyseal fossae (posdf).

The neural spine is short (32.3 mm) relative to the centrum height as in *Desmatosuchus spurensis* (MNA V9300) and *Typothorax coccinarum* (TTU P-9214). The spine is

PeerJ Preprints | https://doi.org/10.7287/peerj.preprints.1924v1 | CC-BY 4.0 Open Access | rec: 3 Apr 2016, publ: 3 Apr 2016

anteroposteriorly elongate, equal in length to the proximal portion of the neural arch, and the distal end is mediolaterally expanded (spine table). The anterior and posterior margins of the neural spine possess paired vertical spinoprezygapophyseal (sprl) and spinopostzygapophyseal (spol) laminae as in *Desmatosuchus spurensis* (MNA V9300).

The postzygapophyses bound deep oval spinopostzygapophyseal fossa (spof). This fossa is much taller than wide and is bounded laterally by thin, nearly vertical intrapostzygapophyseal laminae (tpol). These laminae meet medially at a thickened triangular area dorsal to the neural canal. Here the vertebra bears a strong posteriorly pointed projection that inserts into the ventral portion of the spinoprezygapophyseal fossa just above the ventral bar. That projection is also present in *Calyptosuchus wellesi* (e.g., UCMP 139795). Ventrolateral to the postzygapophyses there are two deep centropostzygapophyseal fossae (cpof) in the proximal portions of the transverse processes.

The transverse processes extend laterally with a length of 81.6 mm in PEFO 34045/FF-51. However, in two of the other vertebrae (PEFO 34045/14-R; PEFO 34045/19-V) the transverse processes are directed more dorsolaterally (Figures 12d-e). This difference also occurs in *Stagonolepis robertsoni* (Walker 1961) and occurs in the more anteriorly positioned trunk vertebrae. Furthermore, the ventral surface of the centrum in these two vertebra (PEFO 34045/14-R; 19-V) is more constricted forming a blunt ventral ’keel‘. The keel and the orientation of the transverse process are the only visible differences between and anterior and mid-trunk vertebrae in *Scutarx deltatylus*.

Posterior trunk vertebrae

The currently available material of *Scutarx deltatylus* includes seven posterior trunk vertebrae; three from PEFO 34045, three from PEFO 31217, and one from PEFO 34919. As in

PeerJ Preprints | https://doi.org/10.7287/peerj.preprints.1924v1 | CC-BY 4.0 Open Access | rec: 3 Apr 2016, publ: 3 Apr 2016

Desmatosuchus spurensis (MNA V9300; Parker 2008a), the posterior trunk vertebrae are much more robust than the anterior and mid-trunk vertebrae (Figures 12g-h; 13a-c). Notable differences between the mid- and posterior trunk vertebrae in *Scutarx deltatylus* include an increase in the height of the neural spines and a lengthening of the transverse processes, which coincide with the loss of distinct parapophyses and diapophyses along the series. Furthermore, the centra become anteroposteriorly shorter than they are dorsoventrally tall (Figure 12h). The neural spine characteristics are identical to those of the mid-trunk vertebrae with regard to the presence of the various vertebral laminae and associated fossae. An isolated posterior trunk vertebra from PEFO 31217 (Figure 13c) shows that the prezygodiapophyseal laminae are even more strongly developed and extend farther laterally than in the more anterior trunk vertebrae. In the more posterior vertebra, the length ratio between the transverse process length (86.84 mm) and centrum width (53.26 mm) equals 1.63, thus the process is more than 1.5 times the width of the centrum. This is comparable to a ratio of 1.58 for the mid-trunk vertebrae.

This same vertebra from PEFO 31217 also lacks distinct diapophyses and parapophyses and a single-headed rib is fused onto the distal end of the process (Figure 13c). This is also seen in *Desmatosuchus spurensis* (Parker 2008a), *Stagonolepis robertsoni* (Walker 1961), and *Calyptosuchus wellesi* (UMMP 13950). An isolated posterior trunk vertebra from PEFO 34045 (Figures 13a-b) preserves the entire transverse processes and the associated fused ribs. However, the specimen differs from the previously described vertebra from PEFO 31217 in that the parapophysis and diapophysis are distinct and the rib is double-headed (Figures 13a-b). Although the ribs and transverse processes are fused, the fusion is incomplete; gaps are present within the individual articulations and a gap is apparent between the anterior surface of the distal end of the transverse process and the medial surface of the capitulum of the rib (Figure 13b). This suggests

PeerJ Preprints | https://doi.org/10.7287/peerj.preprints.1924v1 | CC-BY 4.0 Open Access | rec: 3 Apr 2016, publ: 3 Apr 2016

that several vertebrae in the posterior trunk series fuse with the ribs, and loss of a distinct parapophysis and diapophysis of the transverse process and of the tuberculum and capitulum of the dorsal ribs only occurred in the last one or two presacrals. Examination of UMMP 13950 (Case 1932; Long & Murry 1995) suggests that this loss occurs in the last three presacrals. In *Stagonolepis robertsoni* that condition occurs in the final two presacral vertebrae (Walker 1961). There is no evidence in *Scutarx deltatylus* that the last presacral was incorporated into the sacrum as in *Desmatosuchus spurensis* (Parker 2008a). The last presacral in PEFO 31217 also shows a distinct vertical offset in the ventral margins of the articular faces of the centra with the anterior face situated more ventrally. This is also the case in *Stagonolepis robertsoni* (Walker 1961) and *Desmatosuchus spurensis* (Parker 2008a).

Another posterior trunk vertebra, PEFO 34045/22 (Figures 12g-h), lacks the transverse processes, but preserves other key characteristics of the posterior presacrals. Its neural spine is taller (81.94 mm) than the height of the centrum (61.24 mm), differing from the condition in the anterior and mid-trunk vertebrae where the neural spine is shorter than the centrum (Figure 12g). This transition occurs at the beginning of the posterior trunk vertebrae series, because the specimen from PEFO 34045 with the fused ribs, but distinct rib facets (Figures 13a-b), has a centrum and neural spine of equal height. PEFO 34045/22 also preserves the pointed posterior projection above the neural arch that is present throughout the trunk series (Figure 12h).

Sacral vertebrae

A sacral vertebra, probably the second, is visible in ventral view in PEFO 31217 in articulation with the rest of the pelvis (Figure 14). It is recognizable by the presence of a strong, broad sacral rib that laterally expands anterodorsally to contact the posterodorsal margin of the left ilium. Unfortunately no other details are available for that specimen.

PeerJ Preprints | https://doi.org/10.7287/peerj.preprints.1924v1 | CC-BY 4.0 Open Access | rec: 3 Apr 2016, publ: 3 Apr 2016

748 ***Caudal series.***

749 ***Vertebrae***

750 Eight vertebrae occur in semi-articulation in PEFO 31217 posterior to the sacral vertebra
751 described above (Figure 14). The first two are robust with thick flaring rims on the centra. The
752 first vertebra has a length of 57.3 mm, and its anterior face is indistinguishable from the posterior
753 face of the preceding sacral vertebra. Furthermore, the centrum is constricted which is unusual
754 for an aetosaur, because the sacrals and anterior caudals usually have wide ventral surfaces (e.g.,
755 *Desmatosuchus spurensis*, MNA V9300). The vertebra in PEFO 31217 lacks a ventral groove
756 and chevron facets. It is possible that this is a sacral vertebra that has been forced backwards, but
757 the poor preservation of the specimen does not allow a firm determination. The second caudal
758 vertebra (assuming the first described is from the caudal series) has a centrum length of 52.2 mm
759 and a width of 61.6 mm, thus it is wider than long as is typical for the anterior caudals of
760 aetosaurians (Long & Murry 1995). The centrum is ventrally broad and a chevron is articulated
761 to the posterior margin. The base of the caudal rib originates from the base of the neural arch, but
762 laterally the rib is incomplete.

763 Two anterior caudal vertebrae are also known from PEFO 34045, which roughly
764 correspond in morphology to the second and third caudal centra of PEFO 31217 (Figures 15a-f).
765 These two vertebrae have blocky centra that are wider (flared centrum faces) than long. The
766 ventral surfaces are broad, with a deep median trough bordered by two lateral ridges. These
767 ridges terminate posteriorly into two posteroventrally facing hemispherical chevron facets
768 (Figures 15d-e). The articular faces of the centra are round in anterior and posterior views, and in
769 lateral view these faces are offset from each other (Figure 15f). The ventral margin of the
770 posterior face is situated much farther ventrally than that of the anterior face, as is typical for
771 aetosaurs (e.g., *Desmatosuchus spurensis*, MNA V9300). Although the neural spines are

PeerJ Preprints | https://doi.org/10.7287/peerj.preprints.1924v1 | CC-BY 4.0 Open Access | rec: 3 Apr 2016, publ: 3 Apr 2016

missing, it is apparent that the neural arch complex was much taller than the height of the centrum (Figure 15c). The neural canal is oval with a taller dorsoventral axis.

The pre- and postzygapophyseal stalks are thickened and the facets are closely situated medially. They are oriented at about 30 degrees from the horizontal. The neural arch is directed posterodorsally and the postzygapophyses project posteriorly significantly beyond the posterior centrum face (Figure 15c). The caudal vertebrae lack diapophyseal and zygapophyseal laminae, but spinozygapophyseal fossae occur between the prezygapophyses (Figures 15a-b). The caudal ribs are fully fused to the centrum. They are anteroposteriorly broad and dorsoventrally thin with flat dorsal surfaces and buttressed ventral margins. The ribs are directed slightly posteriorly and laterally they arc ventrally (Figures 15a-c). Unfortunately their lateral extent is unknown.

The third and fourth caudal vertebrae in PEFO 31217 are longer than wide, with the centrum narrowing mediolaterally and with reduced flaring of the rims as in the previous vertebrae (Figure 14). The posteroventral margins possess chevron facets. The caudal ribs are broad, flat, and were elongate, as in *Desmatosuchus spurensis* (MNA V9300), even though the distal ends are not preserved. The third centrum has a length of 56.4 mm and the fourth has a length of 56.4 mm. Details of the neural arches and spines are buried in the block and irretrievable by mechanical preparation.

The fifth and sixth caudal vertebrae are mostly concealed beneath armor, bone fragments, and what are probably the eighth and ninth caudal vertebrae. Only the left caudal ribs are apparent, jutting out of the block. They are dorsoventrally flat and laterally elongate, typical for aetosaurs, but they are poorly preserved and no other details are apparent.

The anterior face of what is probably the seventh caudal vertebra is visible underneath matrix and an osteoderm about six centimeters behind where the sixth caudal vertebra is buried

PeerJ Preprints | https://doi.org/10.7287/peerj.preprints.1924v1 | CC-BY 4.0 Open Access | rec: 3 Apr 2016, publ: 3 Apr 2016

795 in the block, breaking the line of articulation. The neural canal is prominent on this vertebra and
796 what is visible of the neural arch shows that it was tall. The centrum is amphicoelous and
797 mediolaterally constricted. The ventral surface consists of a median ventral groove bounded
798 laterally by two sharp ridges. The ridges would terminate posteriorly with the chevron facets,
799 but the relevant area is obliterated. A vertebra from approximately the same position is
800 preserved in PEFO 34919 (Figures 16a-c) and provides more details.

801 The centrum is much longer than wide (57 mm to ~30 mm), mediolaterally compressed,
802 and grooved ventrally. Its rims flare minimally, but the articular faces are deeply concave (Figure
803 16b-c). The neural arch is dorsoventrally shorter than in the more anteriorly positioned caudal
804 vertebrae, but the neural spine was certainly tall in this position as well (Figure 16b). The
805 zygapophyses are reduced and each pair is closely situated medially. The postzygapophyses do
806 not project far posteriorly. The caudal rib is situated anteroventrally on the neural arch. It is
807 broad and flat, extends laterally (~50 mm), and is slightly arcuate in anterior view (Figure 16b).

808 What are probably the eighth and ninth caudal vertebrae are well-preserved at the edge of
809 the block in PEFO 31217 (Figure 14). The centra are much longer than wide. The ninth centrum
810 has a length of 66.3 mm and a width of 40.2 mm. The lateral faces of the centrum are concave
811 and, as on the preceding centra, the ventral face is narrow with a deep median groove terminating
812 at the chevron facets. The neural arches and spines are complete and tall, with a height of 100.9
813 mm in the eighth vertebra and 98.4 mm in the ninth. The neural spines are tall and roughly
814 triangular in lateral view, with an anteroposteriorly broad base and tapering distally. The
815 zygapophyses are closely situated medially and extend anteriorly and posteriorly beyond the
816 articular faces of the centra. The caudal ribs are greatly reduced in lateral length.

PeerJ Preprints | https://doi.org/10.7287/peerj.preprints.1924v1 | CC-BY 4.0 Open Access | rec: 3 Apr 2016, publ: 3 Apr 2016

An isolated vertebra from PEFO 34045 represents the mid-caudal series (Figure 16d). The centrum is longer than tall (65 mm to 35 mm) and mediolaterally compressed. Its articular faces are deeply concave and oval with the longest axis situated dorsoventrally. The neural arch is dorsolaterally reduced and mediolaterally compressed. The caudal ribs are greatly reduced and eroded. The neural spine is elongate, but its full dorsal extent is unknown (Figure 16d).

Chevrons

Only half of a single chevron and part of the head of a second are preserved in PEFO 34045 (Figures 17a-b). A few are smashed beneath other elements in PEFO 34919 and a badly preserved chevron is present beneath the second caudal vertebra of PEFO 31217. Although the details are poor the latter suggests, in accordance with the lack of facets on the first caudal vertebra of PEFO 31217, that chevrons started on the second centrum. This is different from the condition in *Desmatosuchus spurensis*, in which they first appear on the third caudal centrum (Parker 2008a), but similar to the condition in *Typothorax coccinarum* (Heckert et al. 2010). The two preserved chevrons in PEFO 34045 are of the 'slim' elongate type and, therefore, from the anterior portion of the tail (Parker 2008a).

Ribs

Presacral

No cervical ribs are preserved in any of the specimens, but trunk ribs are common. The sacral and caudal ribs have been described above along with their associated vertebrae. The anterior and mid-trunk ribs are double-headed (Figure 17c-d). They extend laterally for the first quarter of their total length and then sharply turn ventrolaterally, are straight for another two quarters of the length, and then gently turn more ventrally. Proximally the rib body is oval in

PeerJ Preprints | https://doi.org/10.7287/peerj.preprints.1924v1 | CC-BY 4.0 Open Access | rec: 3 Apr 2016, publ: 3 Apr 2016

cross-section, becoming ovate and then flattened more distally; it is broadest at the point of the sharp ventrolateral turn.

The capitulum is oval in cross-section, with a sharp posterior projection. The capitulum and tuberculum are separated along the neck by 44 mm. The dorsal surface of the neck is marked by a transverse groove that terminates at a fossa on the proximal surface of the tuberculum (Figure 17e). That groove probably hosted the ventral portion of the vertebrarterial canal as in *Alligator* (Reese 1915). A thin flange of bone originates on the dorsal surface of the tuberculum and extends laterally, becoming confluent with the rib body just lateral to the ventrolateral hook. That flange forms a deep, elongate groove along the posterodorsal surface of the rib. Dorsally the rib is flattened and forms a thin anterior blade.The posteriormost ribs are single headed and fused with the transverse processes of the trunk vertebrae (Figure 13c).

Gastralia

It has been suggested that aetosaurians lack gastralia (Nesbitt 2011), but they are present in *Typothorax coccinarum* (Heckert et al. 2010). In that taxon (e.g., NMMNH P-56299), the gastralia are preserved in the posteroventral portion of the thoracic region, are medially fused and laterally elongate. A single gastralia set is preserved in PEFO 34616 demonstrating that they were present in *Scutarx deltatylus* as well (Figure 17f). This set consists of incomplete but medially fused ribs with a short anterior projection.

Appendicular Girdles

Scapulocoracoid

The left scapulocoracoid is preserved in PEFO 31217; unfortunately the coracoid is covered by osteoderms that cannot be removed without causing significant damage, so only the dorsal-most portion of the coracoid where it sutures to the scapula, is visible. In lateral view the

PeerJ Preprints | https://doi.org/10.7287/peerj.preprints.1924v1 | CC-BY 4.0 Open Access | rec: 3 Apr 2016, publ: 3 Apr 2016

general outline of the scapula of PEFO 31217 (Figure 18a) strongly resembles the scapulocoracoid of *Stagonolepis robertsoni* (Walker 1961: fig. 12a). The proximal end is expanded anterolaterally with the posterior projection situated more dorsally than the anterior projection. The posterior projection has a rounded posterior margin, as in *Stagonolepis robertsoni* (Walker 1961) differing from the pointed projection in *Stagonolepis olenkae* (ZPAL AbIII/694). The anterior projection is poorly preserved but appears to be pointed as in *Stagonolepis robertsoni* (Walker 1961). The scapular blade is gently bowed medially and the posterior edge is straight except for a slight posterior projection (the triceps tubercle) about 62 mm above the glenoid lip (Figure 18a). The anterior edge of the blade is straight for most of its length until it strongly flares anteriorly, forming a prominent deltoid ridge (=acromion process; Brochu 1992; Martz 2002). Below this there is a prominent foramen, although its anterior edge is broken away. Likewise the ventral margin of the posterior edge of the scapular blade strongly flares posteriorly forming the supraglenoid buttress. The glenoid facet opens posteriorly. Laterally there is a sharp ridge, which probably represents deformation and crushing along the scapulocoracoid suture.

Ilium

Ilia are preserved in PEFO 34919 (right ilium) and PEFO 31217 (both ilia). The ilia of *Scutarx deltatylus* were oriented in life so that the acetabula faced ventrally; however, to avoid confusion in this description, the anatomical directions will be provided as if the reader is viewing the ventral surface laterally (see Figure 18b-c). The right ilium of PEFO 34919 is nearly complete, missing only a portion of the anterior margin of the acetabulum (Figures 18b-c). As usual for the bones from this specimen, the ilium is covered with a thin layer of weathered hematite that cannot be removed without damaging the underlying bone. The iliac blade is complete with a

PeerJ Preprints | https://doi.org/10.7287/peerj.preprints.1924v1 | CC-BY 4.0 Open Access | rec: 3 Apr 2016, publ: 3 Apr 2016

length of 196 mm and a mid-height of 66.8 mm. The 'dorsal' margin of the iliac blade is mediolaterally narrow, expanding anteriorly so that the dorsal margin of the anterior process is thicker and more robust than the rest of the blade. The anterior portion of the iliac blade is triangular in lateral view, and does not extend anteriorly beyond the edge of the pubic peduncle. There is a prominent recess on the dorsal surface between the supraacetabular crest and the posterior iliac blade (Figure 18b) that appears to be unique to *Stagonolepis deltatylus*.

The posterior portion of the iliac blade quickly narrows in its dorsoventral height posteriorly, terminating in a point. From there the posteroventral margin slopes anteroventrally into a curving posterior margin that distally hooks posteriorly and thickens to form the ischiadic peduncle. The posterior projection of the ischiadic peduncle is proportionally larger and more pointed than the same structure in *Aetosauroides scagliai* (PVL 2073) and *Stagonolepis robertsoni* (NHMUK R4789a), and more like that of TMM 31100-1, which represents a desmatosuchine aetosaurine. The ventral margins of the pubic and ischiadic peduncles meet at an angle of 90 degrees ventral to the acetabulum, with the ilium contributing to the majority of the acetabulum. In ventral view the margins of the peduncles are comma-shaped, thinning into the ventral margin of the broadly concave acetabulum. The medial side of the acetabulum is smooth and slightly convex.

Dorsal to the iliac neck, the medial side of the posterior portion of the iliac blade bears a prominent ventral ridge that forms a shelf for sacral rib articulation (Figure 18c). The rib scar is situated just above the ridge and forms a concave sulcus that extends anteriorly to just dorsal to the anterior margin of the neck.

Both ilia are present in PEFO 31217 as portions of a complete sacrum. Of the two the left is the better preserved. The acetabula are deeply concave and oriented ventrally (Figure 14).

PeerJ Preprints | https://doi.org/10.7287/peerj.preprints.1924v1 | CC-BY 4.0 Open Access | rec: 3 Apr 2016, publ: 3 Apr 2016

908 Originally this was thought to be the result of crushing of the pelvis; however, the acetabula are
909 oriented ventrally in many other uncrushed aetosaurian specimens including *Aetosauroides*
910 *scagliai* (PVL 2073) and the holotype of *Typothorax antiquus* (Lucas, Heckert & Hunt 2003).
911 The supraacetabular ridge in these ilia is strongly produced, but not as strong as in rauisuchids.
912 As in PEFO 34919 there is a deep fossa/recess on the dorsal surface between the supraacetabular
913 ridge and the posterior portion of the iliac blade, a condition that appears to be autapomorphic
914 for this taxon. That fossa is bordered posteroventrally by the thickened margin of the neck, a
915 feature which is ventrally confluent with the ischiadic peduncle. The left iliac blade measures
916 188.6 mm in length and 67.4 mm in height, producing a relatively tall iliac blade. The posterior
917 portion of the iliac blade has a posterior margin that projects well beyond the iliac peduncle. The
918 extent of the ventral portions of the ilia is hard to determine because they are indistinguishably
919 fused to the ischia and pubes; however, the left acetabulum is more or less rounded, 116.5 mm
920 tall and 111 mm wide.

921 ***Ischium***
922 The left ischium and part of the right are present, but poorly preserved. The ischium
923 consists of the main body with a sharp, rounded acetabular rim, and an elongate posterior
924 process. The upper margin of the posterior process slopes gradually from the posterior margin of
925 the ischiadic peduncle, and the entire ischium measures 183 mm in length. The anteroventral
926 margin is flat where the two ischia are fused, forming a wide, slightly concave ventral shelf.
927 Overall the ischium is similar to that of other aetosaurians such as *Stagonolepis robertsoni*
928 (Walker 1961), but lacks the prominent ventral kink found in *Desmatosuchus spurensis* (MNA
929 V9300; Parker 2008a).

PeerJ Preprints | https://doi.org/10.7287/peerj.preprints.1924v1 | CC-BY 4.0 Open Access | rec: 3 Apr 2016, publ: 3 Apr 2016

Pubis

Both pubes are present and in articulation with the pelvis although they are moderately distorted by crushing and were damaged by weathering before collection. The body of the pubis consists of an elongate, narrow 'tube' that curves anteroventrally and expands medially into two broad sheets of bone that meet in a median symphysis. This pubic apron is convex anteriorly and concave posteriorly. It is dorsoventrally short, barely extending past the ventral margin of the puboischiadic plate, more like the condition in *Typothorax coccinarum* (Long & Murry 1995) rather than the extremely deep pubic apron found in *Desmatosuchus spurensis* (MNA V9300). Two distinct oval foramina pierce the pubic apron in the proximal part of the element. The bone is broken around the more anterior foramen of the right pubis, but it is clear that it was the larger of the two openings (Figure 14). Two pubic foramina are also described for *Stagonolepis robertsoni* (Walker 1961), and the upper (anterior) opening considered homologous to the single foramen found in other aetosaurs (e.g., MNA V9300, *Desmatosuchus spurensis*). The distal ends of the pubes are shaped like elongate commata, narrow and curving into the symphysis (Figure 14), different from the strong, knob-like projections (pubic boots) found in *Desmatosuchus spurensis* (MNA V9300).

Osteoderms

Paramedian osteoderms

Cervical

Cervical osteoderms are present in PEFO 31217, PEFO 34045, and PEFO 34616. All of the osteoderms are wider than long (w/l ratio of 1.85). The cervical osteoderms are dorsoventrally thick with well-developed anterior bars (sensu Long and Ballew, 1985), which bear prominent anteromedial projections. The lateral edges are strongly sigmoidal, and lack anterolateral projections (Figures 19a, c; 20a).

PeerJ Preprints | https://doi.org/10.7287/peerj.preprints.1924v1 | CC-BY 4.0 Open Access | rec: 3 Apr 2016, publ: 3 Apr 2016

954 The dorsal surface is relatively featureless, with the ornamentation poorly developed. The
955 dorsal eminence is low, broad, and mounded, contacting the posterior plate margin (Figures 19a,
956 c). The eminence is also offset medially, closer to the midline margin. The characteristic
957 triangular protuberance that diagnoses *Scutarx deltatylus* is present in the posteromedial corner
958 of the osteoderm, but is greatly reduced in area (Figure 19c). In the cervical paramedian
959 osteoderms the shape of that protuberance is more of a right triangle than the equilateral triangles
960 found in the trunk series (see below).
961 In posterior view, the osteoderms are gently arched (Figures 19b, d). The median margins
962 are sigmoidal in medial view and dorsoventrally thick as is typical for aetosaurians. *Scutarx*
963 *deltatylus* lacks the 'tongue-and-groove' lateral articular surfaces present in *Desmatosuchus*
964 (e.g., MNA V9300) and *Longosuchus meadei* (TMM 31185-84b).
965 The more posterior cervical paramedian osteoderms are similar, but increase in width
966 (w/l ratio of 2.05) and lack the strongly sigmoidal lateral margin. The margin is still sigmoidal
967 but bears a strong anterolateral projection (Figure 20a). Moreover, the anterior and posterior
968 plate margins are gently curved anterolaterally. In posterior view, these osteoderms have a lesser
969 degree of arching and are dorsoventrally thinner than the more anteriorly situated osteoderms.
970 The dorsal eminence is strongly offset medially and slightly more developed, becoming raised
971 and more pyramidal in shape, although this could be an individual variation (see description of
972 caudal paramedian osteoderms).

973 ***Trunk***

974 The osteoderm transition between the cervical and trunk series is difficult to identify, but
975 anterior dorsal trunk osteoderms are considered here to have higher width/length ratios and be
976 dorsoventrally thinner than the cervical paramedian osteoderms. Furthermore, the triangular
977 protuberance is more equilateral. However, it is difficult to differentiate these osteoderms from
978 those of the anterior caudal region.

PeerJ Preprints | https://doi.org/10.7287/peerj.preprints.1924v1 | CC-BY 4.0 Open Access | rec: 3 Apr 2016, publ: 3 Apr 2016

Osteoderms with the maximum width/length ratio (2.72) are found in the mid-trunk region. They bear a strongly raised anterior bar with prominent anteromedial and anterolateral projections. The dorsal eminence is medially offset, and forms a broad, low mound. Anterior to this on the anterior bar is a prominent, pointed anterior projection. The area of the anterior bar medial to this process is 'scalloped out,'and is deeply concave. The length of the anterior bar decreases significantly within the arc of this concavity. The triangular protuberance is equilateral (Figures 19e-k).

The lateral margin is sigmoidal, and the anterior portion just posterior to the anterior bar is slightly embayed for slight overlap of the associated lateral osteoderm. In posterior view the osteoderm is only slightly arched Figure 19h). In what are presumed to be more posteriorly positioned osteoderms, the osteoderme is more strongly arched (Figures 19l-m). The ventral surface of the dorsal trunk paramedian osteoderms are smooth, with a slight embayment situated on the underside of the dorsal eminence.

The surface ornamentation of the dorsal trunk paramedian osteoderms is barely apparent in PEFO 34045, but much better developed in the other specimens. The ornament consists of pitting surrounding the dorsal eminence and radiating grooves and ridges over the rest of the surface.

There is no direct evidence for a constriction ('waist') in the carapace anterior to the pelvis as in *Aetosaurus ferratus* (Schoch 2007), and *Calyptosuchus wellesi* (Case 1932); however, because the lateral osteoderm shapes in *Scutarx deltatylus* are identical to those of *Calyptosuchus wellesi*, it is probable that *Scutarx deltatylus* also possessed a 'waisted' carapace although this cannot be confirmed.

PeerJ Preprints | https://doi.org/10.7287/peerj.preprints.1924v1 | CC-BY 4.0 Open Access | rec: 3 Apr 2016, publ: 3 Apr 2016

Caudal

Like the cervical-trunk transition, the trunk-caudal transition is also difficult to determine in unarticulated aetosaurian carapaces (Parker 2008a). The latter transition is generally characterized by reduction of osteoderm width-length ratios and greater development of the dorsal eminences. The extreme is found in *Rioarribasuchus chamaensis*, in which the barely visible dorsal eminences in the mid-dorsal region transition posteriorly to elongate, anteromedially curved spines in the anterior caudal region (Parker 2007).

The trunk-caudal transition for *Scutarx deltatylus* is best preserved in PEFO 34919 in which the dorsal eminences show a marked increase in height from 16.35 in the mid-trunkregion to 40.07 mm in the anterior dorsal caudal region. Width/length ratios across this same transition are 2.54 to 2.16, showing the corresponding decrease. The dorsal eminence is a tall pyramid, with a posterior vertical keel (Figure 21). In all other respects the anterior caudal osteoderms are similar to those of the trunk region.

Dorsal mid-caudal paramedians are relatively equal in width and length (w/l ratio = 1.08). Those osteoderms still possess the pronounced dorsal eminence (Figures 22a-j), as well as the anteromedial and anterolateral projections of the anterior bar. In PEFO 34045 these osteoderms are extremely thickened (Figures 22a-b, e-f).

The posterior dorsal caudal paramedians (Figures 22k-n) become longer than wide (w/l ratios of 0.73 and 0.66), and the dorsal eminence is reduced to a raised, anteroposteriorly elongate keel with a posterior projection that extends beyond the posterior margin of the osteoderm. Presumably these continue until they become elongate strips of bone as in *Aetosaurus ferratus* (Schoch 2007).

Lateral osteoderms

The best guide for the distribution of the lateral osteoderms is UMMP 13950, the holotype of *Calyptosuchus wellesi*, which preserves the posterior dorsal armor and much of the

PeerJ Preprints | https://doi.org/10.7287/peerj.preprints.1924v1 | CC-BY 4.0 Open Access | rec: 3 Apr 2016, publ: 3 Apr 2016

caudal lateral armor in articulation (Case 1932). *Scutarx deltatylus* possesses lateral plates that are identical in shape to those of *Calyptosuchus wellesi* allowing for determination of caudal and posterior dorsal osteoderms. Therefore, any lateral osteoderms falling outside of those morphotypes probably are from more anterior regions. Anterior dorsal lateral osteoderms are preserved in the articulated holotype of *Aetosauroides scagliai* (PFV 2073), which can be used to help assign isolated osteoderms.

Lateral osteoderms can be distinguished from paramedian osteoderms primarily by the lack of the prominent anterolateral projection. Furthermore, the anteromedial corner of the osteoderm is 'cut-off' and beveled for reception of the anterolateral projection of the associated adjacent paramedian osteoderm (poa; Figure 23).

Cervical

There are no lateral osteoderms in the material present that can unequivocally be assigned to the cervical region.

Trunk

Anterior lateral trunk osteoderms are not preserved in the holotype of *Calyptosuchus wellesi*, but they are preserved in *Aetosaurus ferratus* (Schoch 2007). In *Aetosaurus* those osteoderms are strongly asymmetrical with the dorsal flanges roughly half the dimensions of the lateral flanges. Furthermore, the dorsal flanges are triangular or trapezoidal in dorsal view rather than rectangular, with a slight, medially projecting posterior tongue.

Two osteoderms from the left side in PEFO 34616 and a third from the right side in PEFO 34045 match this anatomy and are probably from the anterior portion of the carapace (Figures 23a-d). In addition to the features just mentioned, those osteoderms possess a distinct anterior bar. The anteromedial corner of the anterior bar is beveled for articulation with the anterolateral process of the paramedian osteoderm. The dorsal eminence of the lateral osteoderm

PeerJ Preprints | https://doi.org/10.7287/peerj.preprints.1924v1 | CC-BY 4.0 Open Access | rec: 3 Apr 2016, publ: 3 Apr 2016

is a prominent pyramidal boss that contacts the posterior plate margin and extends anteriorly, covering two-thirds of the osteoderm length. Surface ornamentation consists of elongate grooves and ridges radiating from the dorsal eminence. In posterior view, the osteoderms are only slightly angulated, with the angle between flanges strongly obtuse (Figures 23b, d). Similarly shaped osteoderms are found in the anterior lateral trunk region of *Aetosauroides scagliai* (PVL 2073).

Posterior-mid trunk osteoderms (from roughly the ninth through 12th positions) are sub-rectangular with a distinct, posteromedially sloping lateral edge (Figures 23e-h; Case 1932). The dorsal flange is sub-rectangular in dorsal view. The medial edge of the dorsal flange is beveled and slightly sigmoidal with a 'cut-off' anterior corner for the anterolateral projection of the paramedian plate. The osteoderm is moderately flexed with the lateral flange extending at about 45 degrees relative to to the dorsal flange (Figures 23f, h). Both flanges are roughly the same size although the sloping lateral edge produces a small anteromedial 'wing' that extends that edge a bit farther laterally and provides a trapezoidal shape for the lateral flange (alw; Figures 23e, g). The dorsal eminence is pyramidal, and the degree of its development differs between specimens, from a low mound in PEFO 34045 to a distinct tall, triangular boss in PEFO 34919. On the dorsal surface a distinct anterior bar is present and the surface ornamentation consists of small pits and elongate grooves radiating from the dorsal eminence. Ventrally the osteoderms are smooth, except for longitudinal striations along the posterior margin where this margin would overlap the anterior bar of the preceding lateral osteoderm.

The posteriormost lateral trunk osteoderms (15th and 16th positions) are similar to the posterior mid-trunk osteoderms but lack the anterolateral 'wing' and are much more strongly flexed, enclosing an angle of approximately 90 degrees in posterior view (Figures 23i-j). They are similar to the posterior lateral trunk osteoderms in *Calyptosuchus wellesi* (Case 1932).

PeerJ Preprints | https://doi.org/10.7287/peerj.preprints.1924v1 | CC-BY 4.0 Open Access | rec: 3 Apr 2016, publ: 3 Apr 2016

Caudal

Caudal lateral osteoderms are more equal in dimension, and bear rectangular dorsal flanges (Figures 23k-p). The angle enclosed between the dorsal and lateral flanges is about 45-50 degrees (Figures 23l, n, p). Overall these osteoderms possess some of the same surficial features as the other osteoderms, such as an anterior bar, radial ornamention, and a posteriorly placed dorsal eminence. However, the anterior caudal osteoderms in some specimens (e.g., PEFO 34919) possess some of the tallest dorsal eminences in the carapace (Figures 21; 23n). The caudal lateral osteoderms also decrease in width posteriorly (Figure 23m-n). The height of the dorsal eminence is gradually reduced and becomes and elongate sharp ridge.

Ventral trunk osteoderms

Ventral trunk osteoderms are preserved in all of the PEFO specimens, including an articulated, but badly preserved, set in PEFO 31217. They consist mainly of square to rectangular osteoderms, with reduced anterior bars, no dorsal eminence and a surface ornamentation of pits and elongated pits in a radial pattern (Figures 24a-f). Because no complete set is preserved the exact numbers of rows and column cannot be determined.

Appendicular osteoderms

A few irregular, small, rounded osteoderms most likely represent appendicular osteoderms that covered the limbs. There are two types: one featureless except for a distinct raised keel, and the other with a surface ornamentation of radial pits (Figures 24g, i). A triangular osteoderm (Figure 24h) from PEFO 34616 could represent a different type of appendicular osteoderm, or it could also be an irregularly shaped osteoderm from the ventral carapace.

PeerJ Preprints | https://doi.org/10.7287/peerj.preprints.1924v1 | CC-BY 4.0 Open Access | rec: 3 Apr 2016, publ: 3 Apr 2016

Broken osteoderms?

An interesting aspect of PEFO 34045 is the presence of many irregularly shaped osteoderms recovered with the specimen (Figure 25). All of the edges on these osteoderms are compact bone and do not represent recent breaks. Close examination shows that these specimens are the lateral ends of dorsal paramedian osteoderms because they possess anterior bars with strong anterolateral projections and sigmoidal edges (Figures 25a-d). It is unclear why these osteoderms are incomplete but two possibilities exist. The first possibility is that these osteoderms were incompletely ossified. Alternatively, they were broken and then the edges rehealed during the life of the animal. However, there is no visible sign of pathology because the edges are smooth and the dorsoventral thickness of the osteoderms remains constant. The osteoderms are also from opposite sides of the body precluding a cause from a single injury if they are pathologic in nature. Histological examination could help determine the ontogeny of these elements. If growth rings are uniform throughout the specimen, it would demonstrate that either damage occurred at a young age or that the remainder of the element did not ossify. If the osteoderms were broken at a later ontogenetic stage and healed, then that should be reflected in the bone histology showing a disruption in the growth rings, or establishment of new rings along the broken edge.

DISCUSSION

Scutarx deltatylus represents another good example of the importance of utilizing a detailed apomorphy-based approach to differentiate Late Triassic archosauromorph taxa (e.g., Nesbitt, Irmis & Parker 2007; Nesbitt & Stocker 2008; Stocker 2010). The material here referred to *Scutarx deltatylus* was originally assigned to *Calyptosuchus wellesi* (Long & Murry 1995; Martz et al. 2013; Parker & Irmis 2005), which was differentiated from *Stagonolepis robertsoni* by the presence of the triangular protuberance on the paramedian osteoderms (Martz et al. 2013).

PeerJ Preprints | https://doi.org/10.7287/peerj.preprints.1924v1 | CC-BY 4.0 Open Access | rec: 3 Apr 2016, publ: 3 Apr 2016

However, reexamination of the holotype of *Calyptosuchus wellesi* (UMMP 13950) as well as referred material from the *Placerias* Quarry of Arizona shows that material of *Calyptosuchus wellesi* actually lacks the triangular protuberance. Moreover, the skull of *Scutarx deltatylus* possesses characters of the braincase (e.g., foreshortened parabasisphenoid) that are more similar to *Desmatosuchus* than to other aetosaurians that are similar to *Stagonolepis*. Unfortunately, the skull of *Calyptosuchus wellesi* is still mostly unknown. The *Placerias* Quarry contains a number of isolated aetosaurian skull bones, most notably basicrania, with differing anatomical characteristics, but none of these can be referred with certainty to *Calyptosuchus wellesi* (Parker 2014). Nonetheless, prior to the discovery of the skull of *Scutarx deltatylus*, *Calyptosuchus wellesi* was assumed to have a skull more like that of *Stagonolepis robertsoni* and *Aetosauroides scagliai* (i.e., with an elongate parabasisphenoid). That assumption can no longer be maintained. A phylogenetic analysis (Parker, 2016) recovers *Scutarx deltatylus* as the sister taxon to *Adamanasuchus eisenhardtae* and forming a clade with *Calyptosuchus wellesi*. The unnamed clade formed by these three taxa is the sister taxon of Desmatosuchini (Parker, 2016) within Desmatosuchinae (Figure 26). The presence of a aetosaurian with armor similar to *Stagonolepis robertsoni* (sensu Heckert and Lucas, 2000), but with a skull more like that of desmatosuchins provides further support that certain characteristic of the armor that were once used to unite taxa, such as paramedian osteoderm ornamentation (Heckert & Lucas 2000; Long & Ballew 1985; Long & Murry 1995), may have wider distributions across Aetosauria than previously recognized (Parker 2008b).

Implications for Late Triassic Vertebrate Biochronology

The holotype and all of the referred specimens of *Scutarx deltatylus* were originally assigned to *Calyptosuchus wellesi* (Long & Murry 1995; Martz et al. 2013; Parker & Irmis 2005;

PeerJ Preprints | https://doi.org/10.7287/peerj.preprints.1924v1 | CC-BY 4.0 Open Access | rec: 3 Apr 2016, publ: 3 Apr 2016

Parker & Martz 2011), a proposed index taxon of the Adamanian biozone (Parker & Martz 2011), which is earliest Norian in age (Irmis et al. 2011). However, all of the recognized specimens of *Scutarx deltatylus* originate only from the Adamanian portion of the Sonsela Member of the Chinle Formation and the middle part of the Cooper Canyon Formation of Texas (Martz et al. 2013; Parker & Martz 2011). The reassignment of this material restricts the stratigraphic range of *Calyptosuchus wellesi* to the Bluewater Creek and Blue Mesa members of the Chinle Formation as well as the Tecovas Formation of Texas (Heckert 1997; Long & Murry 1995), which are stratigraphically lower than the Sonsela Member and middle part of the Cooper Canyon (Martz et al. 2013).

It has been suggested that the Adamanian biozone (*sensu* Martz & Parker In Press; Parker & Martz 2011) could possibly be subdivided into sub-zones (Martz et al. 2013). That hypothesis was supported by a list of Adamanian taxa of the Chinle Formation that noted which are known solely from the Blue Mesa Member and which are known only from the lower part of the Sonsela Member. The list of taxa shared by both units is small and consists of *Placerias hesternus* (a dicynodont synapsid), the archosauromorph *Trilophosaurus dornorum*, the poposaurid *Poposaurus gracilis*, a paratypothoracin aetosaur similar to *Tecovasuchus chatterjeei*, and *Calyptosuchus wellesi* (Martz et al. 2013). The reassignment of the Sonsela material previously placed in *Calyptosuchus wellesi* to *Scutarx deltatylus* further reduces that list. *Scutarx deltatylus* also occurs in the upper Adamanian Post Quarry of Texas, which contains taxa elsewhere only found in the lower part of the Sonsela Member (e.g., *Desmatosuchus smalli*, *Trilophosaurus dornorum*, *Typothorax coccinarum*, *Paratypothorax* sp.; Martz et al. 2013). Thus, *Scutarx deltatylus* can presently be considered an index taxon of the upper part of the

PeerJ Preprints | https://doi.org/10.7287/peerj.preprints.1924v1 | CC-BY 4.0 Open Access | rec: 3 Apr 2016, publ: 3 Apr 2016

Adamanian biozone, which is presently considered to be middle Norian in age (Figure 26; Irmis et al., 2011).

CONCLUSIONS

Scutarx deltatylus is a new taxon of aetosaurian from the middle Norian (late Adamanian) of the American Southwest, based on material that was originally assigned to *Calyptosuchus wellesi*. This taxon is known from several carapaces and includes rare skull material from western North America. *Scutarz delatatylus* differs from all other aetosaurians in the presence of a raised triangular boss in the posteromedial corner of the presacral paramedian osteoderms, a dorsoventrally thickened skull roof, and an anteroposteriorly shortened parabasisphenoid. A phylogenetic analysis places it as the sister taxon of *Adamanasuchus eisenhardtae* near the base of Desmatosuchinae (Parker, 2016). *Scutarx deltatylus* appears to have utility as an index taxon for the late Adamanian biozone.

ACKNOWLEDGEMENTS

Much of this manuscript was a part of a doctoral dissertation submitted to the University of Texas at Austin. Reviews of that earlier version were provided by Tim Rowe, Chris Bell, Sterling Nesbitt, and Hans-Dieter Sues. Thank you to the management and staff of Petrified Forest National Park (PEFO) for their support of this project. For fieldwork assistance at the Petrified Forest I thank Daniel Woody, David Gillette, Sue Clements, Dan Slais, Randall Irmis, Sterling Nesbitt, Jeff Martz, Michelle Stocker, Raul Ochoa, Lori Browne, Chuck Beightol, Rachel Guest, Matt Smith, and Kenneth Bader. Raul Ochoa discovered the type specimen of *Scutarx deltatylus*. I also greatly appreciate the assistance provided by the Maintenance Division staff of PEFO in the final collection of many of these specimens. Preparation of PEFO specimens

1200 was completed by Pete Reser, Matt Brown, Matt Smith, and Kenneth Bader. All specimens were
1201 collected under a natural resources permit from the National Park Service.
1202 Access to specimens under their care was provided by T. Scott Williams and Matt Smith
1203 (PEFO); Pat Holroyd, Mark Goodwin, and Kevin Padian (UCMP); David and Janet Gillette
1204 (MNA); Julia Desojo (MACN); the late Jaime Powell (PVL); Ricardo Martinez (PVSJ); Sandra
1205 Chapman, Lorna Steel, and David Gower (NHMUK); Lindsay Zanno and Vince Schneider
1206 (NCSM); Sankar Chatterjee and Bill Mueller (TTUP); Matthew Carrano (USNM); Tony Fiorillo
1207 and Ron Tykoski (DMNH); Alex Downs (GR); Charles Dailey and Dick Hilton (Sierra College);
1208 Tim Rowe, Lyndon Murray, Matt Brown, and Chris Sagebiel (VPL).
1209 Financial assistance for this project was provided by the Jackson School of Geosciences,
1210 the Lundelius Fund, the Francis L. Whitney Endowed Presidential Scholarship, the Ronald K. DeFord
1211 Scholarship Fund, the Petrified Forest Museum Association, Petrified Forest National Park, the Friends of
1212 the Petrified Forest, the Museum of Northern Arizona, the GSA Geocorp program, the Samuel and Doris
1213 Welles Fund, and the Systematics Association. This is Petrified Forest National Park Paleontological
1214 Contribution number xx.
1215

1216 **REFERENCES**

1217 Brochu CA. 1992. Ontogeny of the postcranium in crocodylomorph archosaurs M.S. University
1218 of Texas
1219 Brochu CA. 1996. Closure of neurocentral sutures during crocodilian ontogeny: implications for
1220 maturity assessment in fossil archosaurs. *Journal of Vertebrate Paleontology* 16:49-62.
1221 Butler RJ, Barrett PM, and Gower DJ. 2012. Reassessment of the evidence for postcranial
1222 skeletal pneumaticity in archosaurs, and the early evolution of the avian respiratory
1223 system. *PLoS One* 7(3):e34094.

1224 Case EC. 1922. New reptiles and stegocephalians from the Upper Triassic of western Texas. .
1225 *Carnegie Institute of Washington Publication* 321:1-84.
1226 Case EC. 1932. A perfectly preserved segment of the armor of a phytosaur, with associated
1227 vertebrae. *Contributions from the Museum of Paleontology, University of Michigan* 4:57-
1228 80.
1229 Colbert EH. 1971. Tetrapods and continents. *Quarterly Review of Biology* 46:250-269.
1230 Cope ED. 1869. Synopsis of the extinct Batrachia, Reptilia, and Aves of North America. .
1231 *Transactions of the American Philisophical Society, ns* 14:1-252.
1232 Cope ED. 1875. Appendix LL: Report on the geology of that part of northwestern New Mexico
1233 examined during the field season of 1874. In: Wheeler GM, ed. *Appendix GI: Annual*
1234 *Report upon the Geographical Explorations and Surveys West of the One Hundredth*
1235 *Meridian, Annual Report of the Chief of Engineers for 1875*. Washington, D.C.: Engineer
1236 Department, U.S. Army, 61-116.
1237 Desojo JB, and Báez AM. 2005. El esqueleto postcraneano de *Neoaetosauroides* (Archosauria:
1238 Aetosauria) del Triásico Superior del centro-oeste de Argentina. *Ameghiniana* 42:115-
1239 126.
1240 Desojo JB, and Báez AM. 2007. Cranial morphology of the Late Triassic South American
1241 archosaur *Neoaetosauroides engaeus*: evidence for aetosaurian diversity. *Palaeontology*
1242 50:267-276.
1243 Desojo JB, and Ezcurra MD. 2011. A reappraisal of the taxonomic status of *Aetosauroides*
1244 (Archosauria, Aetosauria) specimens from the Late Triassic of South America and their
1245 proposed synonymy with *Stagonolepis*. *Journal of Vertebrate Paleontology* 31:596-609.

1246 Desojo JB, Ezcurra MD, and Kischlat E-E. 2012. A new aetosaur genus (Archosauria:
1247 Pseudosuchia) from the early Late Triassic of southern Brazil. *Zootaxa* 3166:1-33.
1248 Desojo JB, and Heckert AB. 2004. New information on the braincase and mandible of
1249 Coahomasuchus (Archosauria: Aetosauria) from the Otischalkian (Carnian) of Texas.
1250 *Neues Jahrbuch für Geologie und Paläontologie Monatshefte* 2004:605-616.
1251 Desojo JB, Heckert AB, Martz JW, Parker WG, Schoch RR, Small BJ, and Sulej T. 2013.
1252 Aetosauria: a clade of armoured pseudosuchians from the Upper Triassic continental
1253 beds. In: Nesbitt SJ, Desojo JB, and Irmis RB, editors. Anatomy, Phylogeny, and
1254 Paleobiology of Early Archosaurs and their Kin: Special Publications of the Geological
1255 Society of London p203-239.
1256 Fraser NC. 2006. *Dawn of the Dinosaurs: Life in the Triassic*. Bloomington: Indiana University
1257 Press.
1258 Gauthier J. 1986. Saurischian monophyly and the origin of birds. *Memoirs of the California*
1259 *Academy of Sciences* 8:1-55.
1260 Gauthier J, and Padian K. 1985. Phylogenetic, functional, and aerodynamic analyses of the origin
1261 of birds and their flight. In: Hecht MK, Ostrom JH, Viohl G, and Wellnhofer P, eds. *The*
1262 *Beginning of Birds: Proceedings of the International Archaeopteryx Conference*.
1263 Eichstätt: Freunde des Jura Museums, 185-197.
1264 Gower DJ, and Walker AD. 2002. New data on the braincase of the aetosaurian archosaur
1265 (Reptilia: Diapsida) *Stagonolepis robertsoni* Agassiz. *Zoological Journal of the Linnean*
1266 *Society* 136:7-23.

PeerJ Preprints | https://doi.org/10.7287/peerj.preprints.1924v1 | CC-BY 4.0 Open Access | rec: 3 Apr 2016, publ: 3 Apr 2016

1267 Heckert AB. 1997. The tetrapod fauna of the Upper Triassic lower Chinle Group (Adamanian:
1268 latest Carnian) of the Zuni Mountains, west-central New Mexico. *New Mexico Museum*
1269 *of Natural History and Science Bulletin* 11:29-39.
1270 Heckert AB, and Lucas SG. 1999. A new aetosaur (Reptilia: Archosauria) from the Upper
1271 Triassic of Texas and the phylogeny of aetosaurs. *Journal of Vertebrate Paleontology*
1272 19:50-68.
1273 Heckert AB, and Lucas SG. 2000. Taxonomy, phylogeny, biostratigraphy, biochronology,
1274 paleobiogeography, and evolution of the Late Triassic Aetosauria (Archosauria:
1275 Crurotarsi). *Zentralblatt für Geologie und Paläontologie* Teil I 1998 1539-1587.
1276 Heckert AB, Lucas SG, Hunt AP, and Spielmann J. 2007a. Late aetosaur biochronology
1277 revisited. *New Mexico Museum of Natural History & Science Bulletin* 41:49-50.
1278 Heckert AB, Lucas SG, Rinehart LF, Celeskey MD, Spielmann JA, and Hunt AP. 2010.
1279 Articulated skeletons of the aetosaur *Typothorax coccinarum* Cope (Archosauria:
1280 Stagonoleopididae) from the Upper Triassic Bull Canyon Formation (Revueltian: early-
1281 mid Norian), eastern New Mexico, USA. *Journal of Vertebrate Paleontology* 30:619-
1282 642.
1283 Heckert AB, Spielmann J, Lucas SG, and Hunt AP. 2007b. Biostratigraphic utility of the Upper
1284 Triassic aetosaur Tecovasuchus (Archosauria: Stagonolepididae), an index taxon of St.
1285 Johnsian (Adamanian: Late Carnian) time. In: Lucas SG, and Spielmann J, eds. *The*
1286 *Global Triassic*. Albuquerque: New Mexico Museum of Natural History and Science, 51-
1287 57.
1288 Hill RV. 2010. Osteoderms of *Simosuchus clarki* (Crocodyliformes: Notosuchia) from the Late
1289 Cretaceous of Madagascar. *Journal of Vertebrate Paleontology Memoir* 10:154-176.

1290 Hopson JA. 1979. Paleoneurology. In: Gans C, Northcutt RG, and Ulinsky P, eds. *Biology of the*
1291 *Reptilia 9, neurology A*. London: Academic Press, 39-146.
1292 Howell ER, and Blakey RC. 2013. Sedimentological constraints on the evolution of the
1293 Cordilleran arc: New insights from the Sonsela Member, Upper Triassic Chinle
1294 Formation, Petrified Forest National Park (Arizona, USA). *Geological Society of*
1295 *America Bulletin* 125:1349-1368. 10.1130/B30714.1
1296 Irmis RB. 2007. Axial skeleton ontogeny in the Parasuchia (Archosauria: Pseudosuchia) and its
1297 implications for ontogenetic determination in archosaurs. *Journal of Vertebrate*
1298 *Paleontology* 27:350-361.
1299 Irmis RB. 2008. Perspectives on the origin and early diversification of dinosaursPhD. University
1300 of California.
1301 Irmis RB, Mundil R, Martz JW, and Parker WG. 2011. High-resolution U-Pb ages from the
1302 Upper Triassic Chinle Formation (New Mexico, USA) support a diachronous rise of
1303 dinosaurs. *Earth and Planetary Science Letters* 309:258-267.
1304 Irmis RB, Nesbitt SJ, Padian K, Smith ND, Turner AH, Woody D, and Downs A. 2007a. A Late
1305 Triassic dinosauromorph assemblage from New Mexico and the rise of dinosaurs.
1306 *Science* 317:358-361.
1307 Irmis RB, Parker WG, Nesbitt SJ, and Liu J. 2007b. Early ornithischian dinosaurs: the Triassic
1308 record. *Historical Biology* 19:3-22.
1309 Jepson GL. 1948. A Triassic armored reptile from New Jersey. In: Johnson ME, ed. *State of New*
1310 *Jersey Department of Conservation Miscellaneous Geologic Paper*. Trenton: New Jersey
1311 Geologic Survey, 5-20.

PeerJ Preprints | https://doi.org/10.7287/peerj.preprints.1924v1 | CC-BY 4.0 Open Access | rec: 3 Apr 2016, publ: 3 Apr 2016

1312 Long RA, and Ballew KL. 1985. Aetosaur dermal armor from the Late Triassic of Southwestern
1313 North America, with special reference to material from the Chinle Formation of Petrified
1314 Forest National Park. *Museum of Northern Arizona Bulletin* 54:45-68.
1315 Long RA, and Murry PA. 1995. Late Triassic (Carnian and Norian) tetrapods from the
1316 southwestern United States. *New Mexico Museum of Natural History & Science Bulletin*
1317 4:1-254.
1318 Lucas SG. 1998. Global Triassic tetrapod biostratigraphy and biochronology. *Palaeogeography,*
1319 *Palaeoclimatology, Palaeoecology* 143:347-384.
1320 Lucas SG, and Heckert AB. 1996. Late Triassic aetosaur biochronology. *Albertiana* 17:57-64.
1321 Lucas SG, Heckert AB, Estep JW, and Anderson OJ. 1997. Stratigraphy of the Upper Triassic
1322 Chinle Group, Four Corners Region. *New Mexico Geological Society Guidebook* 48:81-
1323 108.
1324 Lucas SG, Heckert AB, and Hunt AP. 2003. A new species of the aetosaur *Typothorax*
1325 (Archosauria: Stagonolepididae) from the Upper Triassic of east-central New Mexico.
1326 *New Mexico Museum of Natural History and Science Bulletin* 21:221-233.
1327 Lucas SG, and Hunt AP. 1993. Tetrapod biochronology of the Chinle Group (Upper Triassic),
1328 western United States. *New Mexico Museum of Natural History and Science Bulletin*
1329 3:327-329.
1330 Lucas SG, Hunt AP, Heckert AB, and Spielmann JA. 2007. Global Triassic tetrapod
1331 biostratigraphy and biochronology: 2007 status. *New Mexico Museum of Natural History*
1332 *and Science Bulletin* 41:229-240.
1333 Lucas SG, Hunt AP, and Spielmann J. 2007. A new aetosaur from the Upper Triassic
1334 (Adamanian: Carnian) of Arizona. In: Lucas SG, and Spielmann J, eds. *Triassic of the*

PeerJ Preprints | https://doi.org/10.7287/peerj.preprints.1924v1 | CC-BY 4.0 Open Access | rec: 3 Apr 2016, publ: 3 Apr 2016

American West. Albuquerque: New Mexico Museum of Natural History and Science, 241-247.

Lydekker R. 1887. The fossil vertebrata of India. *Records of the Geological Survey of India* 20:51-80.

Marsh OC. 1884. The classification and affinities of dinosaurian reptiles. *Nature*:68-69.

Martz JW. 2002. The morphology and ontogeny of *Typothorax coccinarum* (Archosauria, Stagonolepididae) from the Upper Triassic of the American Southwest M.S. Texas Tech University.

Martz JW, Mueller BD, Nesbitt SJ, Stocker MR, Atanassov M, Fraser NC, Weinbaum JC, and Lehane J. 2013. A taxonomic and biostratigraphic re-evaluation of the Post Quarry vertebrate assemblage from the Cooper Canyon Formation (Dockum Group, Upper Triassic) of southern Garza County, western Texas. . *Earth and Environmental Science Transactions of the Royal Society of Edinburgh* 103:339-364.

Martz JW, and Parker WG. 2010. Revised lithostratigraphy of the Sonsela Member (Chinle Formation, Upper Triassic) in the southern part of Petrified Forest National Park, Arizona. *PLoS One* 5:e9329, 9321-9326.

Martz JW, and Parker WG. In Press. Revised formulation of the Late Triassic land vertebrate "faunachrons" of western North America. In: Zeigler KE, and Parker WG, eds. *Deciphering Complex Depositional Systems*: Elsevier.

Martz JW, and Small BJ. 2006. *Tecovasuchus chatterjeei*, a new aetosaur (Archosauria: Stagonolepididae) from the Tecovas Formation (Carnian, Upper Triassic) of Texas. *Journal of Vertebrate Paleontology* 26:308-320.

PeerJ Preprints | https://doi.org/10.7287/peerj.preprints.1924v1 | CC-BY 4.0 Open Access | rec: 3 Apr 2016, publ: 3 Apr 2016

1357 Nesbitt SJ. 2011. The early evolution of archosaurs: relationships and the origin of major clades.
1358 *Bulletin of the American Museum of Natural History* 352:1-292.
1359 Nesbitt SJ, Irmis RB, and Parker WG. 2007. A critical re-evaluation of the Late Triassic dinosaur
1360 taxa of North America. *Journal of Systematic Palaeontology* 5:209-243.
1361 Nesbitt SJ, Sidor CA, Irmis RB, Angielczyk KD, Smith RMH, and Tsuji LA. 2010. Ecologically
1362 distinct dinosaurian sister group shows early diversification of Ornithodira. *Nature*
1363 464:95-98.
1364 Nesbitt SJ, Smith ND, Irmis RB, Turner AH, Downs A, and Norell MA. 2009a. A complete
1365 skeleton of a Late Triassic saurischian and the early evolution of dinosaurs. *Science*
1366 326:1530-1533.
1367 Nesbitt SJ, and Stocker MR. 2008. The vertebrate assemblage of the Late Triassic Canjilon
1368 Quarry (northern New Mexico, USA), and the importance of apomorphy-based
1369 assemblage comparisons. *Journal of Vertebrate Paleontology* 28:1063-1072.
1370 Nesbitt SJ, Stocker MR, Small BJ, and Downs A. 2009b. The osteology and relationships of
1371 *Vancleavea campi* (Reptilia: Archosauriformes). *Zoological Journal of the Linnean*
1372 *Society* 157:814-864.
1373 Parker WG. 2005a. Faunal review of the Upper Triassic Chinle Formation of Arizona. *Mesa*
1374 *Southwest Museum Bulletin* 11:34-54.
1375 Parker WG. 2005b. A new species of the Late Triassic aetosaur *Desmatosuchus* (Archosauria:
1376 Pseudosuchia). *Comptes Rendus Palevol* 4:327-340.
1377 Parker WG. 2007. Reassessment of the aetosaur '*Desmatosuchus*' *chamaensis* with a reanalysis
1378 of the phylogeny of the Aetosauria (Archosauria: Pseudosuchia). *Journal of Systematic*
1379 *Palaeontology* 5:41-68. 10.1017/S1477201906001994

PeerJ Preprints | https://doi.org/10.7287/peerj.preprints.1924v1 | CC-BY 4.0 Open Access | rec: 3 Apr 2016, publ: 3 Apr 2016

1380 Parker WG. 2008a. Description of new material of the aetosaur *Desmatosuchus spurensis*
1381 (Archosauria: Suchia) from the Chinle Formation of Arizona and a revision of the genus
1382 *Desmatosuchus*. *PaleoBios* 28:1-40.
1383 Parker WG. 2008b. How many valid aetosaur species are there? Reviewing the alpha-taxonomy
1384 of the Aetosauria (Archosauria: Pseudosuchia) and its implications for Late Triassic
1385 global biostratigraphy. *Journal of Vertebrate Paleontology* 28:125A.
1386 Parker WG. 2014. Taxonomy and phylogeny of the Aetosauria (Archosauria: Pseudosuchia)
1387 including a new species from the Upper Triassic of Arizona Ph.D. The University of
1388 Texas at Austin.
1389 Parker WG. 2016. Revised phylogenetic analysis of the Aetosauria (Archosauria: Pseudosuchia);
1390 assessing the effects of incongruent morphological character sets. *PeerJ* 4:e1583.
1391 10.7717/peerj.1583
1392 Parker WG, and Irmis RB. 2005. Advances in Late Triassic vertebrate paleontology based on
1393 new material from Petrified Forest National Park, Arizona. *New Mexico Museum of*
1394 *Natural History and Science Bulletin* 29:45-58.
1395 Parker WG, and Martz JW. 2011. The Late Triassic (Norian) Adamanian-Revueltian tetrapod
1396 faunal transition in the Chinle Formation of Petrified Forest National Park, Arizona.
1397 *Earth and Environmental Science Transactions of the Royal Society of Edinburgh*
1398 101:231-260.
1399 Parrish JM. 1994. Cranial osteology of *Longosuchus meadei* and the phylogeny and distribution
1400 of the Aetosauria. *Journal of Vertebrate Paleontology* 14:196-209.
1401 Ramezani J, Hoke GD, Fastovsky DE, Bowring SA, Therrien F, Dworkin SI, Atchley SC, and
1402 Nordt LC. 2011. High-precision U-Pb zircon geochronology of the Late Triassic Chinle

1403 Formation, Petrified Forest National Park (Arizona, USA): temporal constraints on the
1404 early evolution of dinosaurs. *Geological Society of America Bulletin* 123:2142-2159.
1405 Rauhut OWM. 2004. Braincase structure of the Middle Jurassic theropod dinosaur
1406 *Piatnitzkysaurus*. *Canadian Journal of Earth Sciences* 41:1109-1122.
1407 Reese AM. 1915. *The Alligator and its Allies*. New York: Knickerbocker Press.
1408 Reichgelt T, Parker WG, Martz JW, Conran JG, Van Konijnenburg-Van Cittert JHA, and
1409 Kürschner WM. 2013. The palynology of the Sonsela Member (Late Triassic, Norian) at
1410 Petrified Forest National Park, Arizona, USA. *Review of Palaeobotany and Palynology*
1411 189:18-28.
1412 Rieppel O. 1985. The recessus scalae tympani and its bearing on the classification of lizards.
1413 *Journal of Herpetology* 19:373-384.
1414 Roberto-Da-Silva L, Desojo JB, Cabriera SF, Aires ASS, Müller ST, Pacheco CP, and Dias-da-
1415 Silva S. 2014. A new aetosaur from the Upper Triassic of the Santa Maria Formation,
1416 southern Brazil. *Zootaxa* 3764:240-278.
1417 Sawin HJ. 1947. The pseudosuchian reptile *Typothorax meadei*. *Journal of Paleontology* 21:201-
1418 238.
1419 Schoch RR. 2007. Osteology of the small archosaur *Aetosaurus* from the Upper Triassic of
1420 Germany. *Neues Jahrbuch für Geologie und Paläontologie Abhandlugen* 246:1-35.
1421 10.1127/0077-7749/2007/0246-0001
1422 Schoch RR, and Desojo JB. 2016. Cranial anatomy of the aetosaur *Paratypothorax andressorum*
1423 Long & Ballew, 1985, from the Upper Triassic of Germany and its bearing on aetosaur
1424 phylogeny. *Neues Jahrbuch für Geologie und Paläontologie Abhandlugen* 279:73-95.

PeerJ Preprints | https://doi.org/10.7287/peerj.preprints.1924v1 | CC-BY 4.0 Open Access | rec: 3 Apr 2016, publ: 3 Apr 2016

1425 Small BJ. 2002. Cranial anatomy of *Desmatosuchus haplocerus* (Reptilia: Archosauria:
1426 Stagonolepididae). *Zoological Journal of the Linnean Society* 136:97-111.
1427 Small BJ, and Martz JW. 2013. A new basal aetosaur from the Upper Triassic Chinle Formation
1428 of the Eagle Basin, Colorado, USA. In: Nesbitt SJ, Desojo JB, and Irmis RB, eds.
1429 *Anatomy, Phylogeny and Palaeobiology of Early Archosaurs and their Kin*. Bath: The
1430 Geological Society Publishing House, 393-412.
1431 Spielmann J, and Lucas SG. 2012. Tetrapod fauna of the Upper Triassic Redonda Formation,
1432 east-central New Mexico: the characteristic assemblage of the Apachean land-vertebrate
1433 faunachron. *New Mexico Museum of Natural History & Science Bulletin* 55:1-119.
1434 Stocker MR. 2010. A new taxon of phytosaur (Archosauria: Pseudosuchia) from the Late
1435 Triassic (Norian) Sonsela Member (Chinle Formation) in Arizona, and a critical
1436 reevaluation of *Leptosuchus* Case 1922. *Palaeontology* 53:997-1022.
1437 Sulej T. 2010. The skull of an early Late Triassic aetosaur and the evolution of the
1438 stagonolepidid archosaurian reptiles. *Zoological Journal of the Linnean Society* 158:860-
1439 881.
1440 Wake MH. 1992. *Hyman's comparative vertebrate anatomy, revised third edition*. Chicago:
1441 University of Chicago Press.
1442 Walker AD. 1961. Triassic Reptiles from the Elgin Area: *Stagonolepis*, *Dasygnathus* and Their
1443 Allies. *Philosophical Transactions of the Royal Society of London Series B, Biological*
1444 *Sciences* 244:103-204.
1445 Walker AD. 1990. A revision of *Spenosuchus acutus* Haughton, a crocodylomorph reptile from
1446 the Elliott Formation (Late Triassic or Early Jurassic) of South Africa. *Philosophical*
1447 *Transactions: Biological Sciences* 330:1-120.

1448 Weinbaum JC. 2011. The skull of *Postosuchus kirkpatricki* (Archosauria: Paracrocodyliformes)
1449 from the Upper Triassic of the United States. *PaleoBios* 30:18-44.
1450 Wilson JA. 1999. A nomenclature for vertebral laminae in sauropods and other saurischian
1451 dinosaurs. *Journal of Vertebrate Paleontology* 19:639-653.
1452 Wilson JA, D'Emic MD, Ikejiri T, Moacdieh EM, and Whitlock JA. 2011. A nomenclature for
1453 vertebral fossae in sauropods and other saurischian dinosaurs. *PLoS One* 6(2):e17114.
1454 Witmer LM. 1997. Craniofacial air sinus systems. In: Currie PJ, and Padian K, eds.
1455 *Encyclopedia of Dinosaurs*. San Diego: Academic Press.
1456 Woody DT. 2006. Revised stratigraphy of the lower Chinle Formation (Upper Triassic) of
1457 Petrified Forest National Park, Arizona. *Museum of Northern Arizona Bulletin* 62:17-45.
1458 Zeigler KE, Heckert AB, and Lucas SG. 2003 [imprint 2002]. A new species of *Desmatosuchus*
1459 (Archosauria: Aetosauria) from the Upper Triassic of the Chama Basin, north-central
1460 New Mexico. *New Mexico Museum of Natural History and Science Bulletin* 21:215-219.
1461 Zittel KA. 1887-1890. *Handbuch der Palaeontologie. 1. Abteilung: Palaeozoologie, 3*. München
1462 & Leipzig.

1463
1464
1465
1466

1467

1468

1469

1470

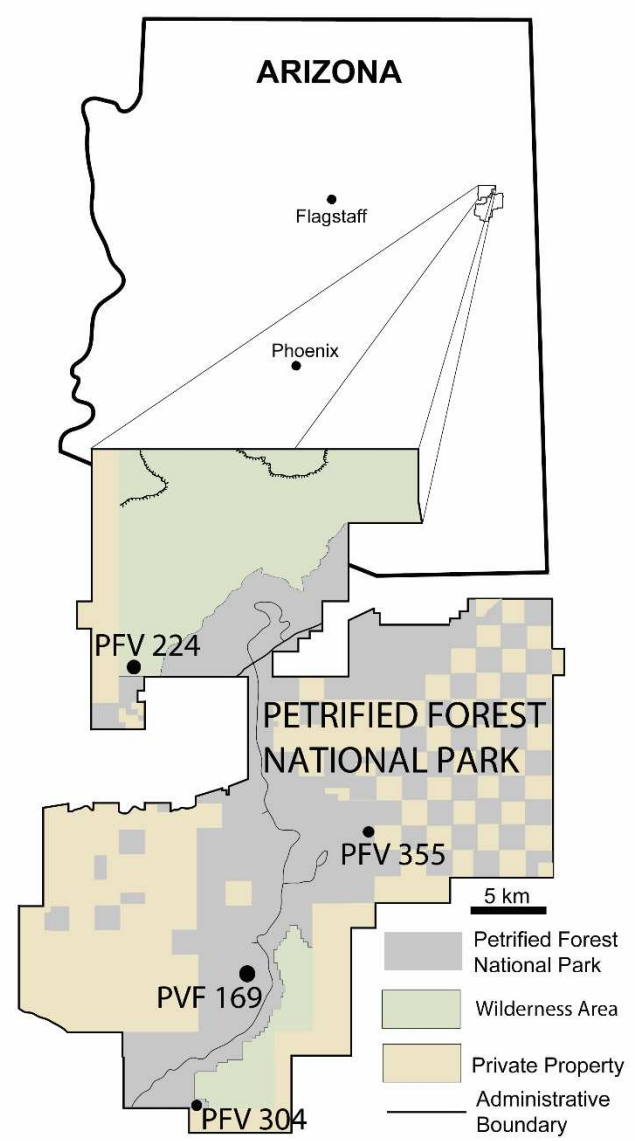

1471

1472

1473 Figure 1. Map of Petrified Forest National Park showing relevant vertebrate fossil localities.
1474 Modified from Parker & Irmis (2005).

1475

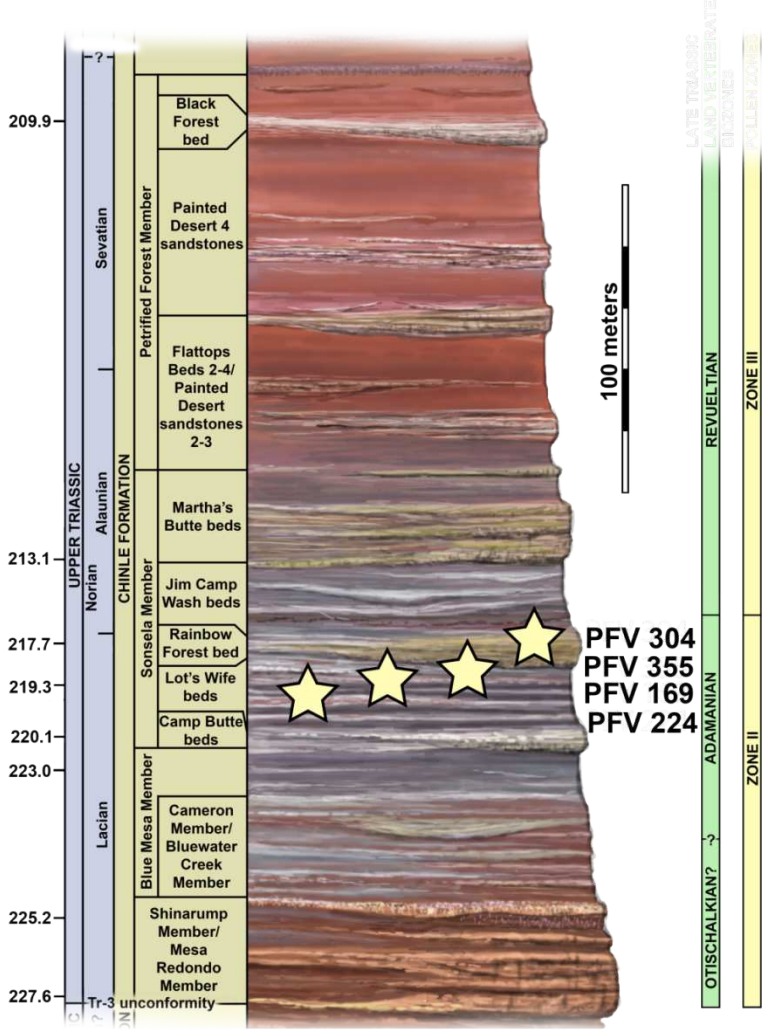

1476

1477

1478 Figure 2. Regional stratigraphy of the Petrified Forest area showing the stratigraphic position of
1479 the localties discussed in the text. All occurrences are in the lower part of the
1480 Sonsela Member of the Chinle Formation and are within the Adamanian biozone.
1481 Stratigraphy from Martz & Parker, 2010. Biozones from Parker & Martz (2011) and
1482 Reichgelt et al. (2013). Ages from Ramezani et al. (2011) and Atchley et al. (2013).

1483

PeerJ Preprints | https://doi.org/10.7287/peerj.preprints.1924v1 | CC-BY 4.0 Open Access | rec: 3 Apr 2016, publ: 3 Apr 2016

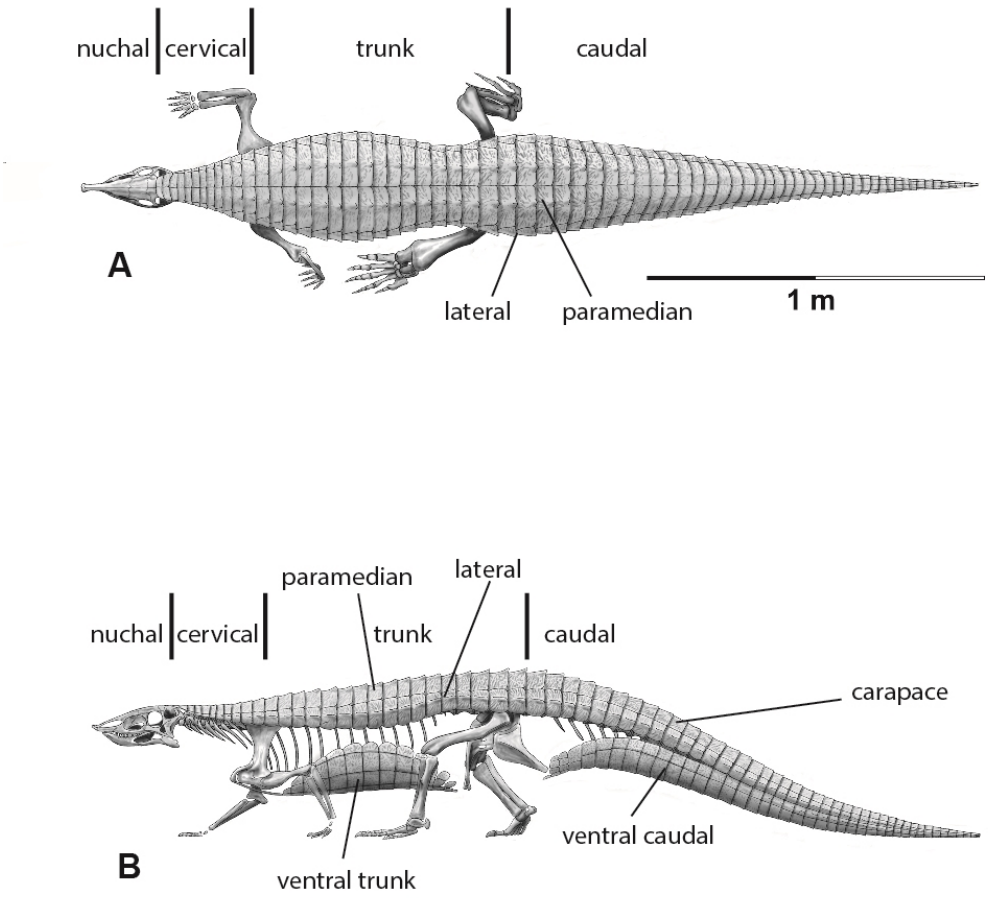

1484

1485 Figure 3. Differention and terminology for aetosaurian osteoderms. Reconstruction

1486 courtesy of Jeffrey Martz.

1487

PeerJ Preprints | https://doi.org/10.7287/peerj.preprints.1924v1 | CC-BY 4.0 Open Access | rec: 3 Apr 2016, publ: 3 Apr 2016

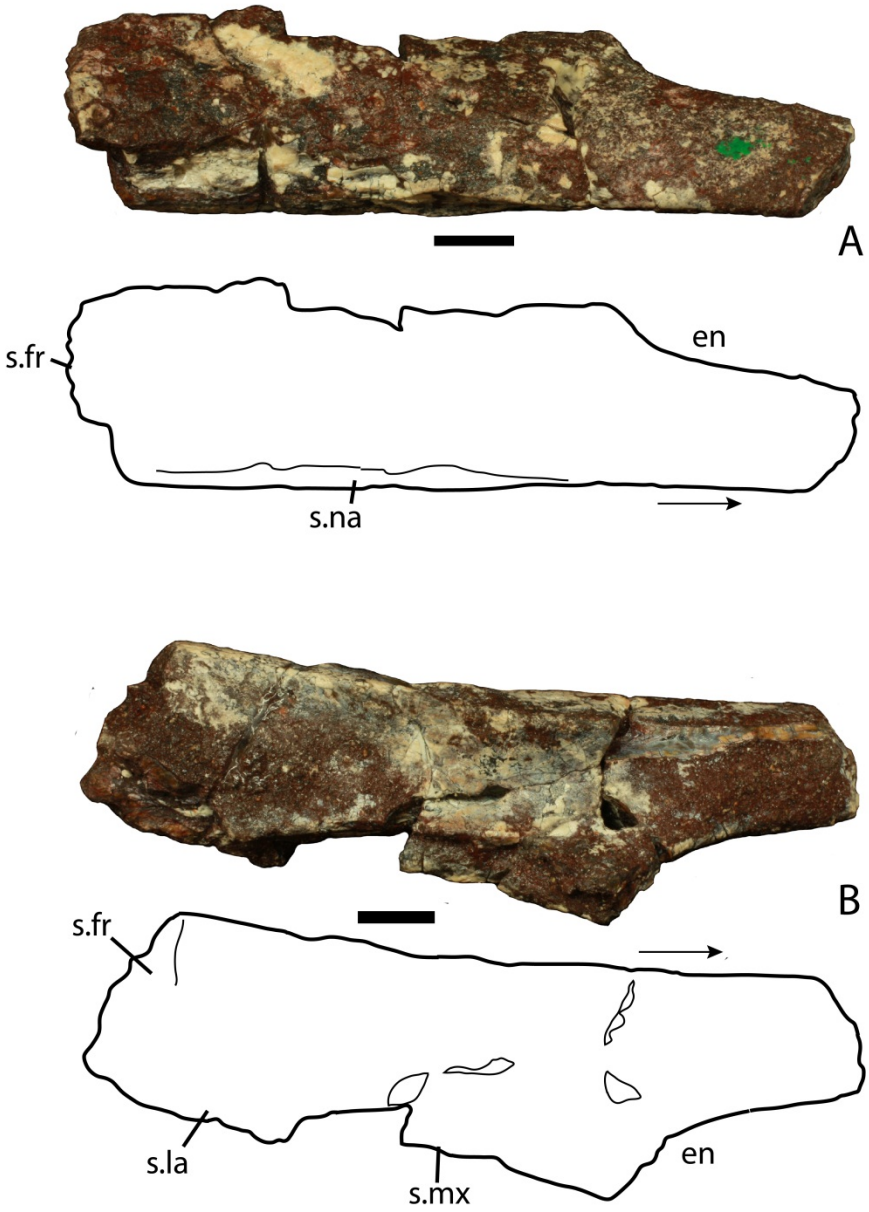

1488

1489

1490 Figure 4. Photos and interpretive sketches of the left nasal (PEFO 34616) in dorsal (A) and
1491 ventral (B) views. Arrows point anteriorly and scale bars equal 1 cm.
1492 Abbreviations: en, external nares; fr, frontal; la, lacrimal; mx, maxilla; s., suture
1493 with listed element.

1494

PeerJ Preprints | https://doi.org/10.7287/peerj.preprints.1924v1 | CC-BY 4.0 Open Access | rec: 3 Apr 2016, publ: 3 Apr 2016

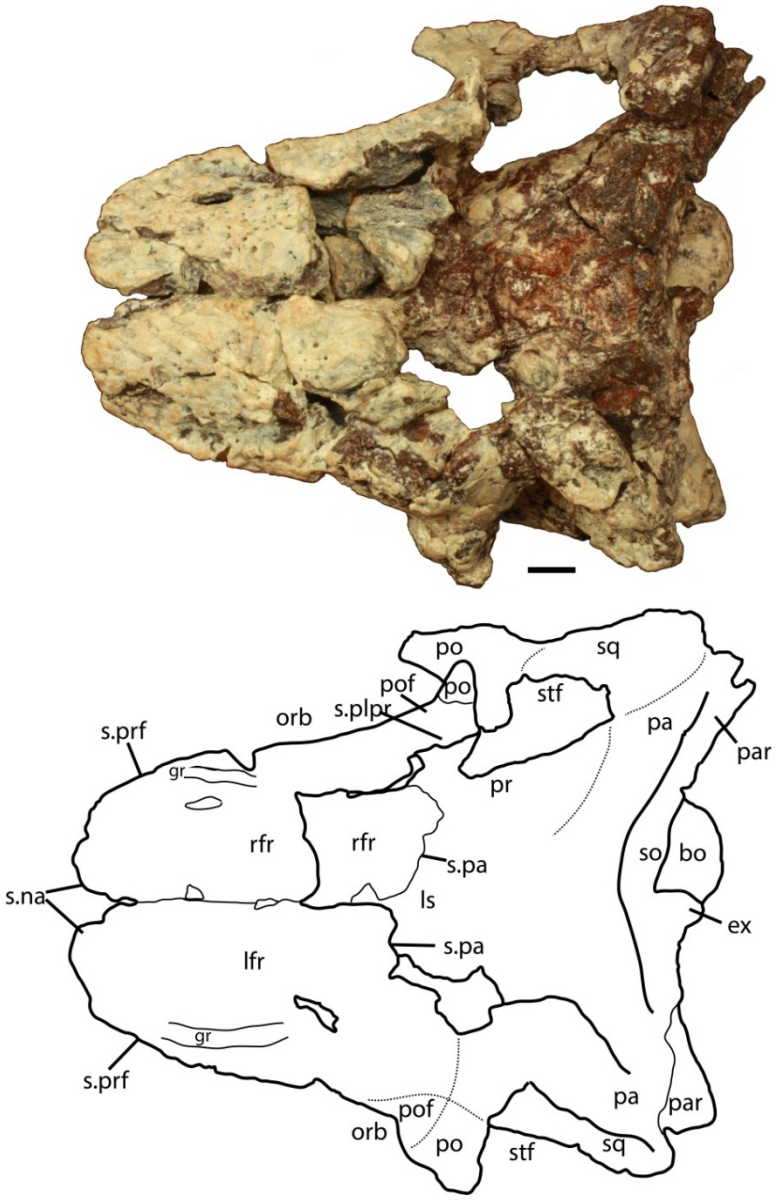

1495

1496

1497 Figure 5. Photo and interpretive sketch of posterodorsal portion of the skull of *Scutarx deltatylus*
1498 in dorsal view. Scale bar equals 1 cm. Abbreviations: bo, basioccipital; gr, groove;
1499 ex, exoccipital; lfr, left frontal; ls, laterosphenoid; na, nasal; orb, orbit; pa, parietal;
1500 par, paroccipital process of the opisthotic; plpr, palpebral; po, postorbital; pof,
1501 postfrontal; pr, prootic; prf, prefrontal; rfr, right frontal; s., suture with listed
1502 element; so, supraoccipital; sq, squamosal; stf; supratemporal fenestra.

PeerJ Preprints | https://doi.org/10.7287/peerj.preprints.1924v1 | CC-BY 4.0 Open Access | rec: 3 Apr 2016, publ: 3 Apr 2016

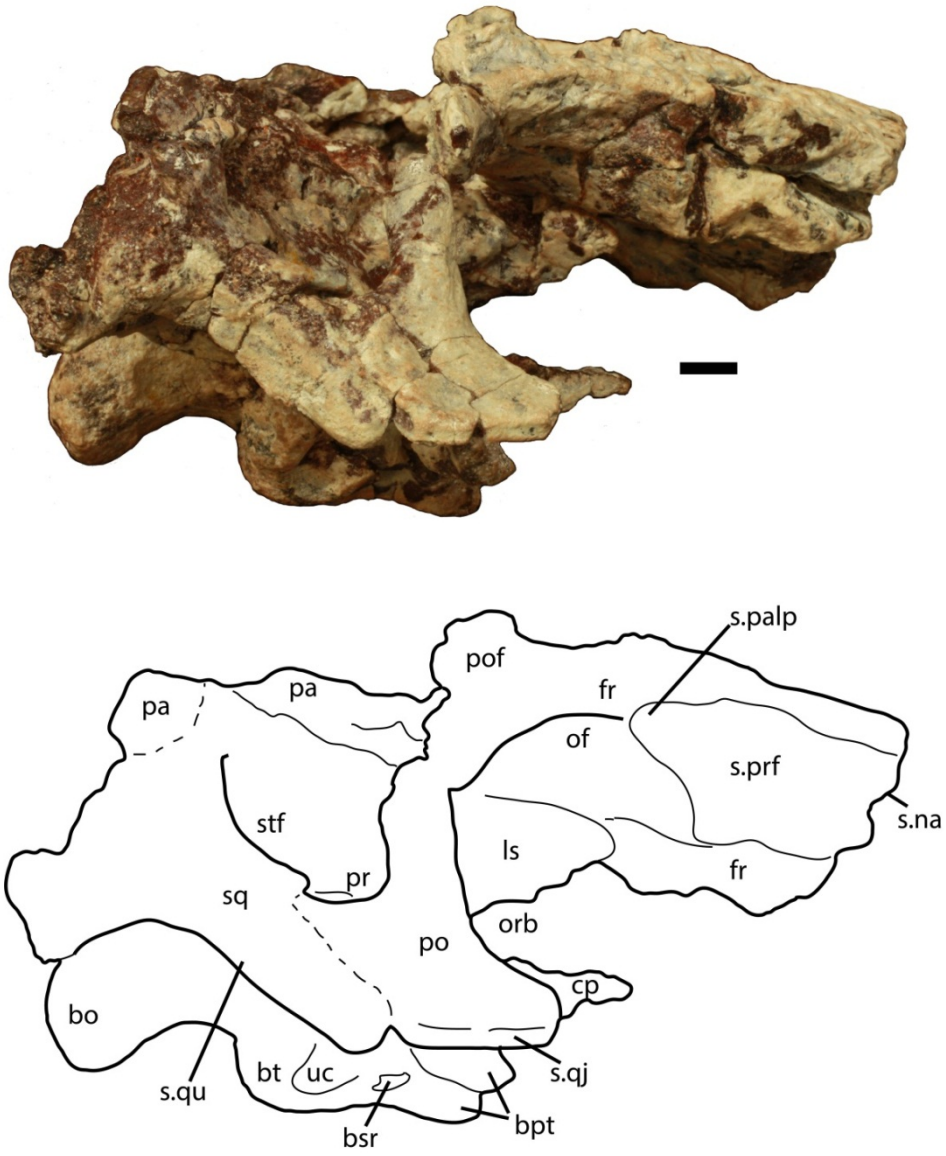

1503

1504

1505 Figure 6. Partial skull of *Scutarx deltatylus* (PEFO 34616) in right lateral view. Scale bar
1506 equals 1 cm. Abbreviations: bo, basioccipital; bpt, basipterygoid processes; bsr, basisphenoid
1507 recess; bt, basal tubera; cp, cultriform process; fr, frontal; ls, laterosphenoid; na, nasal; of, orbital
1508 fossa; orb, orbit; pa, parital; palp, palpebral; po, postorbital; pof, postfrontal; pr, prootic; prf,
1509 prefrontal; qj, quadratojugal; qu, quadrate; sq, squamosal; stf, supratemporal fenestra; uc,
1510 unossified cleft of the basal tubera.

1511

1512

PeerJ Preprints | https://doi.org/10.7287/peerj.preprints.1924v1 | CC-BY 4.0 Open Access | rec: 3 Apr 2016, publ: 3 Apr 2016

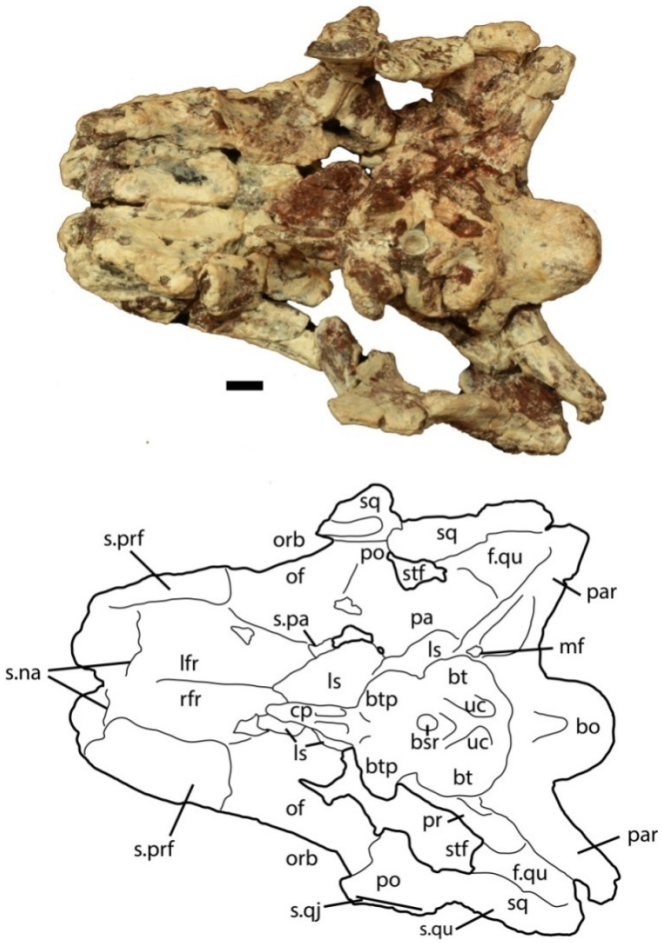

1513

1514

1515 Figure 7. Partial skull of *Scutarx deltatylus* (PEFO 34616) in ventral view. Scale bar
1516 equals 1 cm. Abbreviations: bo, basioccipital; btp, basipterygoid processes; bsr, basisphenoid
1517 recess; bt, basal tubera; cp, cultriform process; f., fossa for specified element; lfr, left frontal; ls,
1518 laterosphenoid; mf, metotic fissure; na, nasal; of, orbital fossa; orb, orbit; pa, parietal; palp,
1519 palpebral; par, paroccipital process of the opisthotic; po, postorbital; pof, postfrontal; pr, prootic;
1520 prf, prefrontal; qj, quadratojugal; qu, quadrate; rfr, right frontal; sq, squamosal; stf,
1521 supratemporal fenestra; uc, unossified cleft of the basal tubera.

1522

PeerJ Preprints | https://doi.org/10.7287/peerj.preprints.1924v1 | CC-BY 4.0 Open Access | rec: 3 Apr 2016, publ: 3 Apr 2016

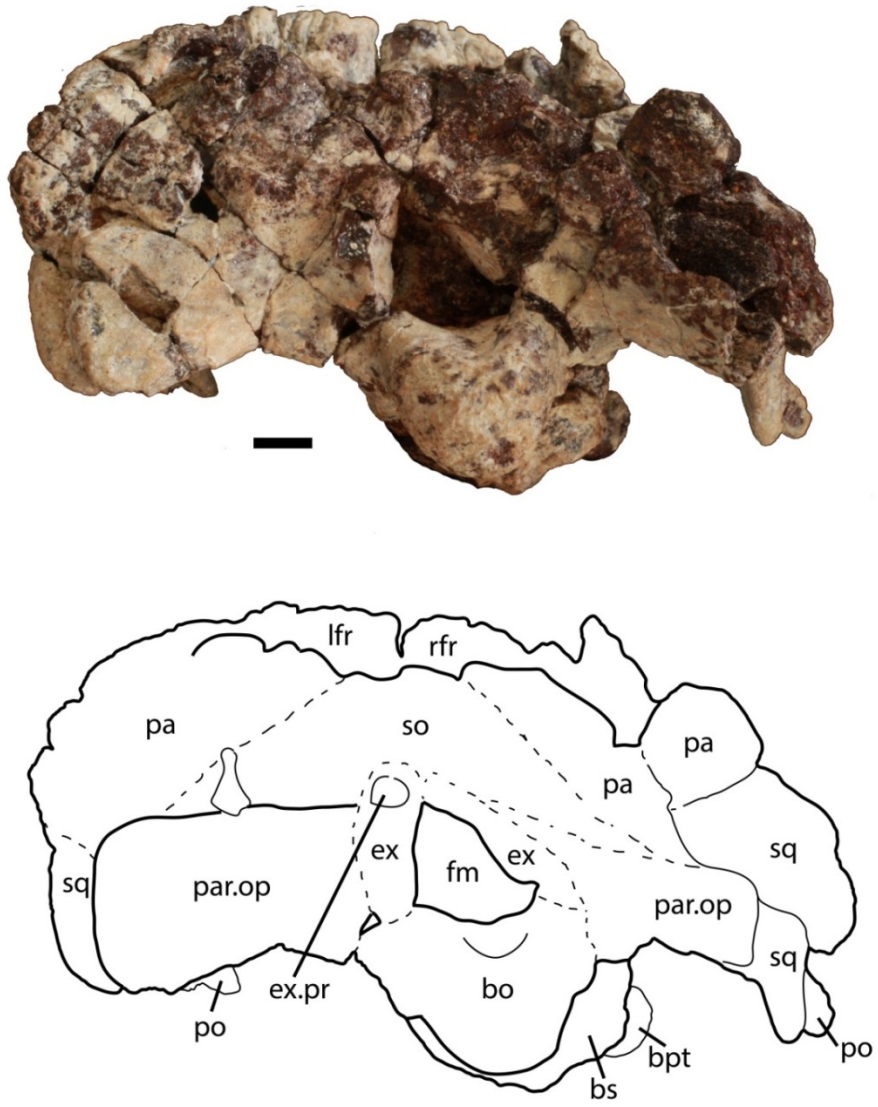

1523

1524

1525 Figure 8. Partial skull of *Scutarx deltatylus* (PEFO 34616) in posterior view. Scale bar
1526 equals 1 cm. Abbreviations: bo, basioccipital; bpt, basipterygoid processes; bs, basisphenoid; ex,
1527 exoccipital; ex.pr; exocippital prong; fm, foramen magnum; lfr, left frontal; pa, parietal; par.op,
1528 paroccipital process of the opisthotic; po, postorbital; rfr, right frontal; sq, squamosal.

1529

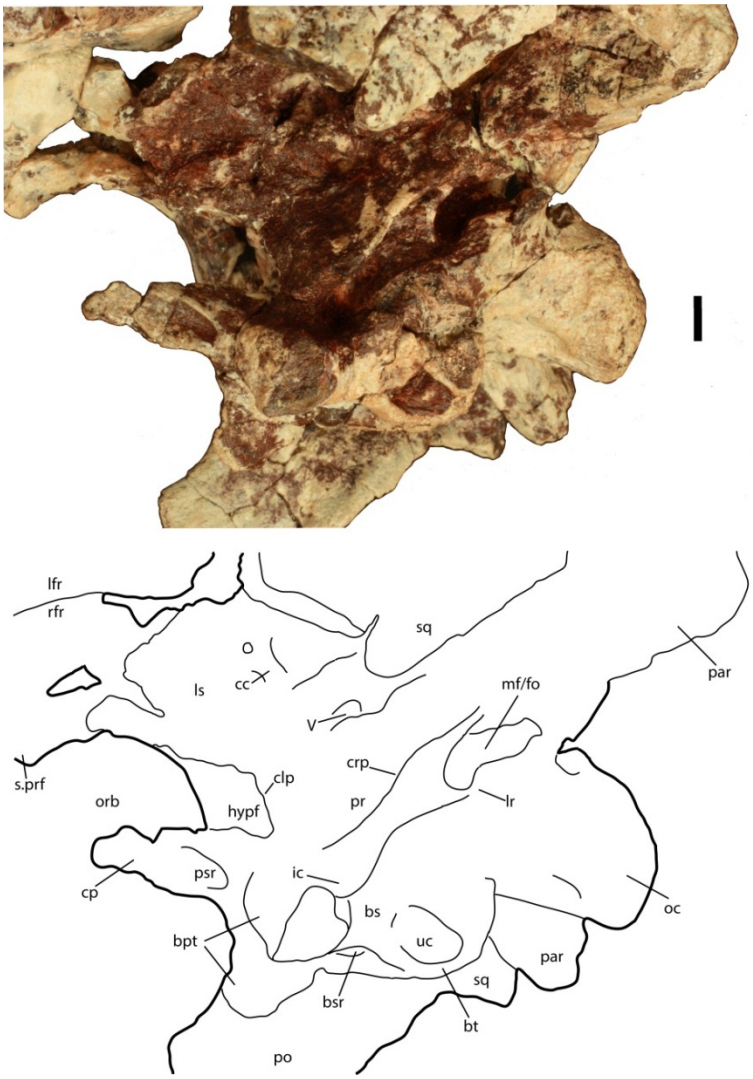

1530

1531

1532 Figure 9. Braincase of *Scutarx deltatylus* (PEFO 34616) in ventrolateral view. Scale bar equals 1
1533 cm. Abbreviations: bpt, basipterygoid processes; bsr, basisphenoid recess; bt, basal
1534 tubera; cc, cotylar crest; clp, clinoid process; cp, cultriform process; crp, crista
1535 prootica; fo, foramen ovale; hypf, hypophyseal fossa; ic, exit area of the internal
1536 carotid artery; lfr, left frontal; lr, lateral ridge; ls, laterosphenoid; mf, metotic
1537 foramen; na, nasal; oc, occipital condyle; orb, orbit; pa, parietal; par, paroccipital
1538 process of the opisthotic; po, postorbital; pr, prootic; prf, prefrontal; psr;
1539 parasphenoid recess; rfr, right frontal; s., suture with designated element; sq,
1540 squamosal; uc, unossified cleft of the basal tubera; V, passageway for the
1541 Trigeminal nerve.

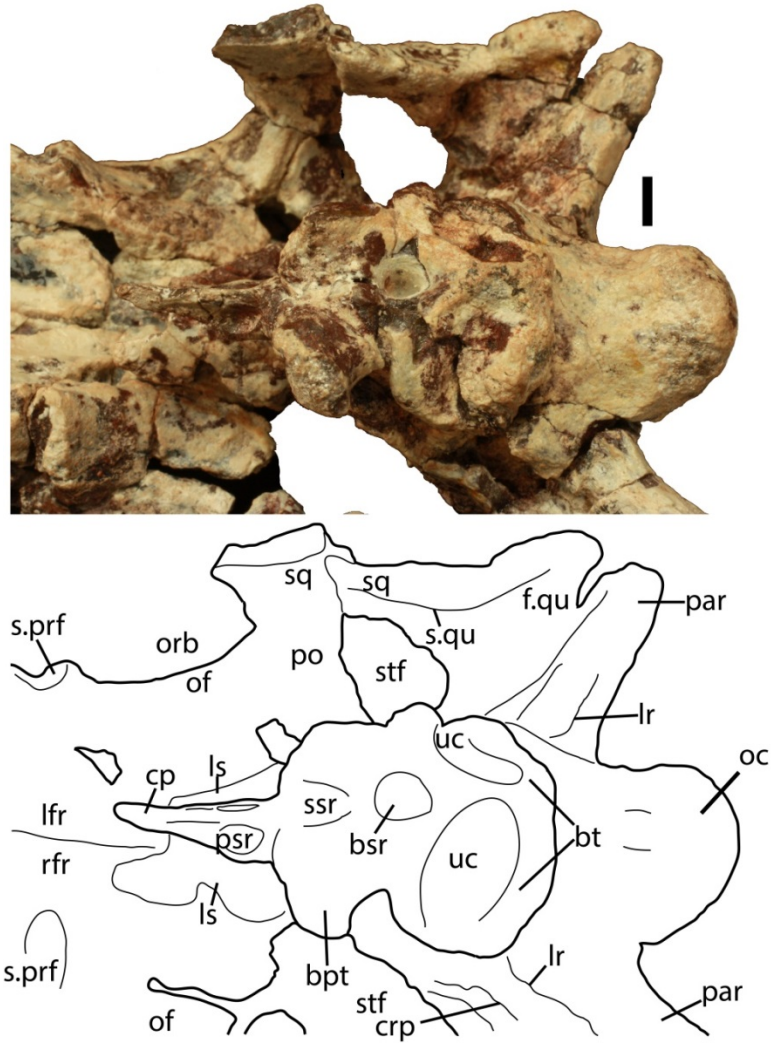

1542

1543

1544 Figure 10. Parabasisphenoid of *Scutarx deltatylus* (PEFO 34616) in ventral view. Scale bar
1545 equals 1 cm. Abbreviations: **bpt**, basipterygoid processes; **bsr**, basisphenoid recess;
1546 **bt**, basal tubera; **cp**, cultriform process; **crp**, crista prootica; **f.**, fossa for specified
1547 element; **lfr**, left frontal; **lr**, lateral ridge; **ls**, laterosphenoid; **of**, orbital fossa; **orb**,
1548 orbit; **par**, paroccipital process of the opisthotic; **po**, postorbital; **prf**, prefrontal; **pr**,
1549 prootic; **prf**, prefrontal; **psr**, parasphenoid recess; quadrate; **rfr**, right frontal; **sq**,
1550 squamosal; **ssr**, subsellar recess; **stf**, supratemporal fenestra; **uc**, unossified cleft of
1551 the basal tubera.

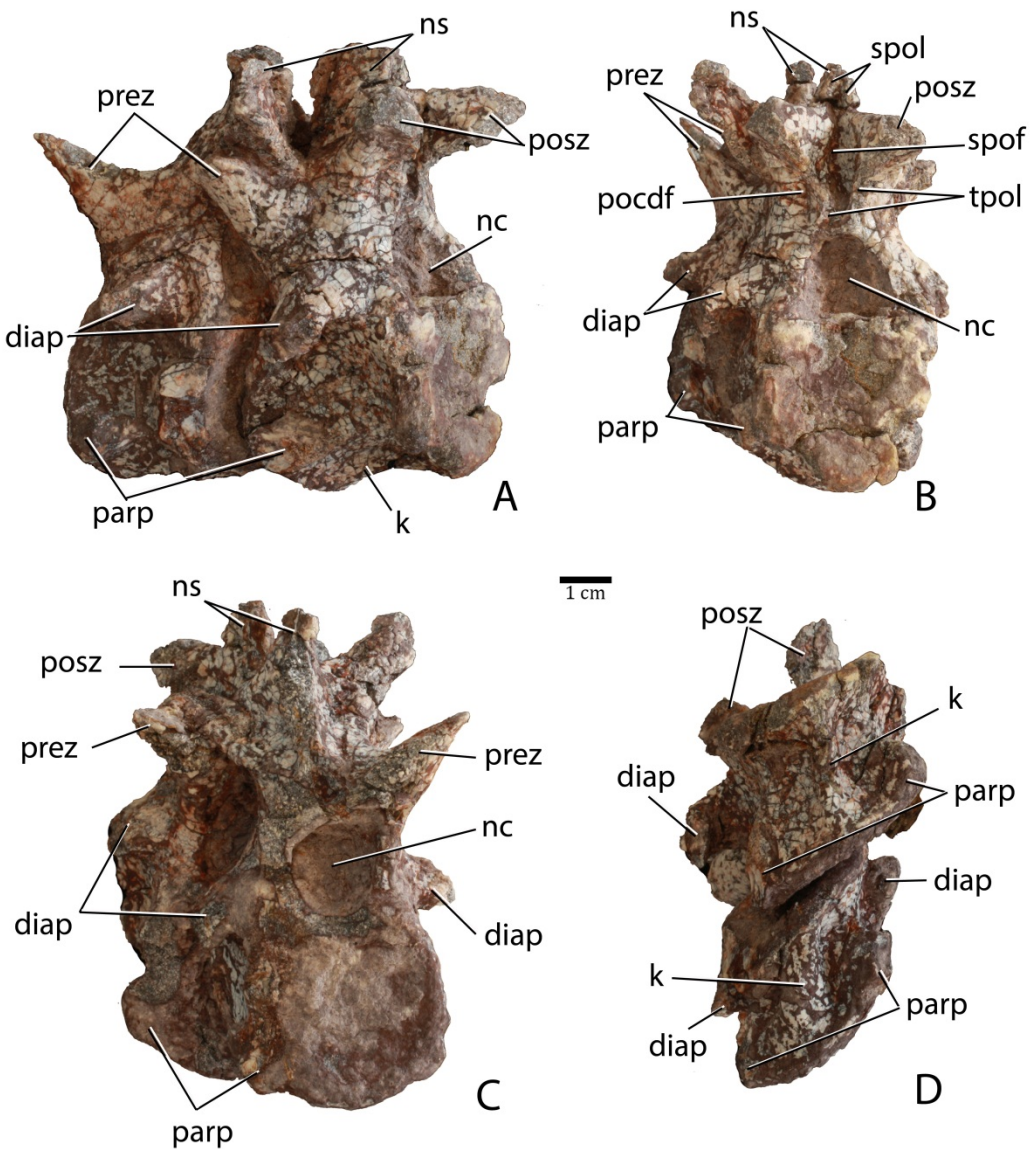

1552

1553

1554 Figure 11. Articulated anterior post-axial vertebrae of *Scutarx deltatylus* (PEFO 31217) in
1555 posterolateral (A), posterior (B), anterior (C), and ventral (D) views. Scale bar
1556 equals 1 cm. Abbreviations: diap, diapophysis; k, keel; nc, neural canal; ns, neural
1557 spine; parp, parapophysis; pocdf, postzygapophyseal centrodiapophyseal fossa;
1558 posz, postzygapophysis; prez, prezygapophysis; spof, spinopostzygapophyseal
1559 fossa; spol, spinopostzygapophyseal lamina; tpol, intrapostzygapophyseal lamina.

PeerJ Preprints | https://doi.org/10.7287/peerj.preprints.1924v1 | CC-BY 4.0 Open Access | rec: 3 Apr 2016, publ: 3 Apr 2016

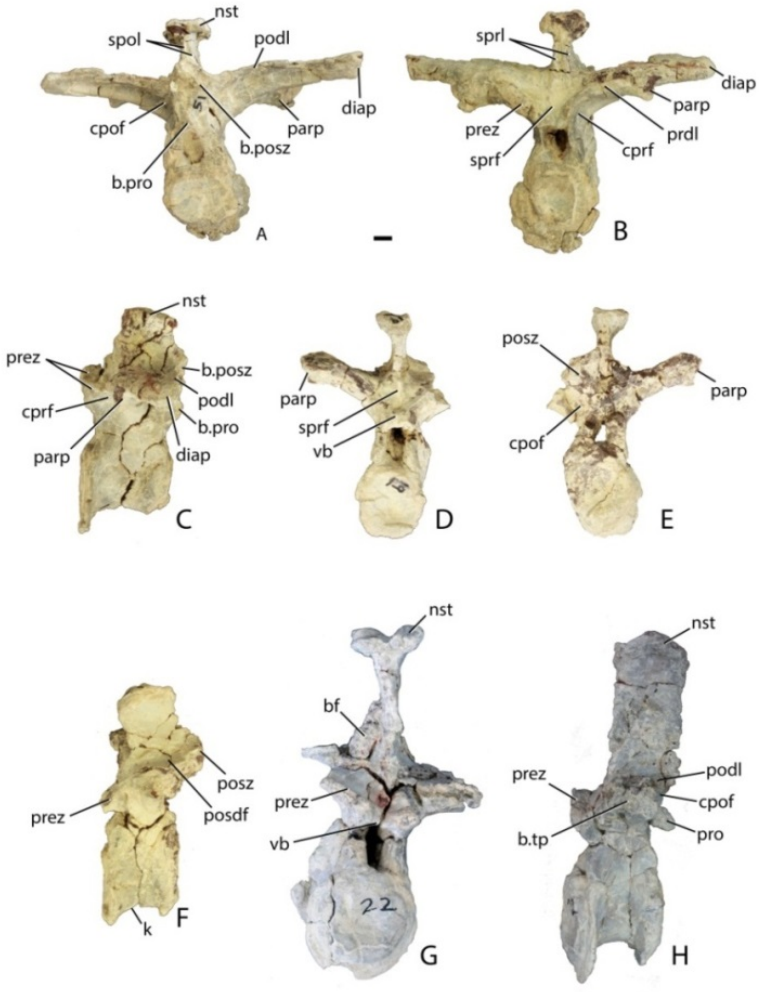

1560

1561

1562 Figure 12. Trunk vertebrae of *Scutarx deltatylus*. A-C, PEFO 34045/FF-51, mid-trunk
1563 vertebra in posterior (A), anterior (B), and lateral (C) views. D-F, PEFO 34045/19, Anterior
1564 trunk vertebra in anterior (D), posterior (E), and lateral (F) views. G-H, PEFO 34045/22,
1565 Posterior trunk vertebra in anterior (G) and lateral (H) views. Scale bar equals 1 cm.
1566 Abbreviations: b., broken designated element; bf, bone fragment; cpof, centropostzygapophyseal
1567 fossa,; cpfr, centroprezygapophyseal fossa; diap, diapophysis; k, keel; nst, neural spine table;
1568 parp, parapophysis; podl, postzygodiapophyseal lamina; posdf, postzygapophyseal
1569 spinodiapophyseal fossa; posz, postzygapophysis; prez, prezygapophysis; pro, projection; sprf,
1570 spinoprezygapophseal fossa; spol, spinopostzygapophyseal lamina; tp, transverse process; vb,
1571 ventral bar.

1572

PeerJ Preprints | https://doi.org/10.7287/peerj.preprints.1924v1 | CC-BY 4.0 Open Access | rec: 3 Apr 2016, publ: 3 Apr 2016

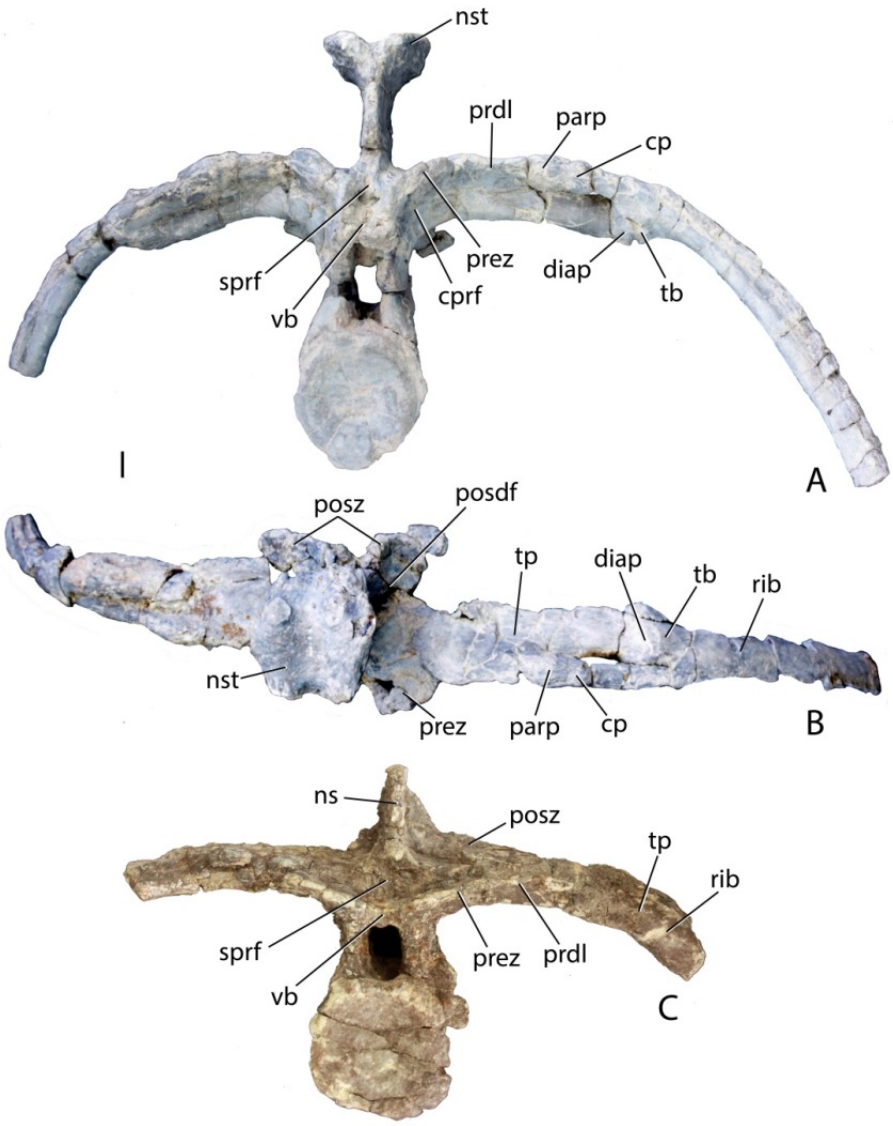

1573

1574

1575 Figure 13. Posterior trunk vertebrae of *Scutarx deltatylus*. A-B, PEFO 34045 in anterior
1576 (A) and dorsal (B) view. C, PEFO 31217 in anterior view. Scale bar equals 1 cm. Abbreviations:
1577 cp, capitulum; cprf, centroprezygapophyseal fossa; diap, diapophysis; ns, neural spine; nst,
1578 neural spine table; parp, parapophysis; prdl, prezygadiapophyseal lamina; posdf,
1579 postzygapophyseal spinodiapophyseal fossa; posz, postzygapophysis; prez, prezygapophysis;
1580 sprf, spinoprezygapophyseal fossa; tb, tuberculum; tp, transverse process; vb, ventral bar.
1581

PeerJ Preprints | https://doi.org/10.7287/peerj.preprints.1924v1 | CC-BY 4.0 Open Access | rec: 3 Apr 2016, publ: 3 Apr 2016

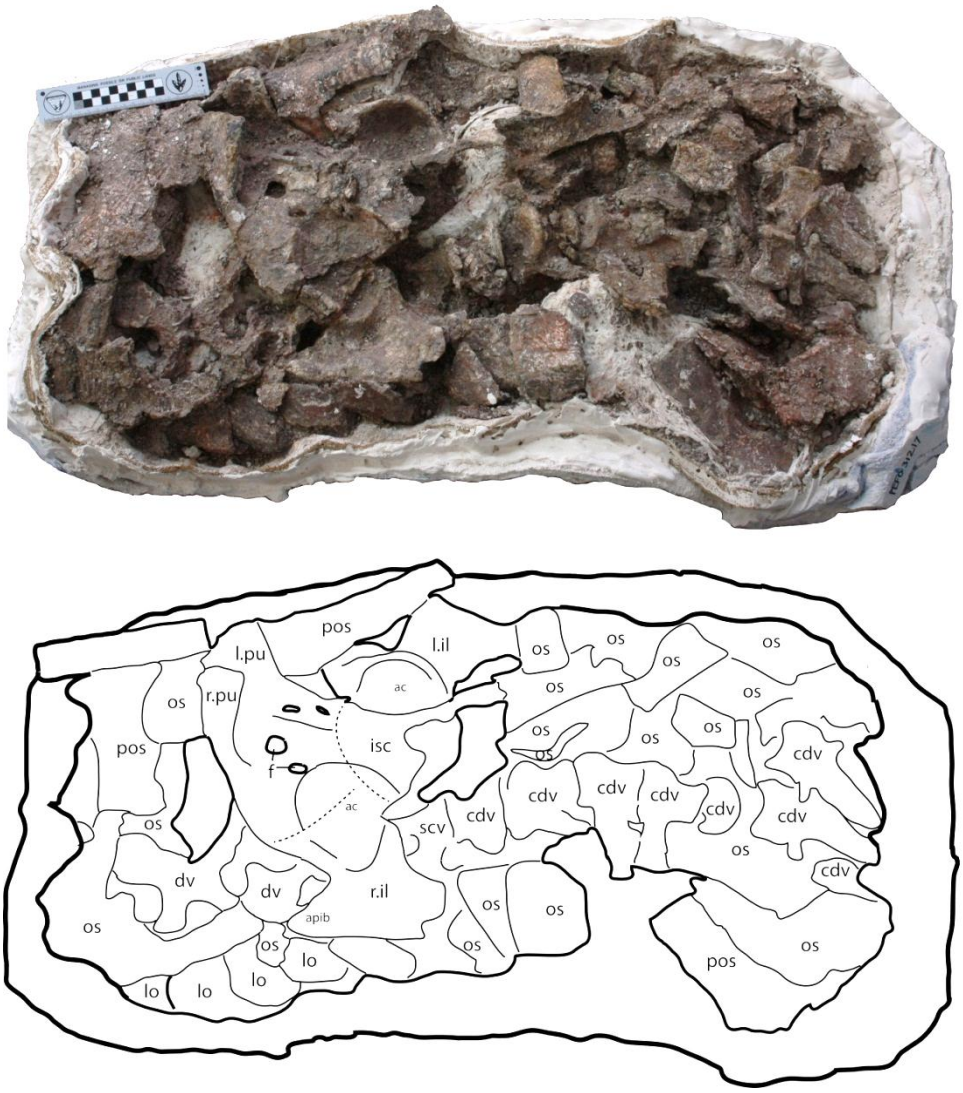

Figure 14. Photo and interpretive sketch of a partially articulated sacrum and anterior portion of the tail of *Scutarx deltatylus* (PEFO 31217). Scale bar equals 10 cm. Abbreviations: ac, acetabulum, apib, anterior process of the iliac blade; cdv, caudal vertebra; dv, trunk vertebra; f, foramen; isc, ischia; l.il, left ilium; l.pu, left pubis; lo, lateral osteoderm; os, osteoderm; pos, paramedian osteoderm; r.il, right ilium; r.pu, right pubis; scv, sacral vertebra.

PeerJ Preprints | https://doi.org/10.7287/peerj.preprints.1924v1 | CC-BY 4.0 Open Access | rec: 3 Apr 2016, publ: 3 Apr 2016

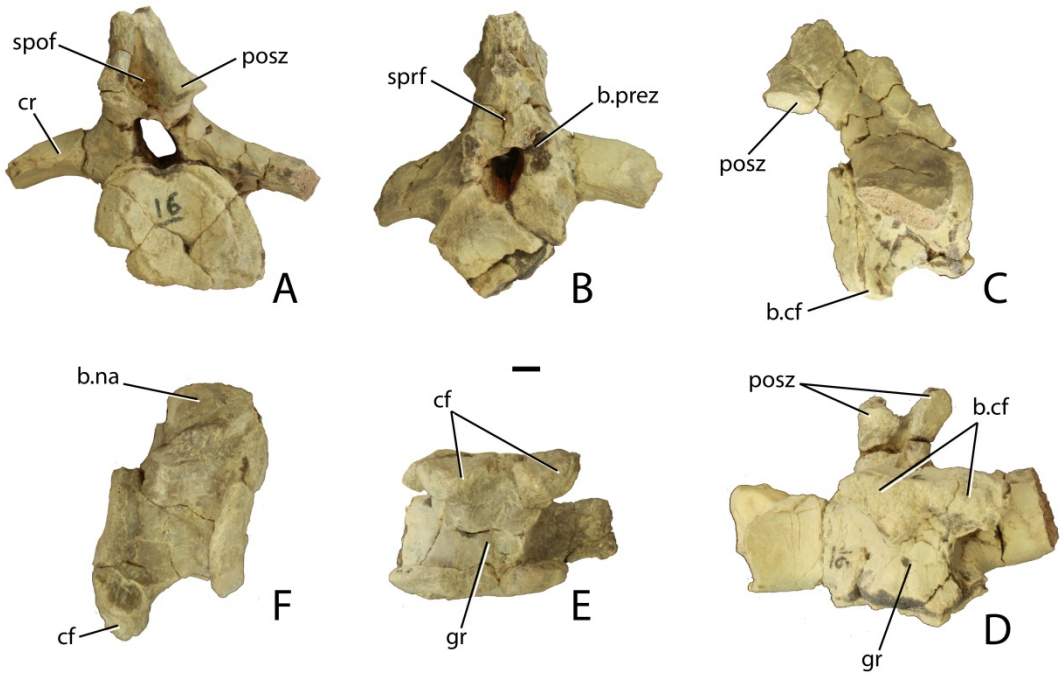

1589

1590

1591 Figure 15. Anterior caudal vertebrae of *Scutarx deltatylus* (PEFO 34045). A-D, anterior caudal in
1592 posterior (A), anterior (B), lateral (C), and ventral (D). E-F, Anterior caudal
1593 vertebra in ventral (E) and lateral (F). Scale bar equals 1 cm. Abbreviations: b.,
1594 broken designated element; cf, chevron facet; cr, caudal rib; gr, ventral groove;
1595 posz, postzygapophysis; prez, prezygapophysis; spof, spinopostzygapophseal fossa,
1596 ; sprf, spinoprezygapophseal fossa.

1597

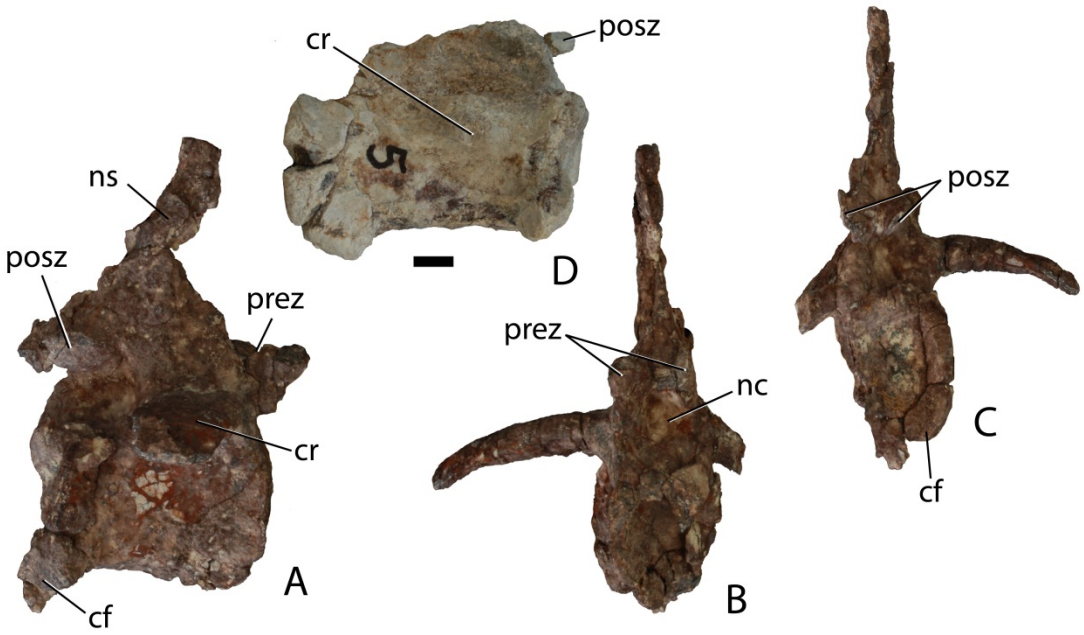

1598

1599

1600 Figure 16. Mid-caudal vertebrae of *Scutarx deltatylus*. A-C, anterior mid-caudal vertebra (PEFO
1601 34919) in lateral (A), anterior (B), and posterior (C) views. D, posterior mid-caudal
1602 vertebra (PEFO 34045) in lateral view. Scale bar = 1 cm. Abbreviations: cf,
1603 chevron facet; cr, caudal rib; ns, neural spine; prez, prezygapophysis; posz,
1604 postzygapophysis.

1605

PeerJ Preprints | https://doi.org/10.7287/peerj.preprints.1924v1 | CC-BY 4.0 Open Access | rec: 3 Apr 2016, publ: 3 Apr 2016

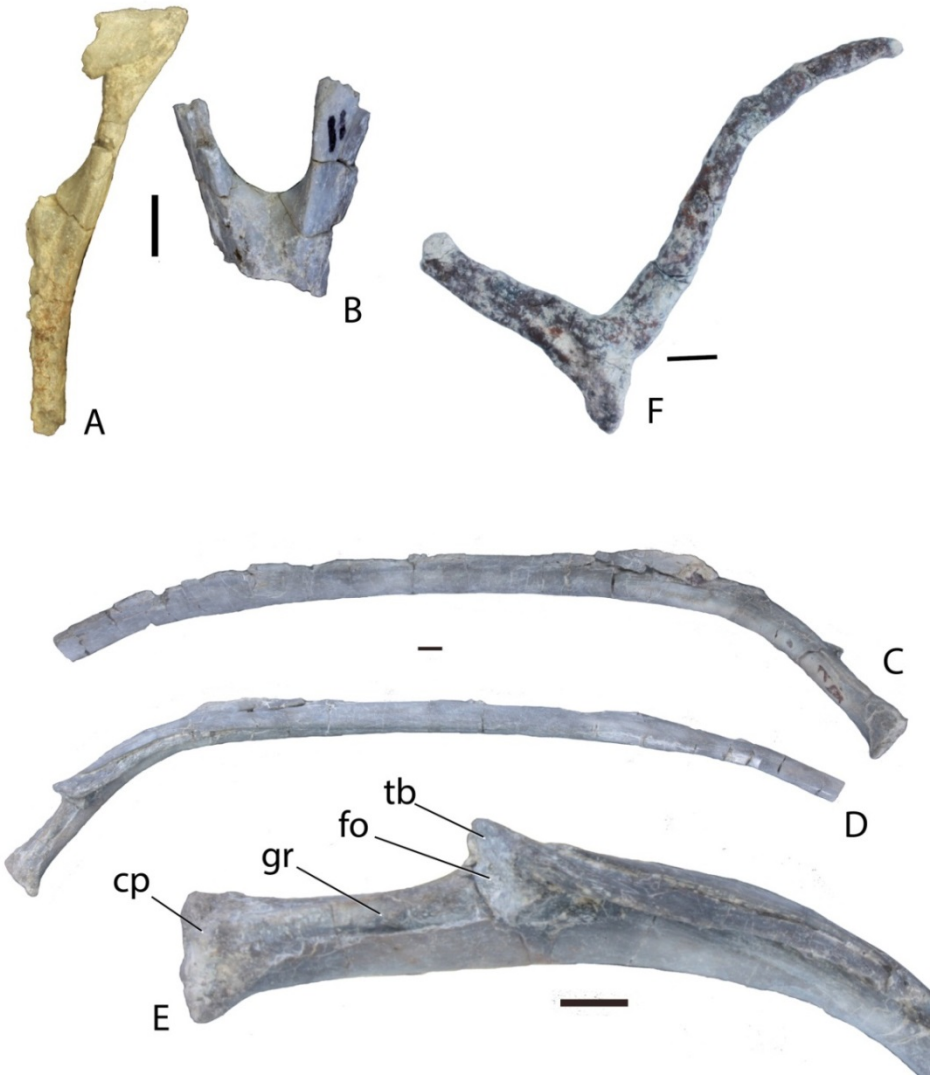

1606

1607

1608 Figure 17. Chevrons and ribs of *Scutarx deltatylus*. A-B, partial anterior chevrons from
1609 PEFO 34045 in posterior view; C-D, left trunk rib from PEFO 34045 in posterior (C) and
1610 anterior (D) views. E, close-up view of head of trunk rib from PEFO 34045. F, paired gastral ribs
1611 from PEFO 34616. Scale bars equal 1 cm. Abbreviations: cp, capitulum; fo, fossa; gr, groove; tb,
1612 tuberculum.

1613

1614

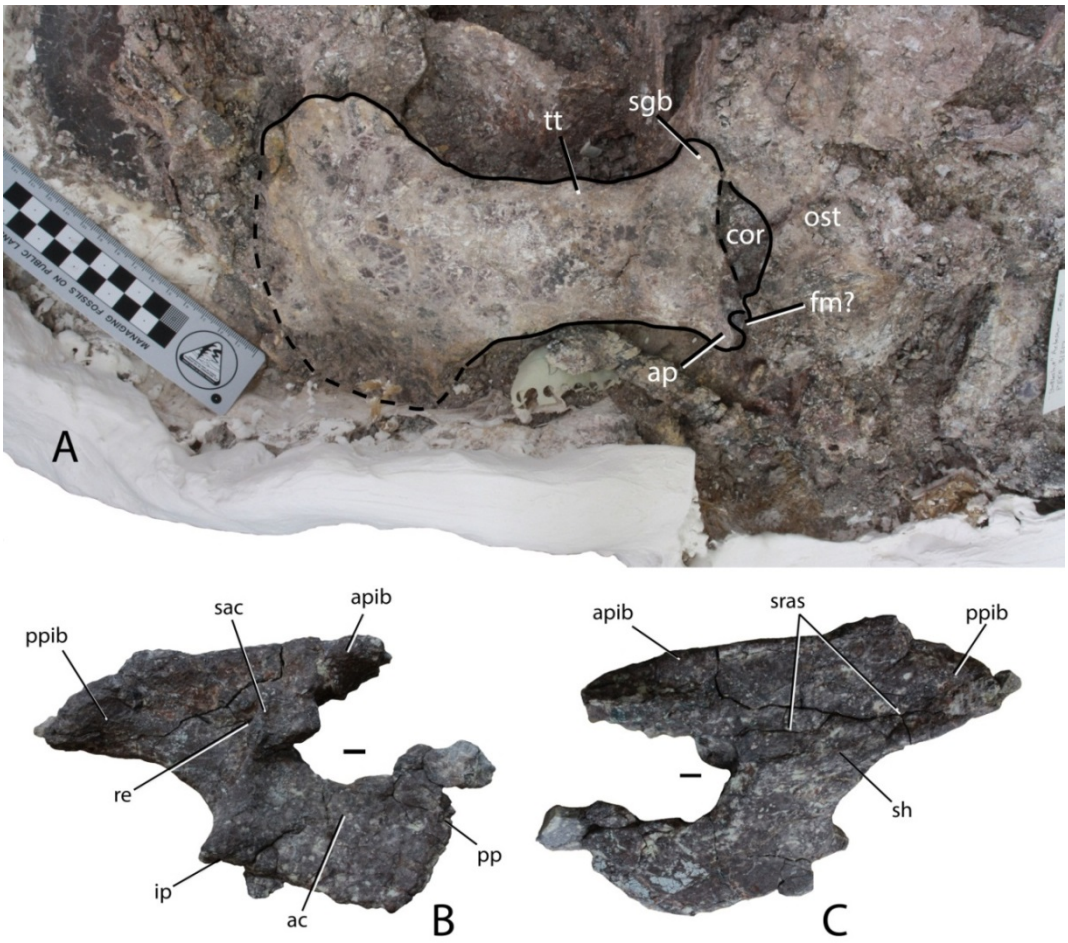

1615

1616

1617 Figure 18. Girdle elements of *Scutarx deltatylus.* A, left scapulocoracoid of PEFO 31217
1618 in lateral view. B-C, right ilium of PEFO 34919 in 'lateral' and 'medial' views (see text for
1619 discussion regarding anatomical direction of the ilium). Scale bars equal 10 cm (A) and 1 cm (B-
1620 C). Abbreviations: ac, acetabulum; ap, acromion process; apib, anterior process of the iliac
1621 blade; cor, coracoid; fm, foramen; ip, ischiadic peduncle; ost, osteoderms; pp, pubic peduncle;
1622 ppib, posterior process of the iliac blade; re, recess; sac, supraacetabular crest; sgb, supraglenoid
1623 buttress; sh, shelf; sras, sacral rib attachment surfaces; tt, triceps tubercle.

1624

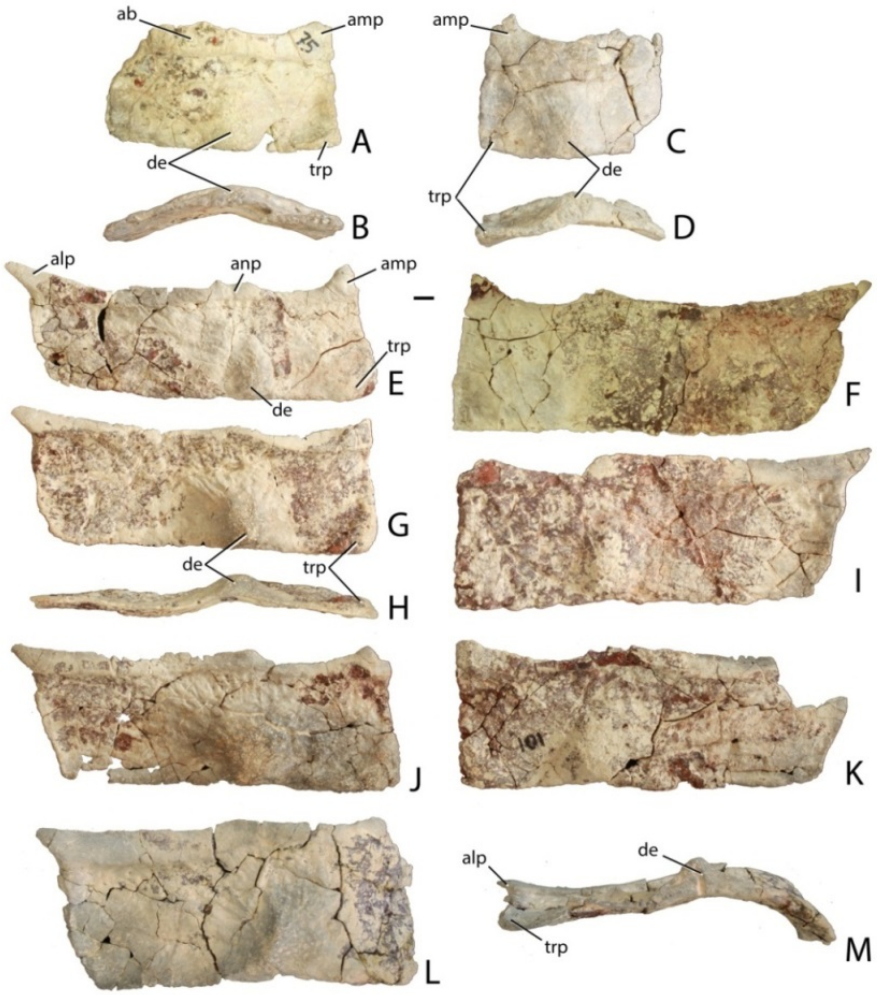

1625

1626

1627 Figure 19. Cervical and dorsal trunk paramedian osteoderms of *Scutarx deltatylus* from
1628 PEFO 34045. A-B, left mid-cervical osteoderm in dorsal (A) and posterior (B) views. C-D, right
1629 mid-cervical osteoderm in dorsal (C) and posterior (D). E-F, left (E) and right (F) dorsal trunk
1630 osteoderms in dorsal view. G-I, left (G, H) and right (I) dorsal trunk osteoderms in dorsal (G, I)
1631 and posterior (H) views. J-K, left (J) and right (K) dorsal trunk osteoderms in dorsal view. L-M,
1632 posterior dorsal trunk osteoderm in dorsal (L) and posterior (M) views. Scale bar = 1 cm.
1633 Abbreviations: ab, anterior bar; alp, anterolateral process; amp, anteromedial process; anp,
1634 anterior process; de, dorsal eminence; trp, triangular protuberance.

1635

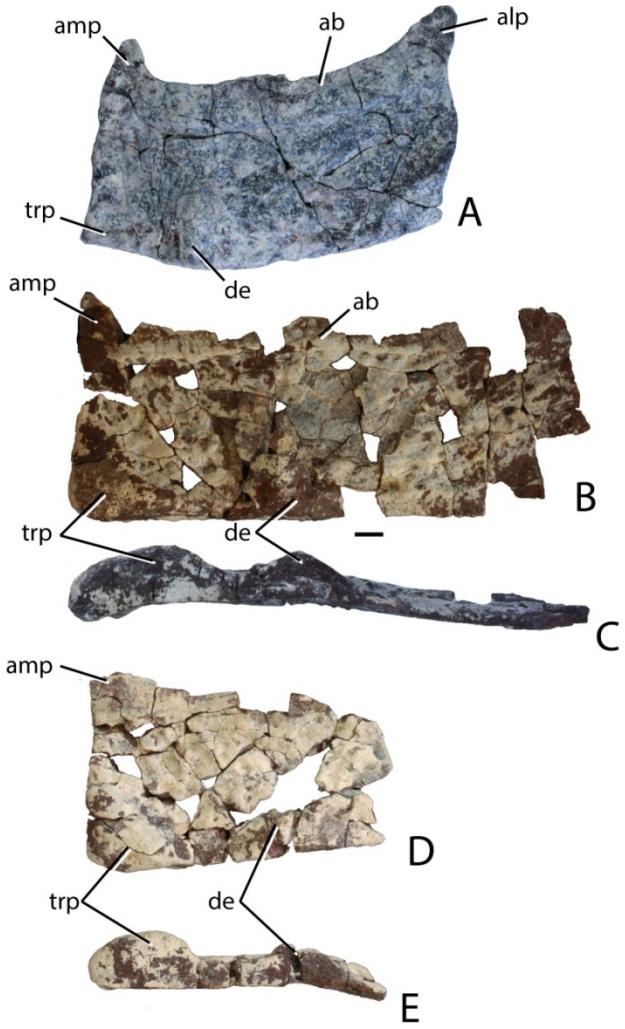

1636

1637

1638 Figure 20. Holotype paramedian osteoderms of *Scutarx deltatylus* from PEFO 34616. A,
1639 posterior cervical osteoderm in dorsal view. B-C, right dorsal trunk paramedian osteoderm in
1640 dorsal (B) and posterior (C) views. D-E, partial right dorsal trunk paramedian osteoderm in
1641 dorsal (D) and posterior (E) views. Note the prominence of the triangular protuberance in the
1642 posterior views. Scale bar equals 1 cm. Abbreviations: ab, anterior bar; alp, anterolateral process;
1643 amp, anteromedial process; de, dorsal eminence; trp, triangular protuberance.

1644

1645

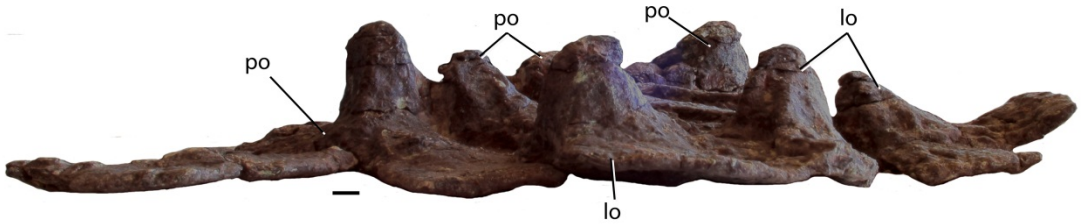

1646

1647

1648 Figure 21. Fused semi-articulated anterior dorsal caudal paramedian and dorsal caudal lateral
1649 osteoderms of *Scutarx deltatylus* (PEFO 34919) in a lateral view showing extreme
1650 development of the dorsal eminences. Scale bar equals 1 cm. Abbreviations: lo,
1651 lateral osteoderm; po, paramedian osteoderm.

1652

PeerJ Preprints | https://doi.org/10.7287/peerj.preprints.1924v1 | CC-BY 4.0 Open Access | rec: 3 Apr 2016, publ: 3 Apr 2016

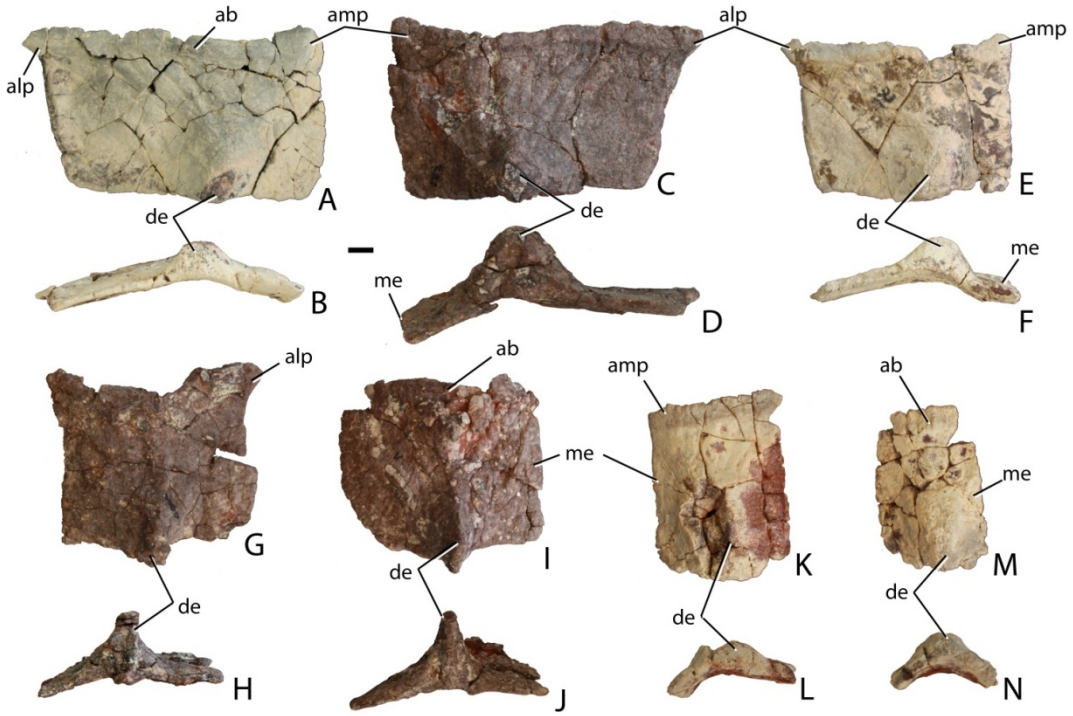

1653

1654

1655 Figure 22. Dorsal caudal paramedian osteoderms of *Scutarx deltatylus*. A-B, left anterior mid-
1656 caudal osteoderm (PEFO 34045) in dorsal (A) and posterior (B) views. C-D, right
1657 anterior mid-caudal osteoderm (PEFO 34919) in dorsal (C) and posterior (D) views;
1658 E-F, left mid-caudal osteoderm (PEFO 34045) in dorsal (E) and posterior (F) views.
1659 G-H, right mid-caudal osteoderm (PEFO 34919) in dorsal (G) and posterior (H)
1660 views. I-J, left mid-caudal osteoderm (PEFO 34919) in dorsal (I) and posterior (J)
1661 views. K-L, right posterior caudal osteoderm (PEFO 34045) in dorsal (K) and
1662 posterior (L) views. M-N, left posterior caudal osteoderm (PEFO 34045) in dorsal
1663 (M) and posterior (N) views. Scale bar equals 1 cm. Abbreviations: ab, anterior
1664 bar; alp, anterolateral process; amp, anteromedial process; de, dorsal eminence; me,
1665 medial edge.

1666

1667

PeerJ Preprints | https://doi.org/10.7287/peerj.preprints.1924v1 | CC-BY 4.0 Open Access | rec: 3 Apr 2016, publ: 3 Apr 2016

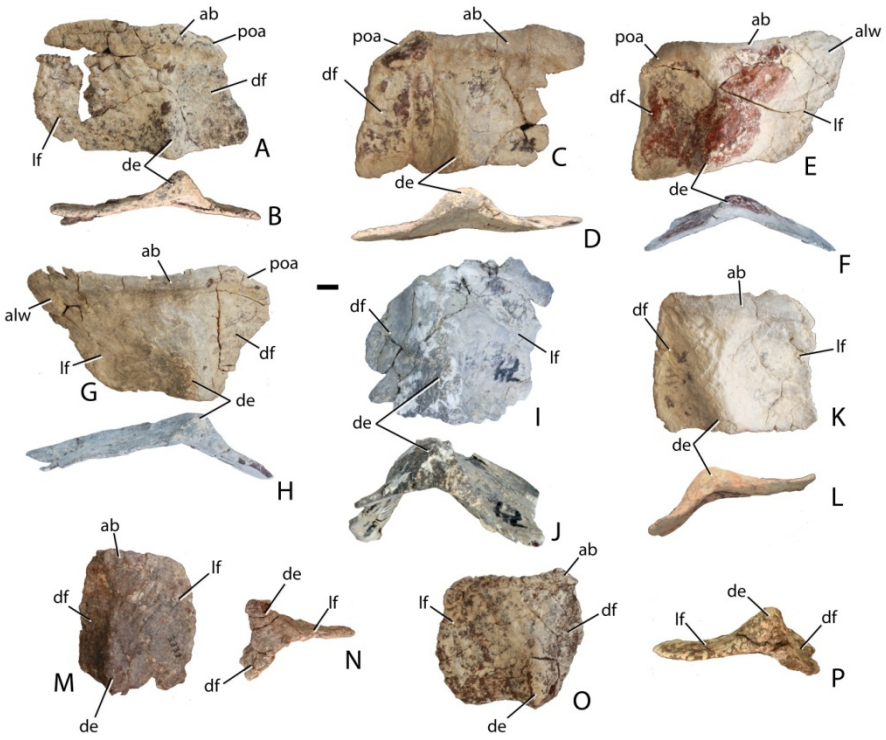

1668

1669

1670 Figure 23. Lateral osteoderms of *Scutarx deltatylus*. A-B, left anterior trunk osteoderm (PEFO
1671 34616) in dorsal (A) and posterior (B) views; C-D, right anterior trunk osteoderm
1672 (PEFO 34045) in dorsal (C) and posterior (D) views; E-F, right posterior mid-trunk
1673 osteoderm (PEFO 34045) in dorsal (E) and posterior (F) views; G-H, left posterior
1674 mid-trunk osteoderm (PEFO 34045) in dorsal (G) and posterior (H) views; I-J, right
1675 posterior trunk osteoderm (PEFO 34045) in dorsal (I) and posterior (J) views; K-L,
1676 right anterior dorsal caudal osteoderm (PEFO 34045) in dorsal (K) and posterior (L)
1677 views; right posterior dorsal mid-caudal osteoderm (PEFO 34919) in dorsal (M) and
1678 posterior (N) views; O-P, left dorsal mid-caudal osteoderm (PEFO 34616) in dorsal
1679 (O) and posterior (P) views. Scale bar equals 1 cm. Abbreviations: ab, anterior bar;
1680 alw, anterolateral wing; de, dorsal eminence; df, dorsal flange; mf, medial flange;
1681 poa, paramedian osteoderm articular surface.

1682

1683

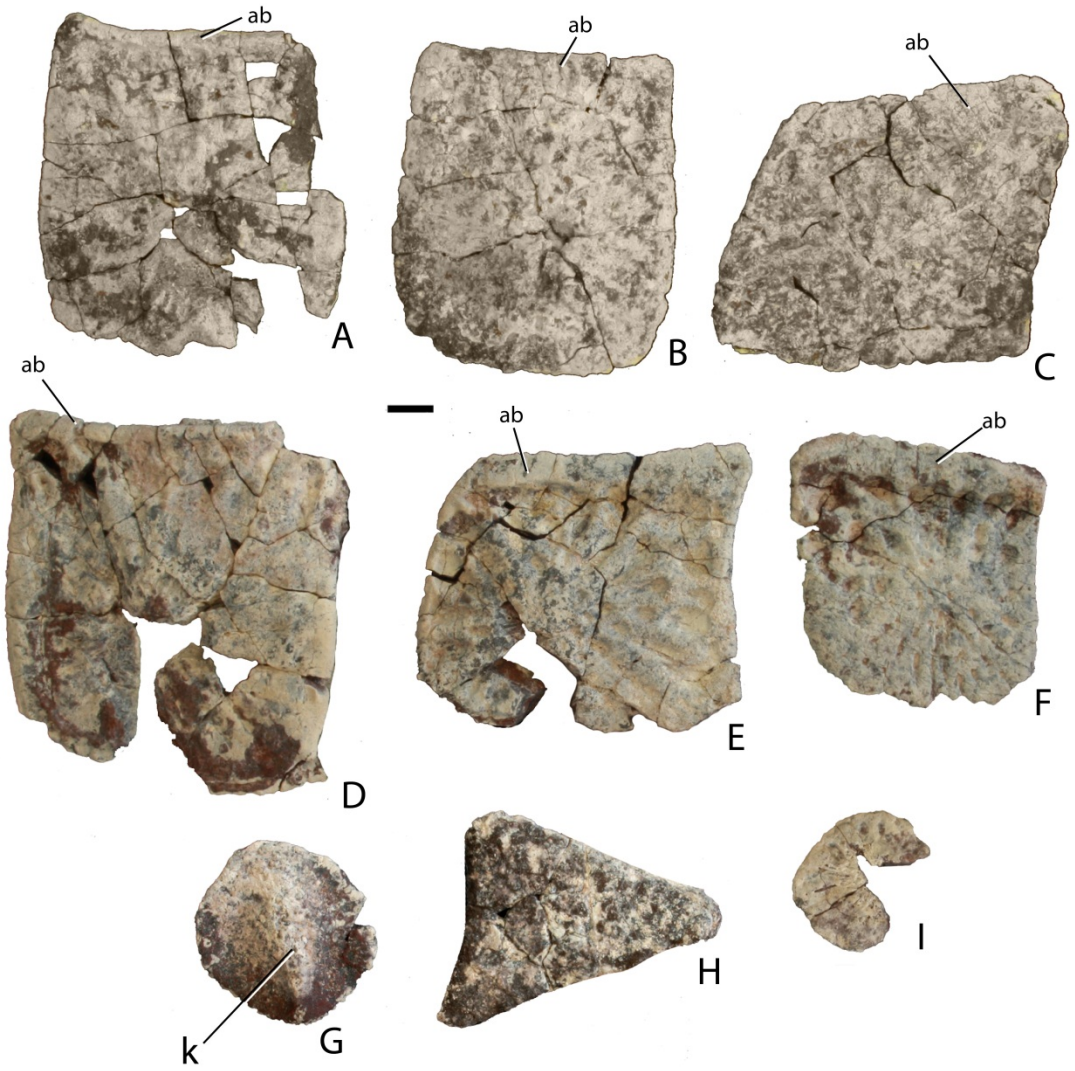

1684

1685

1686 Figure 24. Ventral trunk and appendicular osteoderms of *Scutarx deltatylus* from PEFO 34616.
1687 A-F, square ventral osteoderms. G, round, keeled appendicular osteoderm. H,
1688 triangular ventral or appendicular osteoderm. I, round, ornamented appendicular
1689 osteoderm. Scale bar equals 1 cm. Abbreviations: ab, anterior bar; k, keel.

1690

PeerJ Preprints | https://doi.org/10.7287/peerj.preprints.1924v1 | CC-BY 4.0 Open Access | rec: 3 Apr 2016, publ: 3 Apr 2016

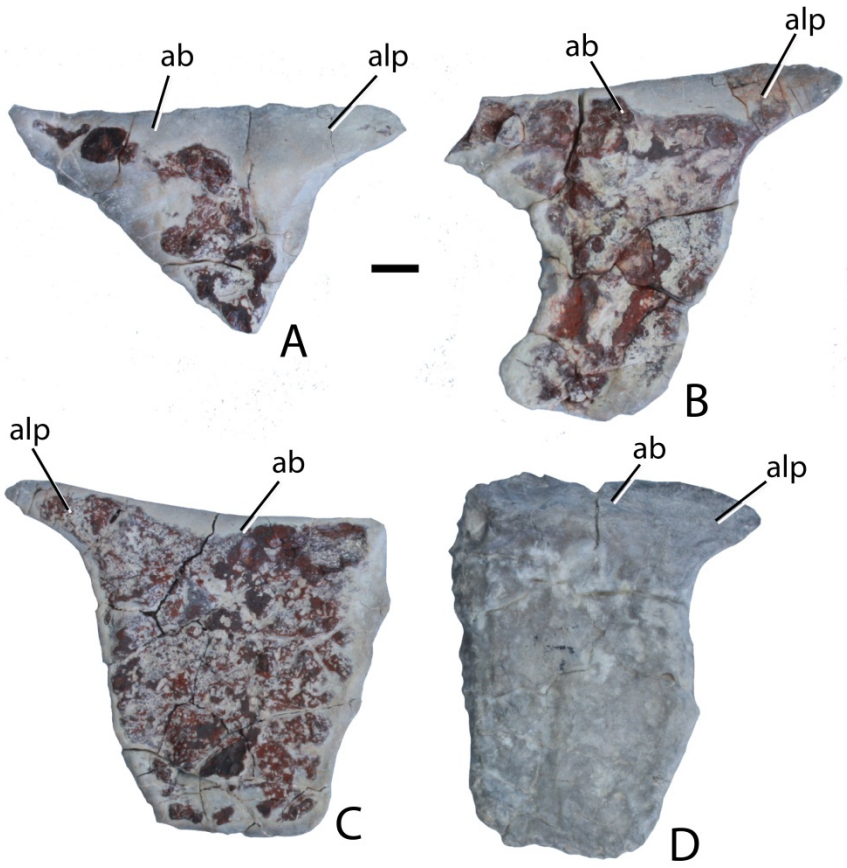

1691

1692

1693 Figure 25. Incompletely formed trunk paramedian osteoderms from PEFO 34045. A-B, right
1694 osteoderms in dorsal view; C, left osteoderm in dorsal view; D, right osteoderm in
1695 dorsal view. Scale bar equals 1 cm. Abbreviations: ab, anterior bar; alp,
1696 anterolateral process.

PeerJ Preprints | https://doi.org/10.7287/peerj.preprints.1924v1 | CC-BY 4.0 Open Access | rec: 3 Apr 2016, publ: 3 Apr 2016

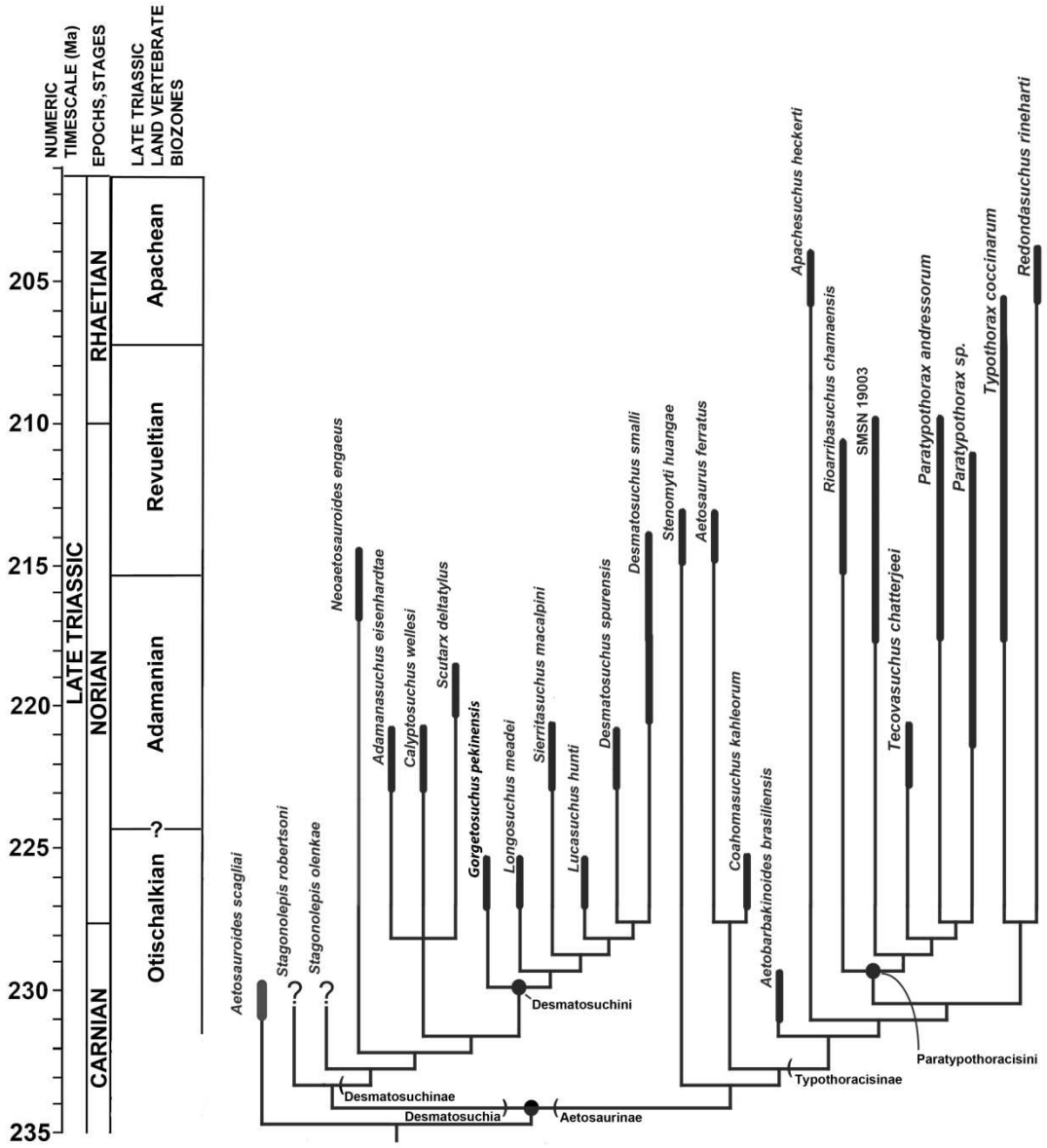

Figure 26. Time-calibrated phylogeny of the Aetosauria showing estimated ranges of taxa in the Triassic stages and associated vertebrate biozones.

PeerJ Preprints | https://doi.org/10.7287/peerj.preprints.1924v1 | CC-BY 4.0 Open Access | rec: 3 Apr 2016, publ: 3 Apr 2016